



Warner Valley Basin Groundwater Flow Model Development and Calibration

FINAL

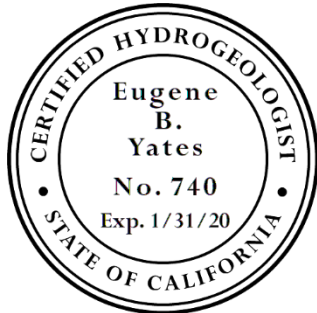
December 2018

Prepared for:
Vista Irrigation District

Prepared By:
TODD 
GROUNDWATER
2490 Mariner Square Loop, Suite 215
Alameda, California 94501

DUDEK
605 Third Street
Encinitas, California 92024

SIGNATURE PAGE



A handwritten signature in black ink that reads "Eugene B. Yates".

Gus Yates, PG, CHg
Senior Hydrologist



A handwritten signature in blue ink that reads "Chad N. Taylor".

Chad Taylor, PG, CHg
Senior Hydrogeologist

Table of Contents

	Page
Executive Summary.....	1
Introduction	4
Purpose of Model	4
Description of Model Area.....	4
Hydrogeologic Conceptual Model	7
Basin Boundaries	7
Basin Fill Materials, Layering and Faults.....	7
Previous Studies.....	7
Stratigraphic Analysis for this Study	8
Cross Sections	8
Available Data and Information.....	9
Cross Section Construction	10
Hydrostratigraphic Evaluation	10
Conceptualization of the Hydrologic System.....	11
Numerical Model Development	12
Software Used for Modeling.....	12
Model Grid and Active Flow Area	12
Model Layers.....	12
Aquifer Characteristics.....	13
Lake Henshaw	13
Simulation Period and Time Increments	14
Initial Water Levels	15
Groundwater Inflows.....	15
Dispersed Recharge	15
Percolation from Streams.....	16
Percolation from Lake Henshaw.....	17
Subsurface Inflow	17
Minor Inflows.....	18
Groundwater Outflows.....	18
Groundwater Pumping	18
Seepage into Streams	19
Seepage into Lakes	19
Water Balance Summary and Change in Storage.....	19
Model Calibration	21
Calibration Approach and Objective.....	21
Calibration Results	22
Calibration Statistics	23
Calibration Discussion.....	24

Sustainable Yield Analysis	26
Scenario Simulations.....	28
Yield of Warner Springs Ranch Resort Area	28
Impact of Climate Change.....	30
Additional Options for Increased District Water Supply Yield	30
Option 1: Lower Lake Levels to Decrease Spills.....	31
Option 2: Lower Lake Levels to Decrease Evaporation	31
Additional Observations	32
References Cited	33

- Appendix A. Comparison of Basin Boundary Delineations
- Appendix B. Documentation of Rainfall-Runoff-Recharge Model
- Appendix C. Comparison of Isohyetal Maps
- Appendix D. Calibration Hydrographs

List of Figures

- 1 Location of Warner Valley Groundwater Basin
- 2 Locations of Wells
- 3 Geologic Map
- 4 Cross Section Map
- 5 Bedrock Elevation Map
- 6 Cross Section A-A'
- 7 Cross Section B-B'
- 8 Cross Section C-C'
- 9 Cross Section D-D'
- 10 Cross Section E-E'
- 11 Cross Section F-F'
- 12 Cross Section G-G'
- 13 Plan View of Model Grid
- 14 Model Layer Extents and Elevations
- 15 Aquifer Parameter Zones
- 16 Boundary Conditions in Groundwater Model
- 17 Lake Henshaw Historical Water Balance
- 18 1945-1977 Design Drought
- 19 Rainfall-Runoff-Recharge Processes
- 20 Map of Recharge Zones
- 21 Map of Stream Segments
- 22 Stream Channel Cross Sections
- 23 Total Bedrock Inflow to Basin
- 24 Locations of Groundwater Pumping 1996-2016
- 25 Annual Groundwater Pumping 1939-2016
- 26 Annual Basin-Wide Groundwater Balances, 1939-2016
- 27 Average Annual Groundwater Balance, 1939-2016
- 28 Hydrographs of Measured and Simulated Groundwater Levels
- 29 Contours of Simulated Groundwater Levels in December 1977
- 30 Contours of Simulated Groundwater Levels in March 1995
- 31 Measured and Simulated Lake Henshaw Levels
- 32 Scatterplot of Simulated and Observed Water Levels
- 33 Simulated Water Levels with Increased VID Pumping
- 34 WSRR Wells and Water Balance Subarea
- 35 Well Hydrographs with Increased WSRR Pumping
- 36 Change in 1977 Water Levels with 1,100 AFY WSRR Pumping
- 37 Groundwater Hydrograph with Climate Change
- 38 Lake Henshaw Area-Capacity Curves

List of Acronyms

AF	acre-feet
AFY	acre-feet per year
AWC	available water capacity
Basin	Warner Valley Groundwater Basin
bgs	below ground surface
cfs	cubic feet per second
CIMIS	California Irrigation Management Information System
City	City of Escondido
District	Vista Irrigation District
DWR	California Department of Water Resources
ET	evapotranspiration
ET ₀	reference evapotranspiration
ft	feet
ft/d	feet per day
GIS	Geographic Information System
gpm	gallons per minute
gpm/ft	gallons per minute per foot
in/d	inches per day
in/yr	inches per year
JMM	James M. Montgomery Consulting Engineers
K _H	horizontal hydraulic conductivity
K _V	vertical hydraulic conductivity
LTMWC	Los Tules Mutual Water Company
NAD83	North American Datum of 1983
NAVD88	North American Vertical Datum of 1988
NED	National Elevation Dataset
NGVD29	National Geodetic Vertical Datum of 1929
SGMA	Sustainable Groundwater Management Act
USGS	U.S. Geological Survey
WSRR	Warner Springs Ranch Resort

Executive Summary

Vista Irrigation District (District) is the largest landowner and water user in the Warner Valley Groundwater Basin (Basin), located in the interior mountains of northern San Diego County (**Figure 1**). The District also owns and operates Lake Henshaw Dam and Reservoir at the downgradient end of the Basin. Groundwater interacts with Lake Henshaw by two pathways: 1) a direct hydraulic connection between groundwater and the lake across the lakebed, and 2) discharge from tens of wells that the District operates in the Basin and pumps into the lake to supplement water supply releases. Those releases serve customers in the District's service area, the City of Escondido (City), the Rincon Band of Mission Indians, and other smaller users along the San Luis Rey River.

The District and the City initiated this study of Warner Basin groundwater to improve estimates of existing and potential future yield and to evaluate the effects of proposed increases in pumping by the other major Basin user, Warner Springs Ranch Resort (WSRR). The scope of the investigation included an updated analysis of Basin hydrogeology, development of a numerical groundwater flow model, and simulation of scenarios including climate change, increased WSRR pumping and increased District pumping.

Major Findings

The sustainable yield of the Basin was investigated relative to the record historical drought period of 1945 through 1977, followed by the recovery period 1978 through 1986. District pumping began in 1953, and average pumping through 1986 was 7,604 acre-feet per year (AFY). Modelling demonstrated that pumping could have been increased by at least 20 percent (to 9,125 AFY) and still allowed groundwater levels to fully recover (although not until 1998 in some locations). For this study, sustainability is defined by complete water-level recovery between droughts. The simulation assumed that existing wells would be capable of producing the same amount of water at water levels up to 60 feet below historical minimums. This is not the case. Obtaining the additional yield and optimizing the use of groundwater storage would require additional wells, different pumps and an evaluation of alternative pumping locations that minimize well interference. Additional factors that would need to be considered include the capacity of the wellfield water conveyance system (ditches and siphons) and any concurrent changes in the operation of Lake Henshaw.

Modeling the interaction of pumping within WSRR with yield within the District area shows that an increase in consumptive use within the WSRR area caused an equal decrease in the conjunctive use yield available to the District. The limiting factor for sustainable yield available to WSRR during the drought of record was not storage recovery, but limited storage due to the relatively small basin thickness near WSRR. The model showed that WSRR consumptive use could successfully be increased to 1,100 AFY. Higher rates caused model cells to go dry, even when additional wells were introduced to spread the pumping stress over a broader area. Although dry cells are partly an artifact of model layering, they correctly reflect the real concern that insufficient saturated thickness could constrain yield during droughts.

Model Development

Basic data were compiled and reviewed for the study. Four different delineations of Basin boundaries have been previously published, for different purposes. Two geologically-based delineations from the 1960s were deemed most suitable for the modeling work, and minor differences between them were reconciled into a new boundary delineation. Previously published contour maps of average annual rainfall were similarly found to have substantial discrepancies. One was selected as most consistent with data from the two long-term stations in the Basin, and minor adjustments were also implemented to improve model calibration. Other basic data included geologic and geophysical logs from wells and boreholes, pumping and water levels from District wells, operations data for Lake Henshaw, and long-term stream flow records for gages on two streams that enter the Basin.

Geologic and geophysical data were imported to a geospatial database that supported preparation of seven cross sections that crossed the Basin along various alignments. The cross-sections confirmed that Basin fill deposits are generally coarse-grained without regional confining layers and that faults divide the Basin into blocks with variable depths to bedrock. Basin thickness is greatest at a down-dropped block in the south-central part of the Basin, where it exceeds 900 feet. Of the roughly ten identified faults crossing the Basin, several have demonstrable effects on groundwater levels.

Hydrologic modeling included rainfall, soil moisture, runoff, stream flow and groundwater processes over the entire watershed tributary to Lake Henshaw, including the Basin and upland areas. A 78-year simulation period of water years 1939-2016 was selected for analysis in order to include the prolonged dry period from 1945-1977. Surface hydrology was simulated on a daily basis.

The groundwater flow model used the MODFLOW 2005 software developed by the U.S. Geological Survey (USGS). The model grid contains three layers and in plan view is divided into uniform 1,000 x 1,000 foot cells. The topmost layer covers the entire Basin area. Layers 2 and 3 are progressively smaller, active only in the deeper parts of the Basin. Where the Basin is sufficiently thick that two or three layers are active, the bottom of layer 1 was set at an elevation approximately equal to the lowest historical water levels to prevent cells from going dry during the calibration simulation.

The groundwater model dynamically simulates flow between streams and groundwater based on the width and permeability of stream channels and the relative difference between the water level in the stream and the adjacent water table elevation. Stream flow is routed from reach to reach (one reach per model cell) from the peripheral boundaries of the Basin to Lake Henshaw. Lake Henshaw was similarly simulated as a surface water body hydraulically coupled to streams and groundwater.

Model parameters were calibrated to achieve reasonable similarity between measured and simulated historical groundwater levels, lake levels and stream flow.

The potential effect of climate change was investigated by running the 1939-2016 calibration simulation with adjustments to reflect future climatic conditions. Monthly factors for adjusting rainfall and reference evapotranspiration were taken from figures developed by the California Department of Water Resources (DWR) by down-scaling global circulation models for the year 2070. The results showed small changes in the groundwater balance and water levels. Relative to the future baseline scenario, groundwater elevations at almost all wells in almost all stress periods changed by less than 2 feet. Overall, the analysis concludes that, while climate change is expected to bring higher evapotranspiration rates and more intense drought and storm cycles, the net effect on sustainable yield in the Warner Basin is expected to be small into the foreseeable future.

An estimate of groundwater yield available to WSRR was obtained by defining a subarea of the Basin around WSRR and calculating the water balance within the subarea with existing amounts of WSRR pumping and hypothetical increases in pumping. Increases in pumping were distributed among existing WSRR wells and two additional hypothetical WSRR wells in such a way that drawdown was relatively uniform throughout the WSRR area. When pumping was increased from the baseline rate of 405 AFY to 1,100 AFY, water level declines during droughts were greater by as much as 40 feet at some WSRR wells but recovered rapidly during wet periods. The increase in pumping by WSRR decreased yield in the rest of the Basin by an equal amount via reductions in groundwater outflow from the WSRR area and changes in stream flow gains and losses.

A simulation in which District pumping was increased by 20 percent over historical amounts during 1953-1995 lowered the minimum water levels (in 1977) by 60 feet in the main District well field, decreasing to 10 feet at distant District wells. Recovery was complete by 1986 in the main well field but not until 1998 in some areas.

District yield could also be increased by maintaining a lower average elevation of Lake Henshaw. A simulation in which the average elevation of Lake Henshaw was decreased by 7 feet increased yield by approximately 2,750 AFY from reduced evaporation losses and by an additional 260 AFY from reduced spill volumes. The District's ability to maintain Lake Henshaw at these lower levels, however, will depend on the wellfield's capacity to increase production during the summer delivery season and possible reoperation of water treatment and delivery infrastructure downstream of the lake.

Introduction

Purpose of Model

Vista Irrigation District (District) is the primary groundwater user in Warner Valley Groundwater Basin (Basin), located in the interior mountain ranges of San Diego County. There are a few other groundwater users in the Basin, including Warner Springs Ranch Resort (WSRR). WSRR is planning to expand, which will increase its water demand; this raises issues about the sustainable yield of the Basin. In addition, the District is concerned about water supply impacts of climate change and is interested in improving its groundwater operations in the Basin.

A numerical groundwater model of the Basin was developed to address several water management questions:

- What would be the impact of increased WSRR pumping on groundwater yield available to the District?
- What is the sustainable yield of the WSRR area?
- Could the District's well field be reconfigured or the timing and location of District pumping be modified to increase groundwater yield available to the District during droughts?
- How connected is Lake Henshaw to the groundwater flow system in the Basin?
- What effects will climate change have on yield available to the District?

The answers to these questions hinge on the interactions of numerous interconnected hydrologic processes, each of which varies in space and time. A numerical groundwater flow model is the best available tool for quantitatively simulating those processes and integrating their effects.

Description of Model Area

The Basin is located in the Peninsular Ranges Geomorphic Province of north-central San Diego County (**Figure 1**). It is a structural basin formed by block faulting between the Elsinore Fault Zone, which forms the southwestern boundary of the Basin and the parallel San Jacinto Fault Zone 10 miles east of the Basin. The Basin is filled with unconsolidated materials derived from erosion of granitic rocks in the mountains surrounding the Basin. The Basin surface is relatively flat and ranges in elevation from about 2,650 feet above sea level at the foot of Henshaw Dam to about 3,200 feet along the eastern and southeastern edges of the valley. Mountains rise steeply around most of the Basin perimeter. Prominent peaks include Mt. Palomar (elevation 6,135 feet) near the northwest corner of the Basin and Hot Springs Mountain (elevation 6,520 feet) near the eastern edge (**Figure 1**).

The Basin is located in the upper watershed of the San Luis Rey River. Henshaw Dam was constructed in 1923 and impounds the river where it leaves the western edge of the Basin. The reservoir impounded by the dam (Lake Henshaw) is currently operated over an elevation range of 2,650-2,690 feet, with a current maximum capacity of 51,700 acre-feet (AF). The dam, lake

and most of the valley floor are owned by the District, which conjunctively operates the lake and groundwater basin for water supply purposes. Water is released from the dam to supply customers of the District, the City of Escondido (City), and the Rincon Band of Mission Indians. Major creeks that drain the surrounding mountains and flow into the Basin are (clockwise from the northwest): West Fork San Luis Rey River, Cañada Aguanga, San Luis Rey River, Ward Creek, Agua Caliente Creek, Cañada Agua Caliente, Cañada Verde, San Ysidro Creek, Buena Vista Creek, Matagual Creek, Carrizo Creek and Carrista Creek (**Figure 1**).

The dominant land use in Warner Valley is non-irrigated range land for cattle. Small recreational resorts are located at Lake Henshaw and Warner Springs, and a small tract of roughly 100 residences is served by Los Tules Mutual Water Company (LTMWC) next to Warner Springs along the eastern margin of the Basin. WSRR was initially developed decades ago around Warner Hot Spring and presently consists of a number of guest cabins, a golf course and clubhouse. The locations of WSRR and LTMWC are shown in **Figure 2**. Vegetation consists primarily of annual grasses on the valley floor and xeric shrubs on hillslopes in the tributary watershed areas. Published vegetation maps disagree in detail, but most show patches of more mesic vegetation including riparian scrub (willows), wet meadows, and riverine and palustrine (non-flowing) wetlands with various durations of seasonal inundation along some of the waterways (San Diego County, 2017; The Nature Conservancy, 2018). The degree to which these areas of more mesic vegetation are supported by shallow groundwater appears to be variable, based on a comparison of groundwater levels and the vegetation patterns. For example, groundwater levels are commonly at or near the ground surface along Buena Vista Creek where it crosses the Warner Ranch fault and nearby parallel unnamed fault, and also at locations farther north along the Agua Tibia South fault. In contrast, water levels are rarely less than 15 feet below the ground surface in wells along both forks of San Luis Rey River and the lower ends of Ward Canyon and Agua Caliente Creeks, which suggests that the fairly extensive patches of mesic vegetation reported for those areas are dependent more on rain and surface flows than on groundwater.

The climate is semiarid with rainfall ranging from 16-20 inches per year (in/yr) on the valley floor to over 30 in/yr on Palomar Mountain. Typically, about 80 percent of annual precipitation falls during November-March. Daily maximum temperatures range from an average of 60 degrees in December-February to 92 degrees in July-August.

After the District acquired Lake Henshaw and most of the land in the Basin in 1946, it installed a number of wells in the early 1950s. During droughts, the District pumps groundwater from the wells and conveys it to Lake Henshaw by ditches (some lined, some unlined). This conjunctive use strategy increases the overall yield of water for downstream users because groundwater storage as well as lake storage can be accessed during droughts and refilled during wet years. Currently, the District operates 28 wells around the Basin for this purpose. The locations of wells in the Basin are shown in **Figure 2**. Lake Henshaw is typically drained to 5-10 percent of its 51,700 AF capacity in the Fall. This leaves a substantial amount of vacant storage capacity that can capture and temporarily retain high inflows in wet years. Consequently, unregulated spills of water from Lake Henshaw are rare and occur only in very wet years. Since the dam spillway was lowered in 1981 due to seismic safety concerns, the dam has only spilled twice, in

1983 and 1993. The dam did not spill in the period between its construction in 1922 and when it was lowered in 1981.

Hydrogeologic Conceptual Model

The most detailed hydrogeologic studies of the Basin were completed in the 1960s. Scheliga (1963) completed substantial original geologic mapping and interpretation of borehole logs. He documented bed offsets of up to a few hundred feet and localized rotational tilting of beds associated with faults within the Basin. James M. Montgomery Consulting Engineers, Inc. (JMM) completed a study of the Basin for the District in 1969 that focused less on geology and more on groundwater. However, the study shared Scheliga's general conceptualization of the Basin as a fault-segmented structural depression filled with unconsolidated, irregularly-layered silts and clays derived from weathering of the surrounding mountains.

Basin Boundaries

Four previous delineations of the Basin boundary were found to have numerous discrepancies ranging from minor to major. The four delineations were from the California Department of Water Resources (DWR), San Diego County, Scheliga (1963) and JMM (1969). A detailed comparison and evaluation of the boundaries is presented in **Appendix A**. For this study, a new boundary delineation was created that essentially combined the Scheliga and JMM boundaries, resolving their minor differences. The boundary represents the contact between unconsolidated basin fill materials (alluvium, Pauba Formation and Temecula Arkose) with consolidated rocks (Lakeview Tonalite, Bonsall Tonalite and Mesozoic rocks). It includes the Lake Henshaw area between Monkey Hill Horst and the Elsinore Fault Zone. The new boundary is used in the map figures in this report (see **Figure 2**, for example).

Basin Fill Materials, Layering and Faults

Previous Studies

The Temecula Arkose is the principal geologic formation in the Basin. It consists of poorly sorted silts and fine to coarse sands with less common clay or gravel lenses. It rests unconformably on granitic basement rocks and has been logged to a depth of 900 feet in one borehole (VID Well 80). Scheliga (1963) and JMM (1969) did not note any extensive confining layers or distinct stratigraphic depth intervals within the arkose. They reported that it contains weakly-defined layers typically several feet thick. No individual layer appeared to be laterally very extensive, but collectively the layers produced increasing confinement of groundwater with depth. In the 1950s, numerous deep wells had water levels above the ground surface, indicating confined groundwater conditions at the depth of the well screen (JMM, 1969).

Two relatively thin surficial deposits locally overlie the Temecula Arkose. These are the gravelly Pauba Formation and alluvium associated with geologically recent stream deposition. These formations are thin and mostly above the water table. They play a role in groundwater recharge but not in groundwater flow and storage. **Figure 3** shows the surficial outcrops of bedrock, Temecula Arkose, Pauba Formation, and alluvium. It also shows the locations of faults mapped by JMM (1969).

Bookman-Edmonston (2002) concluded that four depth zones could be identified within the Basin based on changes in lithology and well specific capacity. The top-most "perched water"

zone is up to 70 feet thick, separated from the main aquifer zone by layers of clay or alluvium and in some locations containing groundwater at an elevation higher than in the main aquifer. The second layer is termed the “upper” or “main” aquifer, which reportedly consists of fining-upward sand-gravel sequences 140-260 feet thick. An aquiclude 20-110 feet thick consisting primarily of clays separates the “upper” and “middle” aquifer. The “middle” aquifer consists of 120-180 feet of sands interbedded with silts and clays and is not present in all parts of the Basin. In the deepest part of the Basin (between the Agua Tibia North and South Faults and north of the Warner Ranch Fault), the “middle” aquifer is underlain by another confining layer and a “lower” aquifer consisting of up to 200 feet of consolidated sandstone. As discussed below, this conceptualization was not supported by borehole and geophysical logs reviewed for this study.

Scheliga (1963) and JMM (1969) mapped numerous faults within the Basin. The ones that those reports suggested might influence groundwater flow are included in the geologic map (**Figure 3**).

The deepest part of the Basin is between the Agua Tibia North and South Faults near the Warner Ranch Fault, where unconsolidated materials were logged to a depth of nearly 1,000 feet at VID Wells 80 and 81 (Scheliga, 1963). Elsewhere, the typical depth to bedrock is about 500 feet in the central part of the Basin and more commonly less than 300 feet in peripheral areas (JMM, 1969).

Stratigraphic Analysis for this Study

Although Scheliga (1963) and JMM (1969) discussed layering of Basin materials evident in borehole logs, only Scheliga presented geologic cross sections. Those sections showed only geologic formations, not individual textural layers. The same was true of cross sections in a hydrogeologic study of the WSRR area (Leighton & Associates, Inc., 1981). The Bookman-Edmonston study (2002) showed only a stratigraphic column diagram with no cross sections or well logs.

New texture-based cross sections were developed for this study to investigate textural patterns in Basin fill materials directly from well completion reports. In addition to the greater level of detail shown in the sections, the investigation took advantage of information from wells drilled during the decades since the previous studies.

Cross Sections

Seven hydrogeologic cross sections were constructed to characterize the thickness and distribution of alluvial aquifer sediments and to delineate the hydrostratigraphy within the Basin. The locations and orientations of the cross sections are shown on **Figure 4**.

The goals of constructing cross sections were to identify Basin-wide and local hydrogeologic structures that should be represented in the numerical groundwater model. Construction of the cross sections focused on conditions relevant to hydrostratigraphic layering in the Basin. The assessment was designed to use and combine existing information in the ArcHydro Groundwater (Strassberg et al., 2011) data format that supports application of geographic

evaluation tools within a Geographic Information System (GIS) platform. The information assessed in this evaluation included:

- Surficial geology,
- Faulting,
- Lithologic and geophysical well and borehole logs,
- Well construction logs,
- Bedrock surface elevations, and
- Previously completed local hydrogeologic conceptualizations.

This information was collected and translated into a unified GIS compatible database structure for cross section construction and geographic evaluation. This approach allows any hydrostratigraphic structures relevant to groundwater flow in the Basin to be easily translated from GIS for use in other formats.

Available Data and Information

Existing datasets and information were collected from all available sources. These sources included the following:

- Surficial geology digitized to GIS format (Scheliga, 1963 and JMM, 1969).
- Fault locations and orientations (Scheliga, 1963 and JMM, 1969).
- Fault subsurface expressions (Scheliga, 1963 and JMM, 1969).
- Bedrock elevations (JMM, 1969)
- Locations, lithology, and well construction information for wells and boreholes in the Basin from District, WSRR, and DWR records.
- National Elevation Dataset (NED) ground surface digital elevation model data for San Diego County (USGS, 2018).

These data and information sources resulted in a dataset of 419 locatable wells and boreholes within and near the Basin. Of these, lithologic records are available for 45 wells and boreholes and construction records are available for 46 wells (**Figure 4**). These location, lithologic, and well construction records were combined into a unified dataset covering the Basin. The unified dataset is composed of a series of related tables in a geodatabase that follows the data storage conventions of ArcHydro Groundwater. Construction of the unified database required combination of well location, lithologic, and well construction data from multiple data sources. These data sources sometimes contained different information types. At each stage of the database construction process, care was taken to include all data from each data source. In addition, many records were included in multiple data sources, and often the records from two or more data sources had differences in locations or information for wells. Duplicate well locations or records were combined into single records preserving all information from each individual data source.

Geophysical logs from wells and boreholes in the Basin were identified from all available sources. The available geophysical logs were reviewed for use in cross section development. This data collection and review process resulted in the identification of 17 geophysical logs from

wells and boreholes within the Basin. The short-normal resistivity values from these geophysical logs were digitized for inclusion in the ArcHydro Groundwater database. Digitization was limited to short-normal resistivity because it was the only geophysical data type present in all available geophysical logs.

There are multiple faults in the Basin, as discussed above. To portray these faults on cross sections, it was necessary to estimate orientations and approximate dip angles. Scheliga (1963) includes representation of the subsurface expressions of local faults within the Basin, and apparent fault dip angles were estimated from Scheliga and converted to true dip angles for each fault/cross section intersection (Davis et al., 1996).

Cross Section Construction

Seven cross section transect locations were chosen based on available data to provide lithologic coverage throughout the Basin. **Figure 4** illustrates well locations with available geophysical, lithologic, and construction information throughout the Basin and shows the selected cross section locations and orientations. These sections are designated as A-A' through G-G', as indicated on **Figure 4**. These seven cross sections cover and extend slightly beyond the Basin.

The datasets incorporated into the database discussed above were used to populate the cross sections for use in hydrostratigraphic correlation. The ArcHydro Groundwater extension to ESRI's ArcGIS Desktop software was used to convert two-dimensional map layers (surficial geology, faults, lithologic, construction, and geophysical records, and elevation surfaces) to two-dimensional cross sections. The wells with lithologic, construction, and geophysical information in the vicinity of the sections are shown on **Figure 4**. Each cross section includes information from wells and boreholes within 1,300 feet of the section line.

Geophysical and lithologic data were used to interpret low permeability units (silts and clays) and aquifer units (sands and gravels) in each cross section. Where geophysical and lithologic logs disagreed, the information from geophysical logs was used. In locations where multiple geophysical or lithologic logs were present on a cross section, preference was given to the closest logs. Mapped surface geology (JMM, 1969) and subsurface conditions around the faults (Scheliga, 1963) were used to interpret the locations and relationships of older materials to one another and to local alluvium. Bedrock elevations on each cross section were plotted from the bedrock contours developed by JMM (1969) shown on **Figure 5**, with local modifications based on well and borehole log data.

The resulting cross sections are shown individually with lithology, faulting, bedrock, and well locations on **Figures 6 through 12**. Areas with no well or lithologic data in the alluvial Basin are left white and the transition is indicated by a dashed line.

Hydrostratigraphic Evaluation

In general, the cross sections support and agree with the previous conceptual model described above. Alluvial thickness is generally greatest in the central and west-central portions of the Basin, and those areas have a high percentage of coarse grained material (sands and gravels) throughout. Additional discussion of observations from the cross sections is presented below.

The cross sections generally show relatively high bedrock elevations and small Basin thickness in the eastern part of the Basin (**Figures 6 and 7**). An exception is the area under Lake Henshaw and west of Monkey Hill, where bedrock is also at a shallow depth. The lowest bedrock elevations in the Basin are projected to be in the south-central part of the Basin, near the intersection of cross sections B-B' and F-F'. The total alluvial thickness in this area is near 1,000 feet. This thick portion of the Basin extends throughout the structural block between the Agua Tibia North and Agua Tibia South Faults, as shown on cross section F-F' (**Figure 11**).

The faults in the Basin appear to have caused vertical offset of bedrock, resulting in abrupt changes in alluvial thickness in some areas. The bedrock offsets shown on the cross sections are primarily based on the bedrock surface interpreted by JMM (1969), with local modifications based on well and borehole log data. Available data from existing wells and boreholes are insufficient to confirm whether some or all faults offset unconsolidated deposits in the Basin. However, groundwater elevation data discussed later indicates that at least some fault segments offset alluvium and create resistance to groundwater flow.

The cross sections show heterogeneous conditions in the subsurface unconsolidated deposits, with significant variability in the presence, thickness, and continuity of fine grained (silt and clay) units. This is consistent with the conceptual model and with a depositional environment characterized by episodic alluvial, fluvial, and lacustrine processes.

The lithologic and geophysical logs reviewed for this study do not support some of the detailed stratigraphic interpretation proposed in some previous studies, such as multiple upward-fining depositional sequences and distinct upper, middle and lower aquifer units separated by extensive fine-grained layers (Bookman-Edmonston, 2002).

Conceptualization of the Hydrologic System

The hydrologic system in the Basin can be conceptualized as having three components: tributary watersheds, the groundwater Basin and Lake Henshaw. Rainfall in the tributary watersheds produces surface and subsurface outflows to the groundwater Basin. Surface outflows include direct runoff during storm events and base flow in tributary streams. The latter is derived from infiltration not consumed by plants that flows via the subsurface to nearby creek channels. Some of the percolation below the root zone flows via the subsurface directly to the groundwater Basin. Within the Basin, recharge occurs from deep percolation of rainfall below the root zone, percolation from streams during flow events, and subsurface inflow from the tributary watersheds. Outflows include pumping from wells, seepage into creek channels, and seepage into Lake Henshaw. Lake Henshaw receives inflow from surface runoff that did not percolate from creek channels as it crossed the Basin, from precipitation on the lake surface, from groundwater pumped into the lake, and from groundwater seepage through the lake bed. Outflows are evaporation, water supply releases at the dam, spills at the dam, and seepage from the lake into the groundwater system.

During sequences of dry years, the District pumps water from its well field and conveys it to Lake Henshaw, where it is released to serve downstream water users. Reservoir and groundwater storage decline during those periods. When wet weather returns, reservoir storage and groundwater storage both recover.

Numerical Model Development

A numerical groundwater flow model was developed to answer the hydrogeologic and water-supply questions stated above in the “Introduction” section. The model and its pre-processors together simulate all three components of the hydrologic system: tributary watersheds, groundwater Basin, and Lake Henshaw.

Software Used for Modeling

Hydrologic processes in the tributary watersheds were simulated by a rainfall-runoff-recharge model developed by Todd Groundwater that is non-proprietary and publicly available. It is a Fortran computer program that simulates numerous hydrologic processes on a daily time step, as described in the following sections. Groundwater flow in the Basin, stream flow and Lake Henshaw were simulated using the public-domain MODFLOW 2005 software developed by USGS. The PCG2 solver was selected because of its reliability and speed. However, it simulates only saturated flow and permanently disables model cells that go dry during a simulation. Some of the pre- and post-processing of model inputs and outputs was managed via Groundwater Vistas v.6, which is a commonly used modeling platform commercially available from Environmental Simulations, Inc. Microsoft Excel workbooks and Fortran utility programs created by Todd Groundwater were also used to prepare, manage and display data. ArcGIS software from ESRI was used to manage and display data involving geographic coordinates.

Model Grid and Active Flow Area

A plan view of the MODFLOW 2005 model grid is shown in **Figure 13**. The grid consists of three layers, with 48 rows and 72 columns of uniform cells 1,000 x 1,000 feet in size. Of the total number of cells (10,368), 2,333 cells are active. The remaining cells are in bedrock and are inactive. The grid is rotated 43 degrees clockwise from north-south about the lower-left grid corner, which is located at X = 6,384,700 feet and Y = 2,044,800 feet, California State Plane Zone VI coordinates, North American Datum of 1983 (NAD83). The vertical datum for elevations is North American Vertical Datum of 1988 (NAVD88).

Model Layers

Model layering is not tied to geologic units because the hydrogeologic analysis presented in the preceding section did not reveal consistent layering. Instead, the layers were used to represent variable Basin thickness and to enable testing of the three-layer conceptual model proposed by Bookman-Edmonston (2002). The top elevation of layer 1 is the ground surface elevation obtained digitally from the NED. The bottom of the top model layer (layer 1) is a contoured surface approximately equal to the minimum historical groundwater elevations. This prevented cells from going dry during model calibration. The bottom of layer 2 was set to 200 feet below the bottom of layer 1 or to the bedrock surface, whichever was shallower, and layer 3 included any remaining Basin thickness. In addition, a minimum layer thickness of 20 feet was applied to all of the layers.

Layer 1 is active across the full area of the alluvial deposits in the groundwater Basin. Several “islands” of exposed bedrock in the interior of the Basin are inactive. Layers 2 and 3 have

progressively smaller footprints corresponding to the extent of deeper deposits, as shown in **Figure 14**.

Aquifer Characteristics

The ability of Basin materials to store and transmit water are quantitatively represented by horizontal and vertical hydraulic conductivity, specific storativity, and specific yield. The values for each of these parameters were estimated by model calibration to measured historical water levels. The calibration procedure is described in greater detail below under “Model Calibration”, and it resulted in the zonal pattern of aquifer characteristics shown in **Figure 15**. Identical zones were used for all four parameters. Horizontal hydraulic conductivity (K_h) ranged from 1 to 10 feet per day (ft/d) in the main part of the Basin and 20 ft/d in the Lake Henshaw area. Specific capacities of wells in the Basin tested in the 1950s were 2.9-4.3 gallons per minute per foot (gpm/ft) of drawdown. Aquifer transmissivity equals K_h multiplied by the saturated thickness of the aquifer. It can be estimated from specific capacity using an empirical rule of thumb that simply multiplies specific capacity by 270 to obtain transmissivity in feet-squared per day (McClymonds and Franke, 1972). The average screen length of 78 wells for which construction information was available is 160 feet. Multiplying the specific capacities by 270 and dividing by 160 feet produces hydraulic conductivity estimates in the range of 5-7 ft/d. Thus, the calibrated values are similar to the estimates obtained from specific capacity tests.

There are no data for vertical head (water-level) gradients within the Basin other than the observation that flowing wells were present prior to the 1950s (Scheliga, 1963). A vertical hydraulic conductivity value (K_v) of 1 ft/d was used throughout the Basin in all model layers, which produced small downward gradients between model layers where streams entered the Basin. Simulation results were not sensitive to the value of K_v , and at most locations water levels in all active model layers were essentially the same.

Simulation results were not sensitive to the value of specific storativity (S_0), and a typical value of 1×10^{-5} per foot was used throughout the Basin. The magnitudes of simulated multi-year water-level fluctuations were somewhat sensitive to the value of specific yield (S_y). A value of 0.10 was used throughout the main part of the Basin. A larger value (0.20) was used in the Lake Henshaw area to help moderate simulated fluctuations in lake level.

Lake Henshaw

The MODFLOW lake module enables the simulation of open bodies of water embedded in the groundwater flow system. This module was used to simulate Lake Henshaw, which occupied 71 cells in model layer 1, as shown in **Figure 16**. A lakebed 1 foot thick with a hydraulic conductivity of 5 ft/d was assumed, which was sufficiently high not to appreciably limit the flow of water into or out of the lake. Historical monthly operations data were used to specify net evaporation, releases and spills from the lake. Because lake area is constant in the model, net evaporation for each model stress period was adjusted to reflect the actual lake area at that time and converted to an equivalent rate over the lake area in the model. Pumping of groundwater into the lake, water supply releases from Henshaw Dam and spills were all obtained from historical operations data for the 1953-2016 period of record provided by the

District. Annual subtotals of the Lake Henshaw water balance are shown in **Figure 17**. The importance of exceptionally wet years is obvious in the graph. The five wettest years (1969, 1978, 1980, 1983 and 1993) delivered 42 percent of all inflows during water years 1939-2017. The graph also shows how pumping into the lake and releases from the lake are managed to maintain a relatively constant lake storage volume between the wet years. Spill information was only obtained for the 1983 and 1993 wet years. The large release volume in 1980 reflects high runoff in conjunction with State storage elevation limitations imposed due to concerns over the seismic safety of the dam. Those concerns were addressed in the seismic retrofit and spillway lowering project completed in 1981.

The operations data do not include seepage across the lake bed but do include an estimate of monthly surface water inflow estimated as the residual in the reservoir water balance. In the groundwater model, the MODFLOW stream module provided the surface inflows and the lake module estimated the lake bed fluxes. Considerable effort was expended to calibrate rainfall, runoff, recharge and stream flow parameters to obtain a reasonable match between the simulated and measured lake hydrograph. Small changes in those parameters often produced very large and unrealistic rising or declining trends in simulated lake levels over the 78-year simulation period.

Simulation Period and Time Increments

To address sustainable yield questions, the analysis period should include the most severe drought for which yield needs to be reliable. In the Basin, the prolonged dry conditions during water years 1945-1977 pose the greatest constraint on simulated yield. **Figure 18** shows the magnitude of that drought in terms of the cumulative departure of rainfall at Henshaw Dam (upper plot) and also as the time series of simulated groundwater storage from a previous operations model (Bookman-Edmonston, 2002).

The groundwater model is a transient model that simulates water years 1939-2016. This 78-year period includes several years prior to the design drought—to allow any errors associated with incorrectly specified initial conditions to dissipate before the drought—and continues through 2016, which was the most recent year for which complete model input data were available.

The simulation period is divided into increments (i.e., stress periods) of variable duration. Variable stress periods were employed because stream flow was expected to be a major source of recharge, and flow fluctuates dramatically over hours to days in this region. Stream percolation is not a linear function of flow. Consequently, if flows are averaged over long stress periods the simulated amount of percolation would be incorrect. For example, the amount of stream percolation that would result from one day of flow at 600 cubic feet per second (cfs) followed by 29 days of no flow would be smaller than from 30 days of flow at 20 cfs, assuming a maximum channel percolation capacity of 200 cfs.

Stress periods were selected by means of a time series filtering algorithm that processes a continuous series of daily flows and marks a new stress period whenever flow changes by a certain magnitude or percentage. In addition, minimum and maximum stress period durations can be imposed, as well as a new stress period at the start of each water year to facilitate

subtotaling of simulation results into annual values. For this study, a continuous time series of daily stream flow during 1939-2016 could not easily be constructed for any of the local waterways because of the limited periods of record for local stream gages. Instead, precipitation was used as a surrogate time series. With minimum and maximum durations of 3 and 33 days, and appropriate thresholds for rainfall events, a set of 1,065 stress periods was selected for the model.

Initial Water Levels

Initial groundwater levels for October 1938 were selected by a combination of historical data and iterative adjustments using the groundwater model. The oldest available water-level data are for spring 1951 (Scheliga, 1963). The spring 1951 water levels were copied into the model as initial conditions for October 1938, and simulated hydrographs were then examined for rapid rises or declines in the first few years of the simulation. Such changes indicate that the assumed initial conditions were not consistent with the aquifer characteristics and groundwater inflows / outflows at the start of the simulation. Simulated water levels after the first two years of the simulation were “recycled” back as initial conditions in a new simulation until the simulated hydrographs: 1) exhibited smooth behavior during the first few years of the simulation, and 2) intercepted measured water-level hydrographs (beginning in the early 1950s) at approximately the correct elevation.

Groundwater Inflows

Dispersed Recharge

Groundwater recharge from rainfall is distributed widely across the Basin and the tributary watersheds. It is affected by soil infiltration characteristics, available water capacity of the root zone, and plant evapotranspiration (ET). Rainfall recharge involves nonlinear relationships among these variables, which means that the resulting recharge cannot be accurately estimated on an annual or even monthly basis. Instead, the processes were simulated concurrently using a rainfall-runoff-recharge model with daily time steps, and the estimated daily recharge amounts were subtotaled to stress periods for input to the groundwater model. The rainfall-runoff-recharge model simulates precipitation, interception, direct runoff (from pervious and impervious surfaces), infiltration, soil moisture storage in the root zone, ET, irrigation, leaks from water and sewer pipes, and the attenuating effects of shallow groundwater storage on recharge to deeper aquifers. Although the model has the capability to simulate agricultural and urban hydrology, those are small in this study area. The processes that are significant in the Basin and watershed are illustrated schematically in **Figure 19**.

The variables that influence dispersed recharge are not uniform over the Basin and watershed. Accordingly, recharge simulation was estimated separately for subareas delineated to have relatively uniform rainfall, reference evapotranspiration (ET_0), soil depth and available water capacity, vegetation type, and depth to bedrock. Those subareas were further subdivided along surface drainage boundaries and the groundwater Basin boundary to obtain a total of 165 recharge zones. A map of the zones is shown in **Figure 20**, color-coded to show simulated average annual dispersed recharge. Rainfall is higher in the tributary watershed areas than in

the Basin, but simulated recharge is lower because some of the deep percolation beneath the root zone in the watersheds discharges as base flow in creeks rather than continuing downward to recharge the deeper groundwater system.

The rainfall-runoff-recharge model is complex. Documentation of its governing equations, assumptions, input data sets and calibrated outputs can be found in **Appendix B**. The distribution of rainfall across the watershed significantly influences the overall mass balance of the rainfall-runoff-recharge model, the groundwater model and Lake Henshaw. Four different isohyetal (rainfall contour) maps were obtained and found to be quite different. **Appendix C** compares those data sets and the basis for selecting one of them to be used in the model.

Dispersed recharge from rainfall and irrigation return flow within the Basin ranged from 60 to 27,020 acre-feet per year (AFY) during water years 1939-2016 and averaged 2,770 AFY.

Percolation from Streams

Twenty-two tributary watersheds have creeks of sufficient size to potentially supply significant amounts of recharge along the channel reaches that flow across the groundwater Basin. They merge at various confluences such that eight channels reach Lake Henshaw. The network of stream channel segments included in the groundwater model is shown in **Figure 21**. Each segment is divided into reaches, with one reach for each model cell crossed by the segment. In total, there are 37 segments and 332 reaches. Inflow is specified for each stress period at the upstream end of segments that originate at the Basin boundary. The MODFLOW stream flow routing module calculates flow gains and losses along each segment based on the difference in elevation between the creek water surface and layer 1 groundwater, and on channel length, width and bed hydraulic conductivity. Outflow from each reach becomes the inflow to the next downstream reach. For segments that originate within the Basin, inflow equals outflow from upstream segments plus local valley-floor runoff simulated by the rainfall-runoff-recharge model. This approach allows MODFLOW to simulate stream flow, groundwater-surface water exchange and groundwater flow consistently, conserving mass for both groundwater and surface water.

In each stream reach, water depth and width are calculated as functions of stream flow using the Manning Equation and the channel cross section geometry. Surveyed cross section data were not available, but the larger channels tend to be broad, sandy washes. For modeling purposes, hypothetical cross sections for small and large channels were developed, as shown in **Figure 22**, and segments were assigned one geometry or the other based on their location in the channel network and appearance in aerial photographs. All stream segments were assigned a roughness coefficient of 0.025 within the channel and 0.032 in overbank areas, which reflect sandy channel material and grass or weed vegetation in overbank areas (Barnes, 1967).

The stream bed elevation at each reach was estimated from Google Earth™ imagery. A stream bed thickness of 3 feet was assumed, and stream bed hydraulic conductivity corresponding to that thickness was estimated as a calibration variable. Simulated inflow to Lake Henshaw was somewhat sensitive to stream channel percolation, and a final calibrated hydraulic conductivity of 4.5 ft/d was selected. When the groundwater level in the model cell where a stream reach is located is higher than the stream bed elevation, flow of water between the aquifer and stream

is calculated using the Darcy Equation for saturated groundwater flow. Flow can be into or out of the stream, depending on whether the groundwater level is higher or lower than the level of the creek surface. MODFLOW solves the coupled equations for stream stage and groundwater level iteratively. When the groundwater level is below the elevation of the creek bed, percolation out of the creek channel is at a constant rate that assumes a unit hydraulic gradient.

Annual percolation from stream channels ranged from 1,020 to 56,800 AFY and averaged 9,090 AFY during 1939-2016.

Percolation from Lake Henshaw

Lake Henshaw is simulated using the MODFLOW lake module. Seventy-three cells in layer 1 are treated as open water rather than aquifer. The model tracks the lake water balance and calculates the change in water level at the end of each stress period by spreading the change in storage uniformly among the cells. The lake water balance includes stream inflows from the stream segments that terminate at the lake, groundwater pumped into the lake from District wells, precipitation, evaporation, water supply releases from the lake and spills. The lake area is constant in the model but variable in reality. The combined area of the lake cells is 1,679 acres, which corresponds to a moderately full condition (elevation 2,678 feet and storage of 27,916 AF). For input to the model, one-dimensional precipitation and evaporation were scaled to be proportional to lake surface area based on the simulated elevation in the preceding stress period. Reservoir spill volumes in 1983 and 1993 were manually entered as withdrawals from Lake Henshaw.

The groundwater model also calculates flows between the lake and aquifer, across the lake bed. Like the stream percolation calculations, the flow is calculated by the Darcy Equation using the water-level difference between the lake and adjacent aquifer cells, the lake bed area and lake bed conductance. The lake bed is assumed to be 1 foot thick and have a hydraulic conductivity of 5 ft/d, which is only slightly less than in the surrounding aquifer cells. The direction of flow was almost always from the aquifer into the lake. However, percolation out of the lake occurred at certain times and locations. Annual percolation ranged from 0 to 1,460 AFY and averaged 160 AFY during the simulation period.

Subsurface Inflow

Subsurface inflow through weathered and fractured bedrock from tributary watersheds into the Basin equals the amount of deep recharge in those watersheds as simulated by the rainfall-runoff-recharge model. To account for attenuation of recharge peaks as water moves through the bedrock, a smoothing function is applied so that current-year subsurface inflow equals a weighted average of the current and prior six years of recharge in the watershed, with smaller weights for each progressively older year. The raw and smoothed time series of total bedrock inflow to the Basin are shown in **Figure 23**. After smoothing, estimated annual subsurface inflow ranged from 270 to 16,650 AFY during water years 1939-2016 and averaged 4,140 AFY.

Subsurface inflow from each tributary watershed is distributed among active model cells along the boundary between the watershed and Basin. A subset of the boundary cells is assigned

inflow, with a greater density of inflow cells near creek valleys, where inflow is likely higher (see **Figure 16**).

Minor Inflows

The model does not include return flows from seepage along District conveyance canals or wastewater percolation at WSRR or LTMWC. Over the course of long droughts, canal percolation returns to the groundwater system and would contribute to groundwater outflow to streams or Lake Henshaw. It is an internal flux that would not materially change the estimate of groundwater yield available to the District. Wastewater percolation at WSRR and LTMWC is negligibly small in the context of the Basin-wide water balance.

Groundwater Outflows

Groundwater Pumping

Groundwater pumping by three users, the District, WSRR, and LTMWC, is included in the model. The locations of active wells are shown in **Figure 24**, with symbol area proportional to average annual pumping during 1996-2016, which is a period representative of current land use conditions. The District has drilled numerous wells since 1950, of which only 20 have been used for production since 1996. In recent years, almost all WSRR pumping has been from four wells (WSRR-1, -4, -5 and -17), with three additional wells producing minor amounts (WSRR-6, -16 and -18). LTMWC has one active well and possibly a standby well.

Measured or estimated annual pumping by all three users during water years 1938-2016 is shown in **Figure 25**. For the District, there was no pumping until the well field was installed in the 1950s. Since then, there have been multi-year periods of relatively high pumping (8,000-18,000 AFY) during dry climatic conditions alternating with multi-year periods of relatively low pumping during sequences of normal to wet years. Average annual production during 1953-2016 was 7,805 AFY.

Metered production data for WSRR wells was available for about half the years since 1997 and not at all prior to that period. Well completion reports indicate that the first WSRR domestic well was drilled in 1950, and the second in 1964. For the model, it was assumed that domestic use ramped up from 5 to 20 AFY during 1950-1964 and remained at 20 AFY thereafter based on a brief verbal description of the resort's development history (Grand, 2017). The first golf course well was drilled in 1965, and the second in 1966. Leighton & Associates (1981) estimated an irrigation demand of 480 AFY for the golf course, but 1997-2009 reported WSRR pumping for the golf course averaged only 405 AFY. Reports were not available for 2010-2012, and reports for 2013-2016 showed that total water use had decreased to 220-280 AFY. For the model it was assumed that golf course irrigation was 405 AFY of applied water for all undocumented years during 1965-2012.

No data are available for LTMWC pumping. The first LTMWC well was drilled in 1960, and the second in 1969. Based on aerial photographs, the residential tract now includes approximately 91 large-lot single-family residences with negligible landscaping plus about 17 small multi-family residences. The lots were assumed to be developed gradually from 1960 to 1980. Water

use since then is estimated to equal 15.6 AFY, based on the following factors: 2.5 people per residence, 75 gallons per person per day for indoor use, 70 percent occupancy and no irrigation use. This amount of pumping is too small to be visible in the bar chart on **Figure 25**.

Seepage into Streams

Groundwater seepage into streams occurs whenever the simulated groundwater level at a stream cell is higher than the simulated water level in the stream. It is calculated dynamically during the model simulation by the stream flow routing module described above under “Percolation from Streams”. Examples of stream reaches that typically gained from groundwater discharge include the lower 3 miles of West Fork San Luis Rey River (2-5 cfs) and the 4 miles of San Luis Rey River above the confluence with the West Fork (2-4 cfs). Annual Basin-wide groundwater seepage into streams ranged from 656 to 18,910 AFY and averaged 4,110 AFY.

Seepage into Lakes

Groundwater seepage into Lake Henshaw was simulated using the lake module and the same governing equation as the calculations of seepage out of the lake described above. Subsurface flow into the lake greatly exceeded leakage out of the lake. It ranged from 1,710 to 11,100 AFY and averaged 4,410 AFY.

Water Balance Summary and Change in Storage

The individual inflows and outflows described above are displayed together as a stacked-bar chart of the annual water balances for water years 1939-2016 in **Figure 26**. Inflows are stacked as positive values extending above the X axis, and outflows are stacked as negative values below the axis. The chart shows the dramatic variation in recharge from rainfall and stream percolation from year to year and the importance of wet years in replenishing the Basin. For example, recharge from rainfall and streams in the six wettest years (1969, 1978, 1980, 1983, 1993 and 2005) accounted for 32 percent of all recharge from all sources for the entire 78-year simulation period.

The effect of District pumping is also apparent in the chart. The large, sustained District pumping rates during the 1950s—combined with dry climatic conditions—caused a large cumulative decrease in groundwater storage. Simulation results indicated that the pumping and low water levels during that period probably dried up many of the stream reaches that normally had perennial base flow. However, wetter conditions and reduced pumping during 1966-1969 replenished the storage depletion and reestablished stream base flow. The sequence of pumping, recharge and storage since 1969 exhibits a classic conjunctive use pattern, with four full cycles of storage depletion and replenishment. During sequences of wet years, pumping was reduced and recharge was high, resulting in large increases in storage. During droughts, all three variables were the opposite. The net cumulative increase in groundwater storage over the analysis period does not indicate that the Basin is out of balance. It is probably an artifact of underestimating initial groundwater levels for 1939.

Figure 27 shows pie charts of average annual Basin-wide inflows and outflows. Slightly more than half of Basin recharge is from stream percolation, with the remainder is split fairly evenly between bedrock inflow and rainfall recharge. These are the proportions in the calibrated model, but they are subject to some uncertainty. The groundwater hydrographs used for model calibration did not exhibit patterns that could be uniquely linked to one of the three major sources of recharge. Thus, from a water balance standpoint, the calibration is not unique. A different calibration with different proportions of recharge from rainfall, streams and bedrock could potentially produce equally good results.

Groundwater pumping accounts for nearly half of Basin outflows (43 percent), followed by outflow to streams (34 percent) and outflow to Lake Henshaw (23 percent). A small amount of the outflow to streams probably occurs at locations where some of it percolates back into the Basin farther downstream. Also, from a water supply standpoint, all stream outflow ultimately ends up in Lake Henshaw. Except for evaporation and infrequent spills from the lake, groundwater outflow to Lake Henshaw and to streams is also available for use, along with the well pumping.

Model Calibration

Calibration Approach and Objective

Model calibration is the process of adjusting model input data and parameters so that model output matches observed groundwater elevations and stream flow for a specified historical simulation period. Modifying the initial estimates of model inputs is justifiable because many inputs are imprecisely known or are valid only for selected locations and times. The calibration objective for the general model was to reasonably match measured historical water levels and stream base flow at gages within the Basin. This subjective criterion was deemed to be met when residuals exhibited no further spatial or temporal trends among groups of wells that could be attributed to a hydrologic process and corrected by changing the parameters or data associated with that process. That is, the remaining residuals were random, or were not diminished by adjustments to inputs, or those adjustments increased some residuals while diminishing others.

For individual well hydrographs, the calibration objective was to obtain a simulated hydrograph that matched the dominant trend of the measured water levels, which is the pattern represented by most of the data points. This includes the timing and magnitude of long-term (multi-year) water-level trends and the magnitude of seasonal water-level fluctuations. This objective emphasizes the central tendency of the data rather than minimization of outlier residuals. For many District well hydrographs, numerous data points appear to be influenced by recent pumping. True static water levels form a smooth line at the top of the data cluster, while pumping-affected data points plot in a cloud of points below that line. The model consistently matched static water levels much better than pumping-affected water levels, which is to be expected because simulated water levels are an average for the entire cell area and do not reflect highly localized drawdown in or near a pumping well.

Model calibrations generally are not unique. Often, two or more variables can trade off against each other to produce nearly identical simulated water levels. For example, increasing the estimate of a flow—such as pumping at a well or inflow from recharge—can often be balanced by an increase in hydraulic conductivity to obtain similar results. The calibration objective was to obtain one good calibration using realistic values of all data and parameters, but not to explore possible alternative calibrations.

The groundwater model and rainfall-runoff-recharge model were jointly calibrated by comparing simulated and measured stream flow at gage locations, groundwater levels at 56 District wells and 9 WSRR wells. Calibration to stream flow is discussed in **Appendix B**. Many older District wells have been replaced with new wells drilled close by, and water levels are measured in both wells. The replacement wells have the same number but with an “A” suffix and are the actively pumped wells. For those well pairs, water levels from the older well were used for calibration because they exhibited much smaller short-term fluctuations associated with pumping cycles.

Calibration Results

Figure 28 shows hydrographs of measured and simulated water levels at eight of the calibration wells that exhibit typical calibration patterns for their area. Hydrographs for all of the wells are presented in **Appendix D**. In the main District pumping region (see hydrographs for VID Wells 32 and 34) there are substantial multi-year water-level declines during periods of substantial District pumping. These are followed by rapid recovery over several years. The model correctly reproduced the timing and approximate magnitude of these fluctuations at all wells in this region. At many of those wells, however, simulated water levels were slightly high during the last 12 years of the simulation but more accurate in prior years. VID Well 79 is one of three District wells with significant amounts of pumping in the west-central part of the Basin. Simulated water levels closely track measured static water levels, particularly in the last 15 years of the simulation. VID Well 92 is one of four wells with little pumping in the southwest part of the Basin. This hydrograph exhibits fluctuations that are probably related to pumping at VID Wells 76, 78 and 79. VID Well 61 is one of three District wells at the northern corner of the Basin and is actively pumped. Simulated water levels closely match the observed static water levels but not the much lower pumping water levels, as expected. VID Well 55 is one of numerous little-used wells southeast of the main well field and between the Agua Tibia North and South Faults. It has a long record of measured water levels. Simulated water levels closely match measured water levels in the last 30 years of the simulation, but the model produced too little drawdown during the heavy pumping period in the 1950s and 1960s. VID Well 81 is south of Warner Ranch Fault and the parallel unnamed fault to the north. Water levels in several wells in that area (VID Wells 51, 80, 81, 82 and 83) rose to and remained near the ground surface beginning at various dates between 1983 and 1997. Obstruction of groundwater flow by the faults might have contributed to this shallow groundwater condition. The simulated hydrograph for WSRR Well 5 shows responses to stream recharge events along Cañada Verde because it is relatively shallow and located in a stream cell. Simulated water levels match measured static water levels reasonably closely.

Contours of simulated groundwater elevations in December 1977 are shown in **Figure 29**. In most locations, these were the lowest water levels during the calibration period. The general direction of groundwater flow is from the edges of the Basin toward Lake Henshaw. Even at these low elevations, groundwater flowed to the lake. In other words, the lake did not become a source of recharge supplying District wells in the western part of the Basin even at the end of the largest drought in the simulation period. A pumping trough is evident around the main District well field that captured groundwater flow from roughly the northern half of the Basin.

Some fault segments impeded groundwater flow, as indicated by closely-spaced contours. Only a few of the fault segments could be calibrated, which consisted of adjusting the hydraulic conductance across the fault plane. Along most segments there was insufficient well density to differentiate between a continuously sloping water-level surface (small fault effect) and a stair-step surface (large fault effect). The south end of the Agua Tibia South Fault needed a low conductance to raise simulated water levels on the upgradient (east) side to match measured water levels. In contrast, the north end of that fault—where it passes through the main District well field—appears to have little effect on groundwater flow. The south end of the Agua Tibia North Fault near WSRR Wells 1, 1A and 2 was assigned a very high conductance (that is, zero

effect on groundwater flow) in an attempt to lower simulated water levels at those wells. The eastern spur of the unnamed westernmost fault in the Basin was assigned a moderately low conductance to simulate a small offset in water levels between VID Well 76 and nearby VID Wells 78 and 79. No other fault segment conductances were adjusted during model calibration.

Some of the highest groundwater elevations during the simulation period occurred in March 1995, and contours of those elevations are shown in **Figure 30**. Water levels were 20-40 feet higher than in 1977 throughout much of the Basin and up to 80 feet higher between the Agua Tibia North and South Faults near Warner Ranch Fault. Regional flow patterns were generally the same as in 1977, with a few differences. District pumping was low in 1995, and consequently there was little localized water-level depression around the main well field. The water-level drop across the south end of the Agua Tibia South Fault was 80-100 feet greater than in 1977. West of that fault, water-level gradients sloped moderately toward Lake Henshaw, in contrast to the relatively flat water-level surface in 1977 that had developed during the 1945-1978 dry period.

The simulated Basin-wide increase in storage from 1977 to 1995 was 150,000 AF. Simulated Basin storage was at a minimum in 1965, at which time it was 70,000 AF lower than in 1977. Thus, the difference between maximum and minimum storage during the simulation was 220,000 AF.

Hydrographs of measured and simulated water elevation in Lake Henshaw during 1939-2016 are shown in **Figure 31**. The simulated hydrograph includes the major inflow events associated with large storms in the watershed, and the long-term trend in lake level is approximately correct. However, the simulated hydrograph dropped below the actual minimum lakebed elevation (2,649 feet) at various times. In practice, calibration of the simulated lake hydrograph proved to be very difficult. Small changes in rainfall-runoff parameters or stream channel percolation upstream of the lake often produced large upward or downward long-term trends in lake level. Reservoir releases and spills were fixed at the historical flows documented in reservoir operations data. They were not dynamically adjusted during the simulation to maintain target lake levels, as they would be under actual operation. The simulated hydrograph shown in the figure is much better than most of the simulated hydrographs generated during the calibration process.

Calibration Statistics

The accuracy of the model calibration is visually apparent in the hydrographs showing simulated and measured groundwater elevations (**Figure 28**). It can also be summarized using a statistical summary of model residuals, which equal the observed water level minus the simulated water level for each data point. For the statistics to be meaningful, water level measurements affected by recent pumping in the well need to be omitted, because the model does not simulate well hydraulics and localized drawdown in the immediate vicinity of wells. This was done in two steps. First, in cases where measurements were made from an active replacement well (indicated by a letter "A" following the well number) and from the nearby retired well that it replaced, only data from the retired well were used. Second, hydrographs were visually screened to omit outlying low measurements likely to reflect short-term

drawdown from recent pumping. These points could be identified with confidence when the effect was large, but not if the effect was small. Only distant outliers were removed. This left a total of 20,951 water-level measurements at 65 wells, mostly in the second half of the simulation period.

Figure 32 shows a scatterplot of the entire set of simulated versus measured water levels, along with the summary statistics. The model clearly has a high bias, meaning that on average simulated water levels were slightly higher than observed water levels (mean residual = - 22.51 feet). This bias likely results from including numerous observed data points that were influenced from recent pumping. A common rule of thumb is that model performance can be considered acceptable if the root-mean-squared residual is less than 10 percent of the total range of measured water levels (Environmental Simulations, Inc., 2011). For the Warner Basin model, the root-mean-squared residual is 8.2 percent, which meets the acceptability criterion.

Calibration Discussion

Lake Henshaw and the groundwater Basin together capture almost all runoff from the watershed upstream of Henshaw Dam. This imposed very tight mass balance constraints on the calibration. All rainfall not consumed by ET must be accounted for by changes in groundwater and reservoir storage, given that groundwater pumping and releases are known. Initial estimates of rainfall and ET produced large upward long-term trends in simulated lake level and insufficient decline in groundwater levels during droughts. Rainfall was adjusted downward slightly in tributary watersheds, ET_0 was adjusted upward, and root depth was increased in tributary watersheds despite shallow published soil depths. These adjustments succeeded in reproducing average annual stream flow in the West Fork San Luis Rey River and Agua Caliente Creek with reasonable accuracy. Additional adjustments to stream bed permeability within the Basin helped to further calibrate the Lake Henshaw elevation hydrograph. Given the discrepancies among published isohyetal maps described in **Appendix C**, adjustments of estimated rainfall are reasonable.

A reasonable calibration to measured water levels at wells in the Basin was achieved with K_h values of 1 to 20 ft/d. This is a very narrow range, given that K_h values of naturally occurring unconsolidated sediments can range over at least ten orders of magnitude (Freeze and Cherry, 1979). Decreasing K_h tends to steepen the regional water-level gradient, raising simulated water levels along the northern, eastern and southern margins of the Basin. However, it also lowers water levels near pumping wells by focusing drawdown within a smaller radius. For example, the small K_h zone of 1 ft/d surrounding WSRR Wells 1, 1A and 2 (**Figure 15**) was implemented simply to demonstrate this local drawdown effect and to lower simulated water levels at those wells. It is not hydrogeologically very realistic.

The final distribution of K_h is counterintuitive. Values near the main well field ("Group 1" wells of Bookman-Edmonston, 2002) are lower than in surrounding areas even though wells in that group have high specific capacities indicating high K_h and efficient wells. Conversely, a relatively high K_h of 20 ft/d was selected to produce a flat water level surface near VID Wells 90-93 even though those reportedly have relatively small specific capacities. The counterintuitive relationship between calibrated K_h values and well specific capacities could stem from

differences in what those variables represent. Calibrated K_h represents the bulk properties of the entire Basin thickness over broad areas, whereas well specific capacities reflect local aquifer conditions near the well screens and the construction of the well. It is also possible that the low calibrated K_h in the main well field area resulted from calibrating to water level measurements that included residual pumping effects. In reality, residual drawdown could be quite localized around each well. To match those water levels at the scale of model cells would require a small K_h value.

The calibration process indicated that some fault segments appear to definitely obstruct groundwater flow while others do not. In general, those patterns were the same as reported in previous investigations (JMM, 1969; Bookman-Edmonston, 2002). South of the bedrock outcrop near the middle of the Basin, the Agua Tibia South Fault appears to obstruct flow (see **Figures 2 and 29**). A small conductance value was needed to raise simulated hydrographs of wells on the upgradient (east) side of the fault (for example, VID Wells 48-51). In contrast, the effect of the fault north of the bedrock outcrop—where it crosses the main well field—appears to be negligibly small in hydrographs and contour maps (**Appendix D and Figure 29**). Simulated water levels in the three wells in the western part of WSRR (WSRR Wells 1, 1A and 2) were consistently too low in simulations during model calibration. These wells are upgradient of the Agua Tibia North Fault. In an attempt to lower the simulated water levels by removing any hydraulic backwater effect of the fault, that segment of the Agua Tibia North Fault was removed entirely from the model. That adjustment did not substantially improve results. It can be concluded, however, that if the fault impedes groundwater flow, its effect on the regional gradient appears to be small.

The unnamed fault parallel to and north of the Warner Ranch fault has a clear effect on groundwater levels. Measured water levels in VID Wells 80-83 on the south (upgradient) side of the fault all rose to the ground surface or nearby creek channel elevation for most of the period from 1993 onward. Nearby wells on the downgradient side (wells 50, 51 and 59) did not exhibit this strong pattern. The final fault segment that appeared to affect groundwater levels based on available data is the fault trace that passes between VID Well 76 and VID Wells 78 and 79. The small, consistent difference in water levels between the wells was successfully replicated by including a moderately small fault conductance. Other fault segments might impede groundwater flow, but measured groundwater levels are not available sufficiently close to the faults to detect the effect.

Sustainable Yield Analysis

The sustainable yield of a groundwater basin is similar to the concept of safe yield used by hydrogeologists in past decades. It can be defined as the maximum amount of groundwater pumping that can be sustained during a complete wet-dry climatic cycle without causing undesirable results. This definition does not assume that pumping is the same every year. In the Warner Valley Basin, the cumulative pumping during the dry-wet cycle is the limiting factor. Sustainable yield is not a fixed natural quantity in groundwater basins with head-dependent boundaries such as streams or land uses that affect recharge, such as irrigation or wastewater disposal. In basins with streams that are hydraulically connected to groundwater—as is the case in the Warner Valley Basin—increased pumping increases percolation from creeks or intercepts groundwater that would have discharged into creeks.

Warner Valley Basin is unlike most groundwater basins in that groundwater is managed so tightly with surface water. All natural groundwater discharge and nearly all groundwater pumping flow into Lake Henshaw, which also captures almost all surface runoff from the Basin and surrounding watershed. Releases from Lake Henshaw then supply water users downstream. For practical purposes, the yield of interest is the overall yield of this conjunctive-use system.

Because the system already captures watershed runoff so efficiently, the greatest opportunity to increase yield is to borrow more heavily from groundwater storage during droughts, allowing the extra depletion to re-fill during subsequent wet years. This strategy could be optimized by adjusting the rates and locations of groundwater pumping. For a preliminary evaluation of the concept, however, a simulation was completed in which historical VID pumping was simply increased by 20 percent. Additional specifications for this future scenario simulation are described in the next section, “Scenario Simulations”. The analysis variables were whether simulated water-level declines during droughts were excessive and whether those water levels fully recovered between droughts. During the historical simulation period, the two droughts best suited for analysis were the 1945-1977 and 1987-1992 droughts.

The results demonstrated that the Basin has ample storage to supply the additional pumping and that recovery rates following droughts were reasonable. **Figure 33** shows hydrographs for wells in several locations that illustrate this pattern. As expected, the largest changes in water levels were in the main well field, where pumping was greatest and the increase in pumping was therefore also greatest. Hydrographs for two wells in the main well field are included in the figure (VID Wells 14 and 34). The uniform increase in pumping lowered water levels by similar amounts during the 1945-1977 and 1987-1992 droughts. Water levels were about 60 feet lower than the baseline simulation at the west end of the main well field, decreasing to about 30 feet at the east end. Streams draining about half of the total watershed area converge near the well field, and recharge capacity is consequently high. Water levels at all of the main well field wells recovered back to baseline levels by 1983 following the first drought and by 1995 following the second drought.

Water-level recovery was slower southeast of the main well field, in the large group of wells numbered in the 40s and 50s. Among those wells, water-level lowering was greater during the 1945-1977 drought than during the 1987-1992 drought. Maximum lowering was by about

22 feet, as illustrated in the figure by the hydrograph for VID Well 45. Water levels did not quite fully recover during the 1978-1986 wet period, but did fully recover by 1995 following the second drought. South of the Warner Ranch Fault, where some pumping occurs at VID Well 83, water levels at nearby VID Well 81 were lower by a maximum of 11 feet, in 1977 (see hydrograph in figure). Farther west, the maximum decrease in water levels also occurred in 1977 and was about 17 feet in the 70s well group and 10 feet in the 90s well group (see hydrographs for wells 79 and 92). Recovery was slower in this region, lingering through 1998 and even later at some wells. At WSRR wells the effect of increased District pumping decreased from west to east. The biggest effect was a lowering of water level by 13 feet at the end of the 1945-1977 in WSRR Well 1. This decreased eastward to a lowering of only 4 feet at WSRR Well 17 (see hydrographs). Recovery was rapid at WSRR wells because several streams flow through the area and wells are relatively shallow due to limited Basin thickness.

These results indicate that the sustainable yield of VID's part of the Warner Basin is at least 20 percent higher than historical pumping, provided sufficient well capacity is installed to produce the targeted amounts of water from water levels that are up to 60 feet lower than historical levels. The maximum yield does not appear to be much greater than the simulated 20-percent increase, based on the slow recovery of water levels in some parts of the Basin following each drought. Increased yield with less additional drawdown would probably be feasible if pumping were distributed more broadly across the Basin. A systematic review of well pumping rates, locations, depths and specific capacities would be needed before recommending a reconfiguration of VID's well field.

Scenario Simulations

The calibrated model was used to address several water management questions. A future baseline simulation was prepared to serve as a reference simulation for comparing the effects of each scenario. The future baseline simulation covered the same hydrologic period as the calibration simulation (water years 1939-2016) but differed in the following respects:

- Initial water levels were the final simulated water levels from the calibration simulation (September 2016).
- WSRR and LTMWC pumping were assumed to be 405 AFY and 16 AFY every year, respectively.
- District pumping was the same as historical, including zero pumping during the first 14 years of the simulation (corresponding to water years 1939-1952).
- Lake Henshaw was converted from the MODFLOW lake module to the MODFLOW constant-head module. The changes in water balance associated with the scenarios were large enough to generate large long-term rising or declining trends in simulated Lake Henshaw elevation. When simulated lake levels exceeded the actual minimum or maximum possible lake elevations, the lake module often became numerically unstable or at least unreliable. The model does not include an operations module that would adjust reservoir releases and/or groundwater pumping into the reservoir to maintain water levels within a realistic range. To overcome this difficulty, the lake was replaced with a patch of constant-head cells located near Henshaw Dam. This ensured that simulated groundwater levels in the western part of the Basin remained within a realistic range. Also, changes in simulated constant-head flux indicated the change in reservoir releases that would be needed to maintain lake levels within a reasonable range.

Yield of Warner Springs Ranch Resort Area

Various amounts of increased WSRR pumping were tested to determine the effect on groundwater levels and groundwater flow to the District's wells. Initial tests revealed a tendency for layer 1 cells to go dry at some of the WSRR wells. The Basin is thinner in the WSRR area than it is farther west, and layer 1 represents almost the entire Basin thickness. Thus, the occurrence of dry cells could not be solved simply by lowering the bottom of layer 1 without altering the interpretation of the bedrock surface. Limited saturated thickness appears to be a real constraint on increased WSRR pumping during droughts. For modeling purposes, it was assumed that pumping would be redistributed among the existing WSRR wells and that two additional wells would be drilled along a line between WSRR Well 1 and WSRR Well 17 so that drawdown would be distributed more uniformly across the WSRR subarea. The locations of the hypothetical wells are shown in **Figure 34**. The figure also shows the model grid region for which water balance information was tabulated ("WSRR Water Balance Area"). The eastern boundary of the WSRR subarea is the edge of the Basin. The northern boundary approximately

follows a groundwater flow pathline midway between Agua Caliente Creek and Ward Canyon, so that flow across the boundary is small. The western boundary coincides with the Agua Tibia North Fault and is between the westernmost WSRR wells and the nearest District wells. The southern boundary of the WSRR subarea follows the Basin boundary and the unnamed fault parallel to and north of the Warner Ranch Fault. This subarea delineation was selected for water balance analysis only; it does not reflect property lines or jurisdictional boundaries. The size of the subarea is 3,096 acres.

Scenarios with two levels of increased WSRR pumping were simulated: 1,100 AFY and 1,800 AFY. For comparison, the baseline simulation includes 405 AFY of WSRR pumping and also includes deep percolation of applied irrigation water on the golf course. Existing irrigation return flow at existing golf course was included in the scenarios with additional pumping, but no other return flows were included. When the WSRR hydrogeological analysis (required as part of the County Specific Plan Amendment process) is made public, a future task may be to model the pumping, consumptive use and return flow patterns of the proposed WSRR project.

Figure 35 shows hydrographs for three WSRR wells and the nearest VID well for the baseline scenario and the two scenarios with increased pumping. The response to pumping was similar at all WSRR wells. Water levels declined more rapidly during droughts, reaching a larger cumulative decline by the end of the drought. For example, water levels with 1,100 AFY of WSRR pumping were about 40 feet lower than the baseline water levels in 1977 at the end of the long 1945-1977 drought. Water levels recovered quickly in wet years, however, reaching the same high levels as the baseline scenario in the early 1980s and mid-1990s. No model cells went dry in the 1,100 AFY pumping scenario. When pumping was increased to 1,800 AFY, however, layer 1 cells at several WSRR wells went dry during the long drought.

At VID Well 54, which is close to the WSRR area, water levels also became gradually lower during the 1945-1977 drought. By 1977, they were 17 feet lower than the baseline water level with 1,100 AFY of WSRR pumping and at least 30 feet lower with 1,800 AFY of WSRR pumping (the dry cells in the WSRR area eliminated subsequent pumping in those cells for the remainder of the simulation). During wet and normal conditions, WSRR pumping had a negligible effect on water levels at VID Well 54. This pattern of impact occurred at all VID wells east of the Agua Tibia South Fault and north of the Warner Ranch Fault, but the magnitude of impact decreased with distance from WSRR.

Figure 36 shows contours of the change in layer 1 water level in December 1977 from the baseline scenario to the scenario with 1,100 AFY of WSRR pumping. For wells in the main well field area, water levels were 10-16 feet lower than in the baseline scenario. This represents an increase in cumulative drawdown during major droughts of 8-23 percent, with the higher percentages toward the eastern end of the well field.

A comparison of average annual water balances for the WSRR area showed that increasing WSRR pumping by 695 AFY (from 405 AFY to 1,100 AFY) was balanced by a 154 AFY decrease in groundwater storage (distributed throughout the Basin) and a 541 AFY decrease in inflow to Lake Henshaw. WSRR pumping decreased groundwater outflow from the WSRR area to the rest of the Basin, and that shift in the groundwater balance in downgradient areas decreased the amount of groundwater discharge into streams and, hence, the amount of surface inflow to

Lake Henshaw. In other words, the increase in consumptive use within the WSRR area caused an equal decrease in the conjunctive use yield available to the District.

These simulation results indicate that the sustainable yield (as net consumptive use but with golf course irrigation return flow) of the WSRR area is about 1,100 AFY and that limited saturated Basin thickness probably constrains yield at higher pumping rates.

Impact of Climate Change

Climate change is altering air temperatures and rainfall patterns throughout the world. The rainfall-runoff-recharge model used to develop inputs to the groundwater model is capable of translating changes in daily time series of rainfall and ET_0 to changes in stream flow and distributed recharge. As part of its role in implementing the Sustainable Groundwater Management Act (SGMA), the DWR has developed monthly time series of change factors for locations throughout California, to be used for evaluating climate change impacts on groundwater resources. DWR developed separate sets of factors for climate conditions in 2030 and 2070, and the latter were selected for the Warner Basin analysis. DWR developed separate factor time series for each cell of a grid that covers the entire state with cells that are approximately 3.75 x 3.75 miles in size. Factors for the 18 grid cells that overlap the Warner Basin watershed were downloaded from DWR's SGMA Data Viewer (DWR, 2018). Recharge zones in the rainfall-runoff-recharge model were assigned to the DWR grid cell that overlapped most of the zone. The monthly change factors were applied to each daily rainfall or ET_0 value in that month.

The climate change factors affected three inputs to the groundwater model: surface inflow at the model boundary and runoff within the Basin, subsurface inflow from bedrock adjacent to the Basin boundary, and distributed rainfall recharge over the surface of the Basin. In general, the changes in these flows were small. Total surface runoff in the watershed increased by 0.9 percent, but simulated percolation from streams in the groundwater model decreased by 0.6 percent, probably because storm events were fewer but larger overall. Average annual distributed recharge decreased by 2.9 percent, and bedrock inflow by 1.4 percent.

Water-level hydrographs at most wells were barely affected. **Figure 37** compares the hydrographs for baseline and climate change conditions at VID Well 14, which exhibited larger differences than most wells. The DWR change factors affected different storm events in different watersheds at different times, resulting in occasional temporary deviations between the hydrographs. The largest difference was in 2007, when water levels with climate change were 9 feet lower than under baseline conditions. Most of that difference was gone by 2016.

Overall, the simulated effects of climate change on groundwater levels and the water balance are small. Those changes would not substantially affect the conjunctive-use yield of water available to the District.

Additional Options for Increased District Water Supply Yield

The yield of water available to the District is a function of the conjunctive operation of the groundwater Basin and Lake Henshaw. Stream flow that does not percolate into the Basin is almost entirely captured in Lake Henshaw and pumping from District wells into the lake allows

stored groundwater to be used on a timely basis. The only true losses from this system are infrequent spills from the lake in exceptionally wet years and evaporation from the lake surface. The feasibility of increasing yield available to VID by increasing groundwater pumping during droughts was discussed above under “Sustainable Yield Analysis”. Two other options for increasing yield are to increase the capture of water that currently spills from Lake Henshaw and decreasing the amount of evaporation loss from Lake Henshaw. Both of these options involve maintaining the lake at a lower average elevation.

Option 1: Lower Lake Levels to Decrease Spills

This option was evaluated by analysis of historical operations data, not the groundwater model. The two most recent spill years were 1983 and 1993. Using 1983 as an example, 21,564 AF of water spilled from Henshaw Dam over a 15-week period. Before reservoir storage began rising rapidly in January 1983, storage was at about 13,300 AF. Even if storage had been zero at that time, approximately 8,200 AF of water would have spilled. Draining the lake completely would be undesirable from an environmental and recreational standpoint. If the average lake surface elevation were lowered from 2,664 feet above sea level (the historical average) to 2,657 feet, average storage would be decreased by 5,500 AF. The relationships between lake elevation, surface area and storage are shown in **Figure 38**. Spills have occurred in perhaps 3 years out of the 64-year record of operations (1978, 1983, 1993). If 5,500 AF of additional water were captured and retained for use in those three years, the 64-year total increase in water supply would be only 16,500 AF. This is a small amount of water in the context of overall conjunctive use operations.

Option 2: Lower Lake Levels to Decrease Evaporation

Loss of water to evaporation from the surface of Lake Henshaw is substantial. At the average lake elevation of 2,664 feet, the surface area is 1,085 acres. Multiplying that area by an annual net evaporative loss of 5.08 feet produces a volumetric loss of 5,512 AFY. Lowering the lake level by the same amount as assumed in the above calculation of spill capture (from 2,664 to 2,657 feet), the average lake area would decrease by half, to 540 acres. This would reduce annual evaporation losses by approximately 2,750 AFY. Because this saving would occur every year, the cumulative savings over 64 years would be 176,000 AF, or more than ten times the benefit achieved by capturing additional water in spill years. However, the evaporation and spill benefits would be additive and total 192,500 AF (or an average of 3,010 AFY).

The groundwater model was used to determine how groundwater levels and flow would change in response to a decrease in average lake level. This was accomplished by changing the specified elevation at the constant-head cells representing Lake Henshaw. Lowering the level of the lake tends to decrease groundwater discharge into the lower reaches of streams that enter Lake Henshaw and increase groundwater seepage directly into the lake. Thus, lower lake levels might adversely impact habitat conditions along some stream reaches.

Additional Observations

The stratigraphic interpretation in this report and the results of the modeling analysis conflict with the hydrogeologic conceptual model and conclusions of the Bookman-Edmonston study (2002). That study interpreted the Basin as having three saturated depth intervals: an upper, middle and lower aquifer. It described wells as “going dry” after a certain volume of groundwater had been pumped during the 1987-1992 drought. They attributed this to well interference, dewatering of the productive upper aquifer, and much lower transmissivity in the middle and lower aquifers. The study concluded that only about 100,000 AF of groundwater can be extracted from the District’s existing wells before pumping rates “rapidly deteriorate”. VID Well 6A was one of the wells that reportedly “went dry” during the drought, and accordingly, it was selected for evaluation in this study. Well construction records show that the pump is set at a depth of 220 feet below ground surface, which is between the upper screen (104-218 feet) and lower screen (240-450 feet). During the drought, water levels at VID Well 6A declined from less than 50 feet below ground surface (bgs) in 1986 to about 200 feet bgs in 1990 and remained at that depth until post-drought recovery commenced in 1993. There are two possible causes of decreased production in VID Well 6A. The first is that the pump might have lost suction when pumping levels declined to the elevation of the pump intake at 220 feet bgs. The second is that the performance curve for the pump is very flat, which means that the pumping rate declines rapidly as the depth to water increases. The pump was selected to produce 1,900 gallons per minute (gpm) at a water-level depth of 120 feet. However, the pump performance curve shows that increasing the depth to water by as little as 20 feet would decrease the pumping rate to 1,300 gpm and that flow would drop to zero at a depth to water of 182 feet (shut-off head). Thus, the pump probably ceased producing water before the water level dropped as low as the intake. When the well stopped producing water, there was still at least 222 feet of saturated screened interval, so the well did not go dry. The geologic and resistivity logs for the well do not indicate a transition to much finer-grained aquifer materials below a depth of 220 feet. It is clear in this case that the loss of production at VID Well 6A was not related to the aquifer or well construction, but rather to the performance curve and possibly the depth setting of the pump.

A comprehensive review of well construction, specific capacity, pump characteristics and performance during the 1987-1992 drought at all District wells was beyond the scope of the present study. Such a review would be desirable as an initial step toward developing a strategy for increasing overall access to Basin storage by District wells. Achieving that objective might include a combination of replacing pumps at existing wells, increasing the number of wells and expanding the distribution of wells and pumping across the Basin.

References Cited

- Barnes, H.H. 1967. Roughness characteristics of natural channels. Water-Supply Paper 1849. U.S. Geological Survey, Washington, D.C.
- Bicknell, B.R., J.C. Imhoff, J.L. Kittle, Jr., A.S. Donigian, Jr., and R.C. Johanson. 1997. Hydrological Simulation Program--Fortran, User's manual for version 11: U.S. Environmental Protection Agency, National Exposure Research Laboratory, Athens, GA. EPA/600/R-97/080, 755 p.
- Bookman-Edmonston Engineering, Inc. May 2, 2002. Evaluation of local water supply. Prepared for City of Escondido and Vista Irrigation District, Escondido and Vista, CA.
- California Department of Water Resources (DWR). 2003. California's groundwater, Update 2003. Sacramento, CA.
- California Department of Water Resources (DWR). 2018. Sustainable Groundwater Management Act on-line data viewer at <https://sgma.water.ca.gov/webgis/?appid=SGMADataViewer> accessed October 9, 2018.
- Davis, G. H. and S.J. Reynolds. 1996, Structural geology of rocks and regions, Second Edition, John Wiley & Sons, Inc.
- Environmental Simulations, Inc. 2011. Guide to Using Groundwater Vistas, Version 6. Reinholds, PA.
- Freeze, R.A. and J.A. Cherry. 1979. Groundwater. Prentice-Hall, Inc., Englewood Cliffs, NJ.
- Grand, Fred. WSRR Partner. August 30, 2017. Personal communication to District staff and consultants during site visit.
- James M. Montgomery consulting Engineers, Inc. (JMM). March, 1969. Hydrogeology of Warner Basin, San Diego County, California. Prepared for Vista Irrigation District, Vista, CA.
- Leighton & Associates, Inc. September 23, 1981. Hydrogeology and ground water management plan for 2,885-acre Warner Springs Ranch, San Diego County, California.
- Li, Weimin. Associate professor, Department of Landscape Architecture, California Polytechnic Institute, Pomona. October 23, 2017. E-mail to Gus Yates, Todd Groundwater.
- McClymonds, N.E., and O.L. Franke. 1972. Water-transmitting properties of aquifers on Long Island, New York. Professional Paper 627-E. U.S. Geological Survey. Washington, D.C.
- Nature Conservancy. 2018. Statewide digital map of natural vegetation communities that can depend on groundwater. Hosted on California Department of Water Resources website: <https://gis.water.ca.gov/app/NCDatasetViewer/#> Accessed October 9, 2018.
- Rantz, S.E. 1969. Mean annual precipitation in the California region. Basic-Data Compilation 1020-01. U.S. Geological Survey, Menlo Park, CA.
- Rawls, W.J., L.R. Ahuja, D.L. Brakensiek and A. Shirmohammadi. 1993. Infiltration and Soil Water Movement. Chapter 5 in D.R. Maidment, ed. Handbook of Hydrology. McGraw-Hill, Inc. New York, NY

San Diego County. 2017. ECO_VEGETATION_CN digital map of terrestrial vegetation published on SanGIS website at <http://www.sangis.org/download/> Accessed October 9, 2018.

Scheliga, J.T., Jr. August 1963. Geology and water resources of Warner Basin, San Diego County, California. M.A. Thesis, Department of Geology, University of Southern California, Los Angeles, CA.

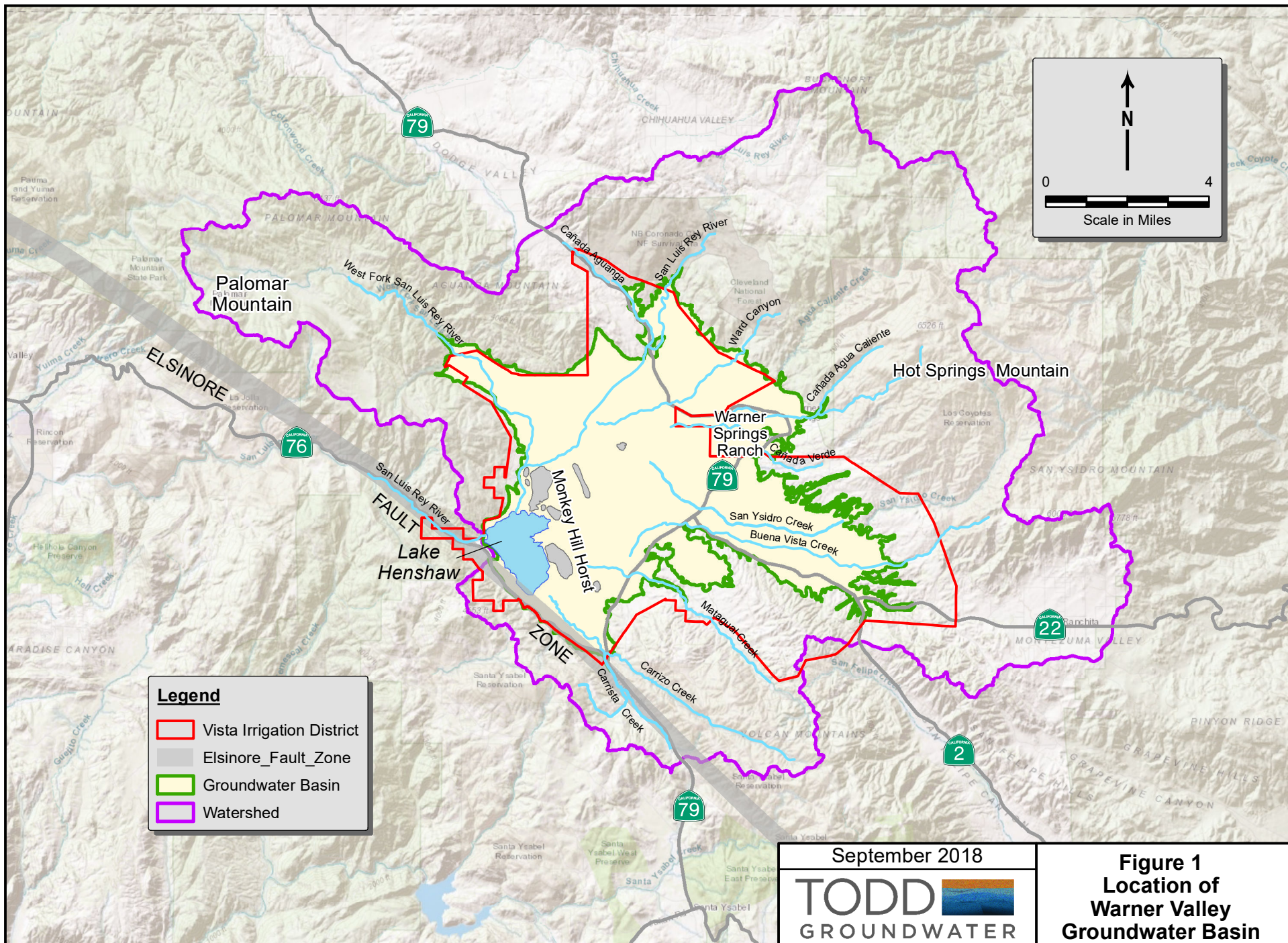
Strassberg, G., N.L. Jones and D.R. Maidment. February 15, 2011, Arc Hydro Groundwater: GIS for hydrogeology. ESRI Press.

United States Geologic Survey (USGS). 2018. National Elevation Dataset (NED) for San Diego County. (Available at: <https://nationalmap.gov/elevation.html>)

Van Mullen, J.A., D.E. Woodward, R.H. Hawkins, and A.T. Hjelmfelt, Jr. No date (but after 2001). Runoff Curve Number Method: Beyond the Handbook. Curve-Number Working Group, Natural Resources Conservation Service, Washington, D.C.

Viessman, W., Jr., J.W. Knapp, G.L. Lewis, and T.E. Harbaugh. 1977. Introduction to Hydrology. 2nd edition. Harper & Row, Publishers. New York, NY.

Figures



Legend

- Vista Irrigation District
- Elsinore Fault Zone
- Groundwater Basin
- Watershed

↑
N

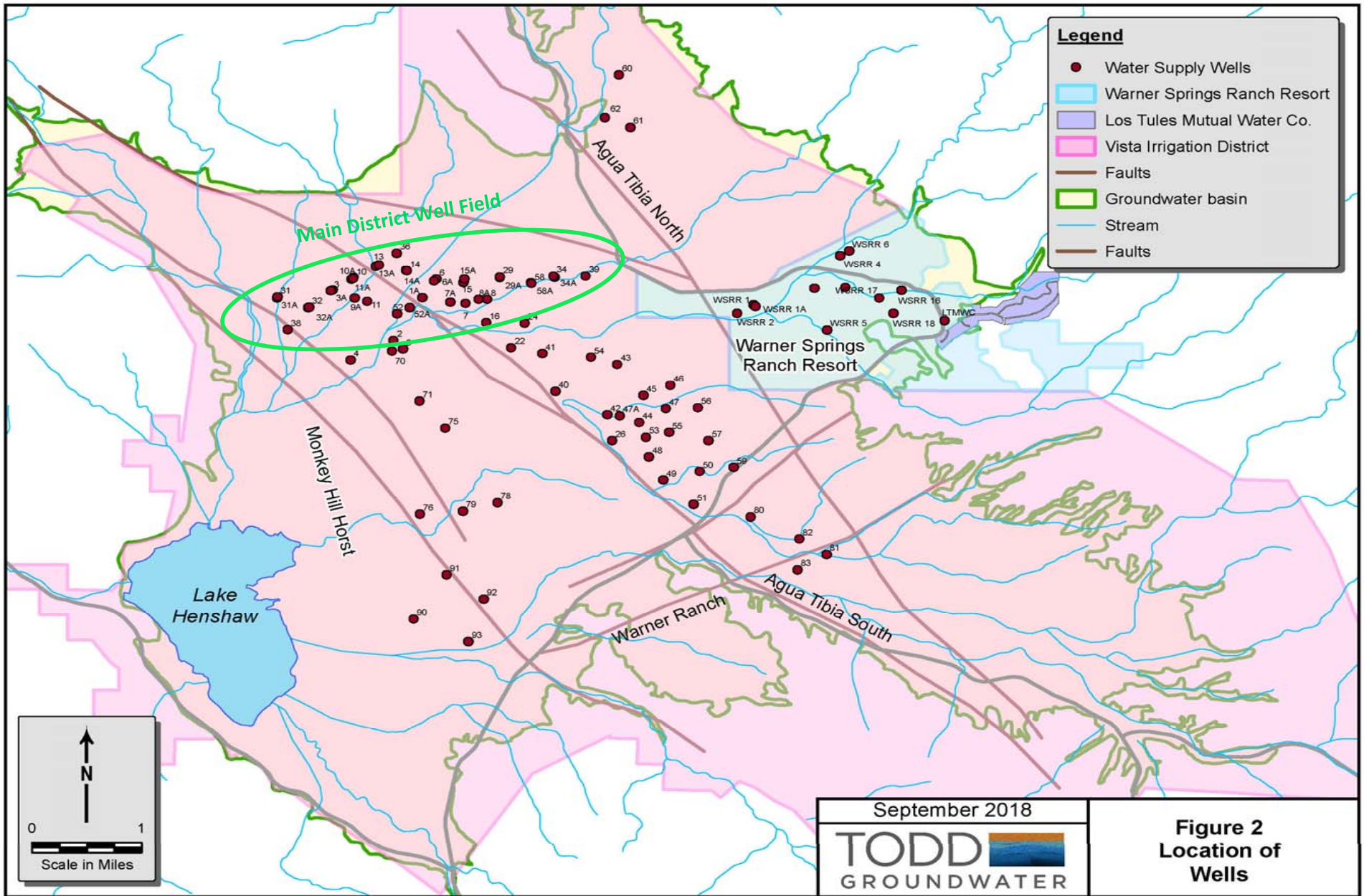
0 ————— 4

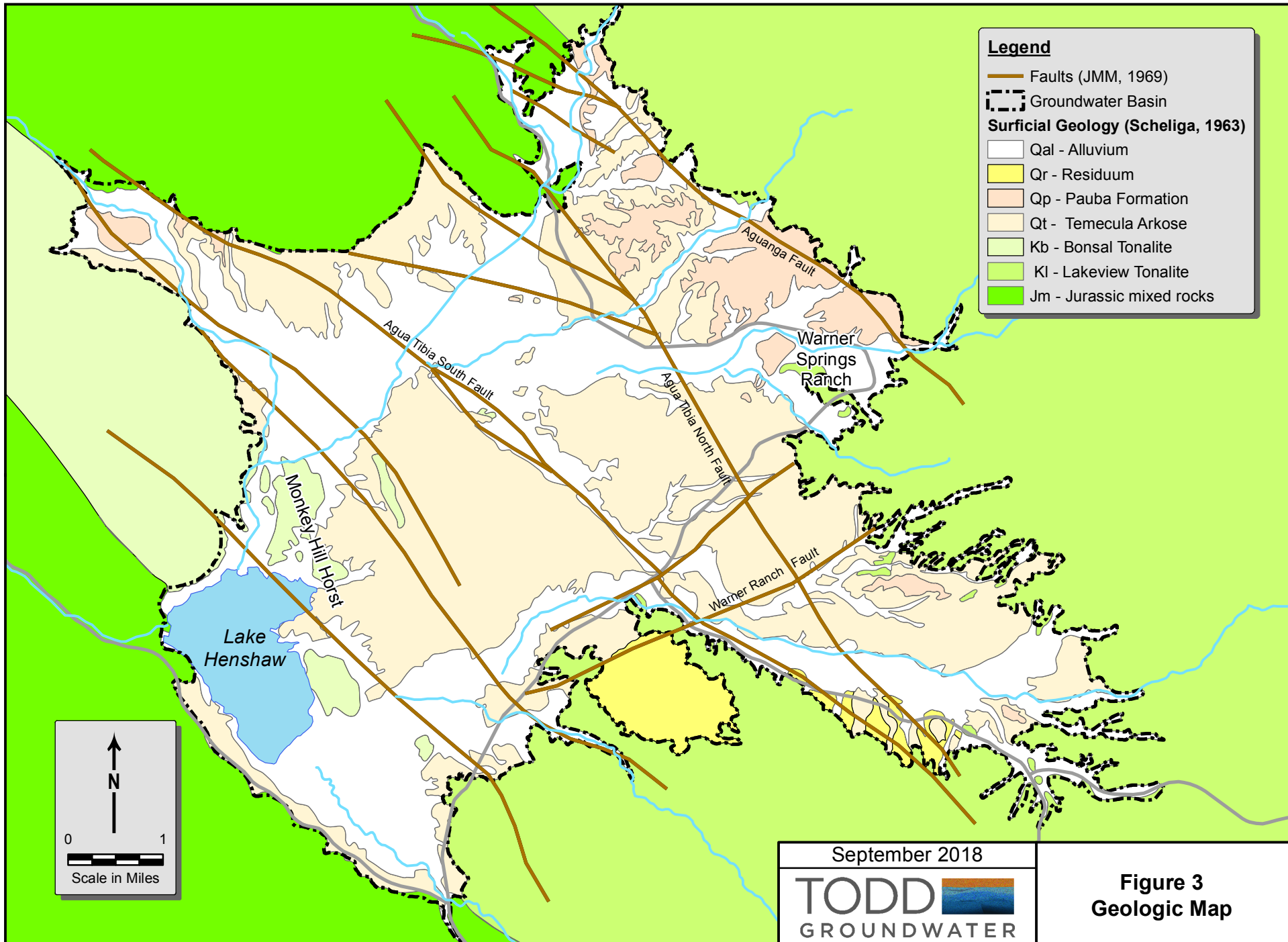
Scale in Miles

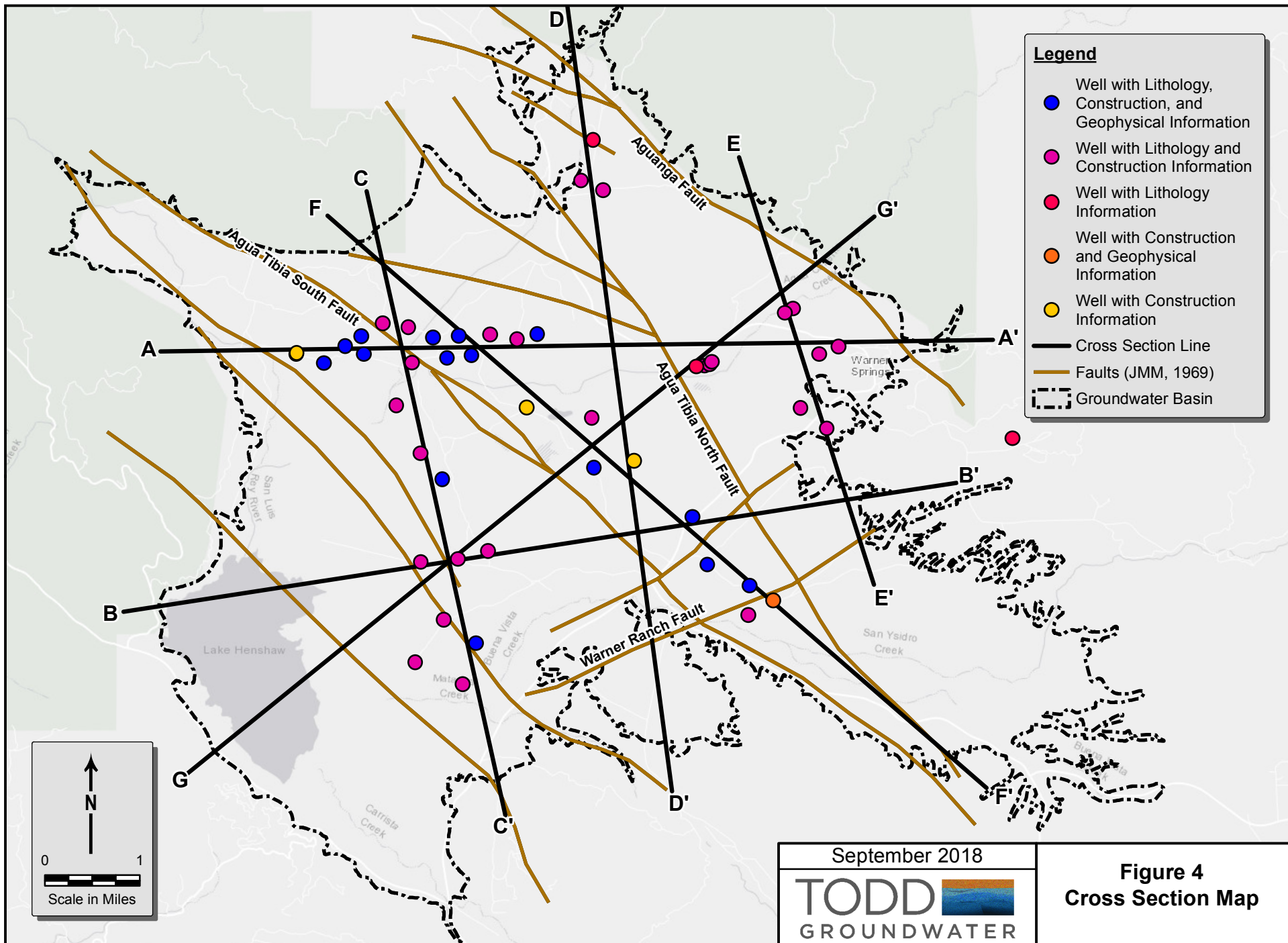
September 2018

TODD **GROUNDWATER**

Figure 1
Location of
Warner Valley
Groundwater Basin







Legend

- Well with Lithology, Construction, and Geophysical Information (Blue circle)
- Well with Lithology and Construction Information (Pink circle)
- Well with Lithology Information (Red circle)
- Well with Construction and Geophysical Information (Orange circle)
- Well with Construction Information (Yellow circle)
- Cross Section Line (Black line)
- Faults (JMM, 1969) (Orange line)
- Groundwater Basin (Dashed line)

Scale in Miles

0 1

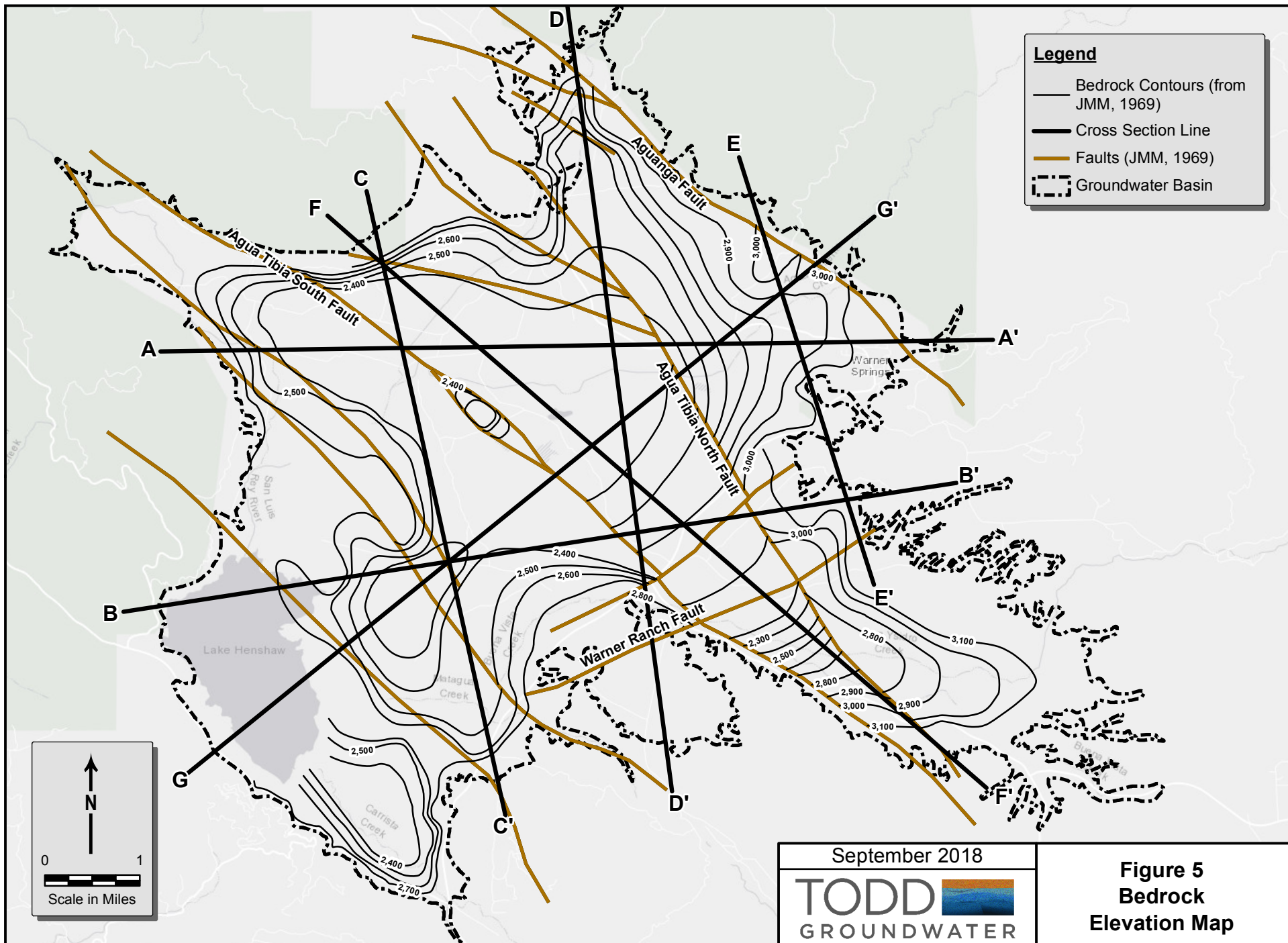
N

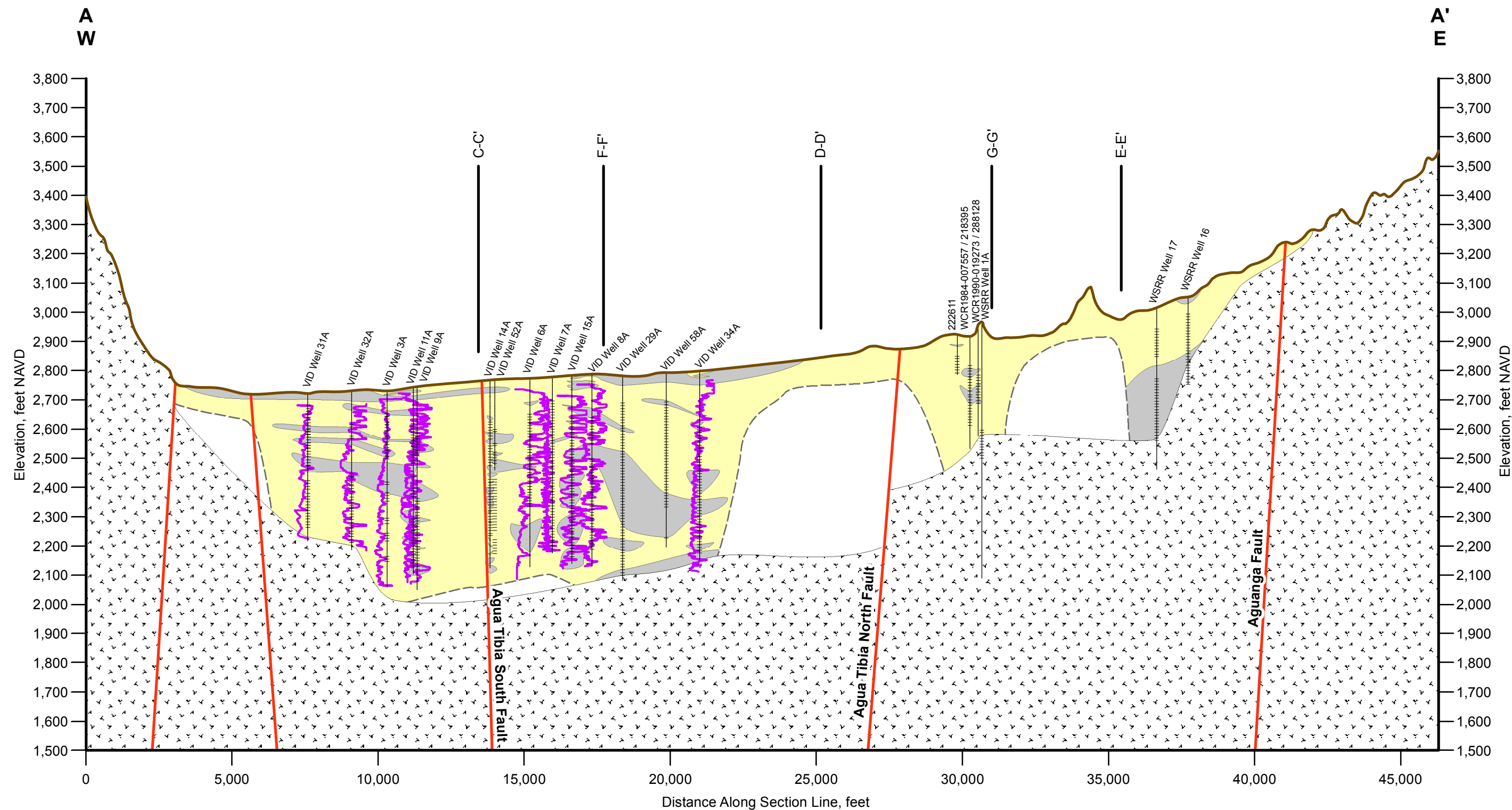
September 2018

TODD 

GROUNDWATER

Figure 4
Cross Section Map





Path: T:\Projects\VID_Water Basin_600\GIS\Maps\Figures\Fig 6 Cross Section A-A'.mxd

- Well Screen
- Total Drilled Depth
- Short Normal Geophysical Log
- Fault
- Sand and Gravel
- Silt and Clay
- Bedrock
- No Information

Notes:
 Cross section only extended to depth of available information.
NAVD 88: North American Vertical Datum of 1988.

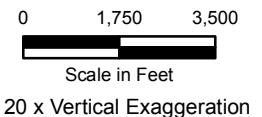
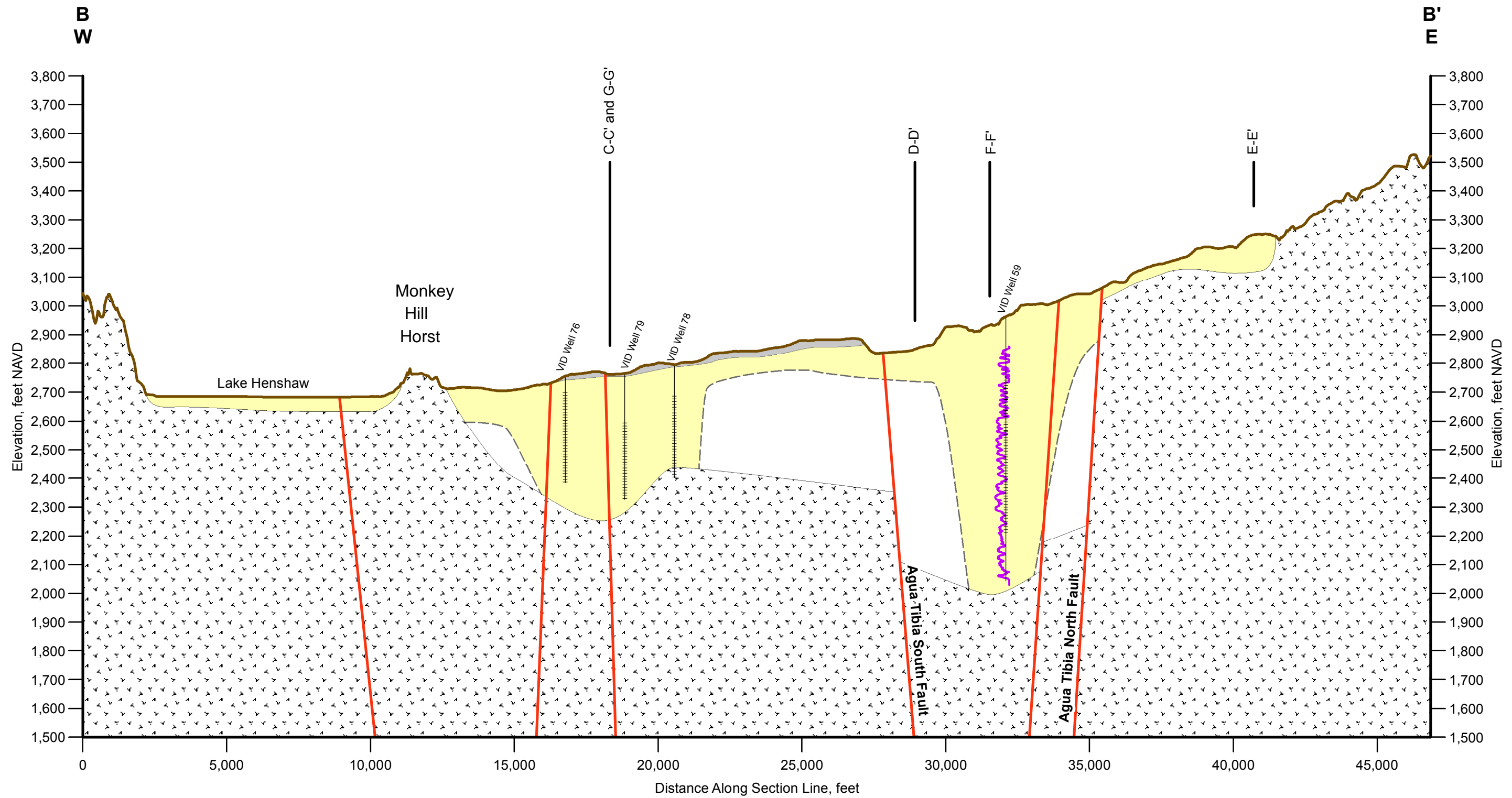


Figure 6
Cross Section A-A'



- Well Screen
- Total Drilled Depth
- Short Normal Geophysical Log
- Fault
- Sand and Gravel
- Silt and Clay
- Bedrock
- No Information

Notes:
Cross section only extended to depth of available information.

NAVD 88: North American Vertical Datum of 1988.

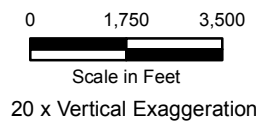
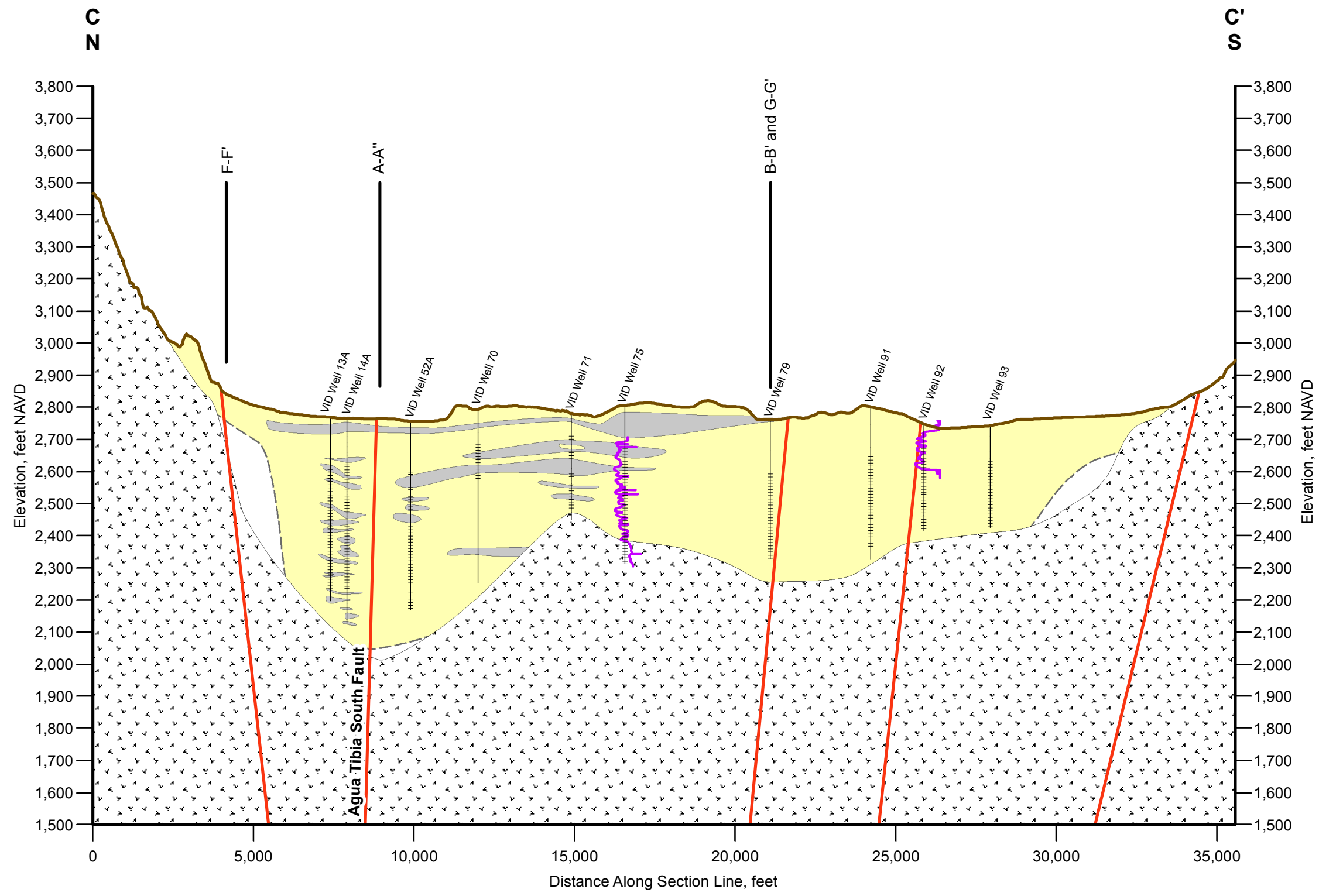


Figure 7
Cross Section B-B'



Path: T:\Projects\VID_Water\Basin_600\GIS\Maps\Figures\Fig 8_Cross Section C-C'.mxd

- Well Screen
- Total Drilled Depth
- Short Normal Geophysical Log
- Fault
- Sand and Gravel
- Silt and Clay
- Bedrock
- No Information

Notes:
 Cross section only extended to depth of available information.
NAVD 88: North American Vertical Datum of 1988.

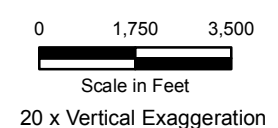
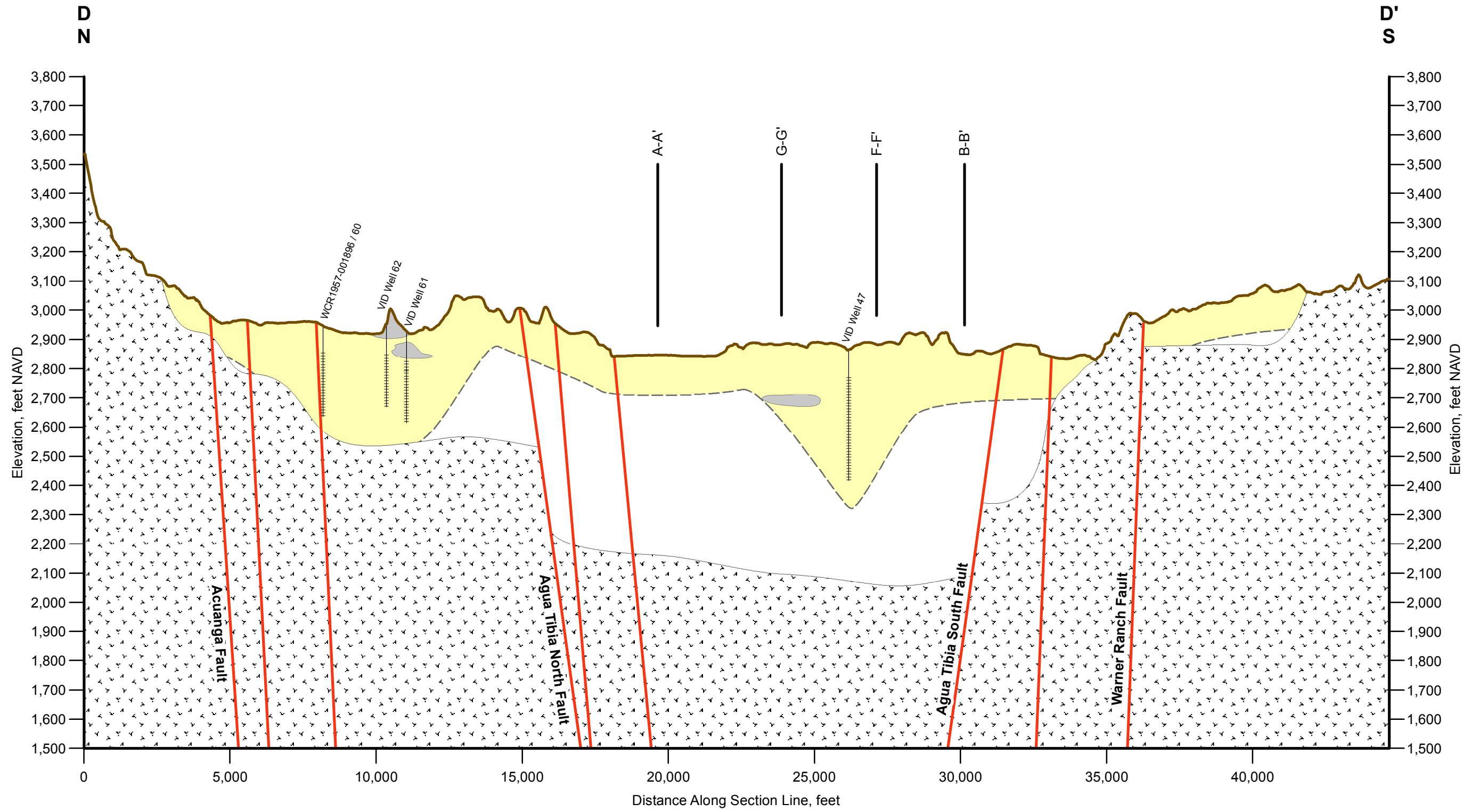


Figure 8
Cross Section C-C'



Path: T:\Projects\VID Warner Basin 600\GIS\Maps\Figures\Fig 9 Cross Section D-D'.mxd

- Well Screen
- Total Drilled Depth
- Short Normal Geophysical Log
- Fault
- Sand and Gravel
- Silt and Clay
- Bedrock
- No Information

Notes:
 Cross section only extended to depth of available information.
NAVD 88: North American Vertical Datum of 1988.

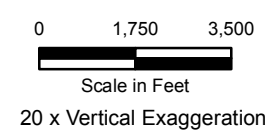
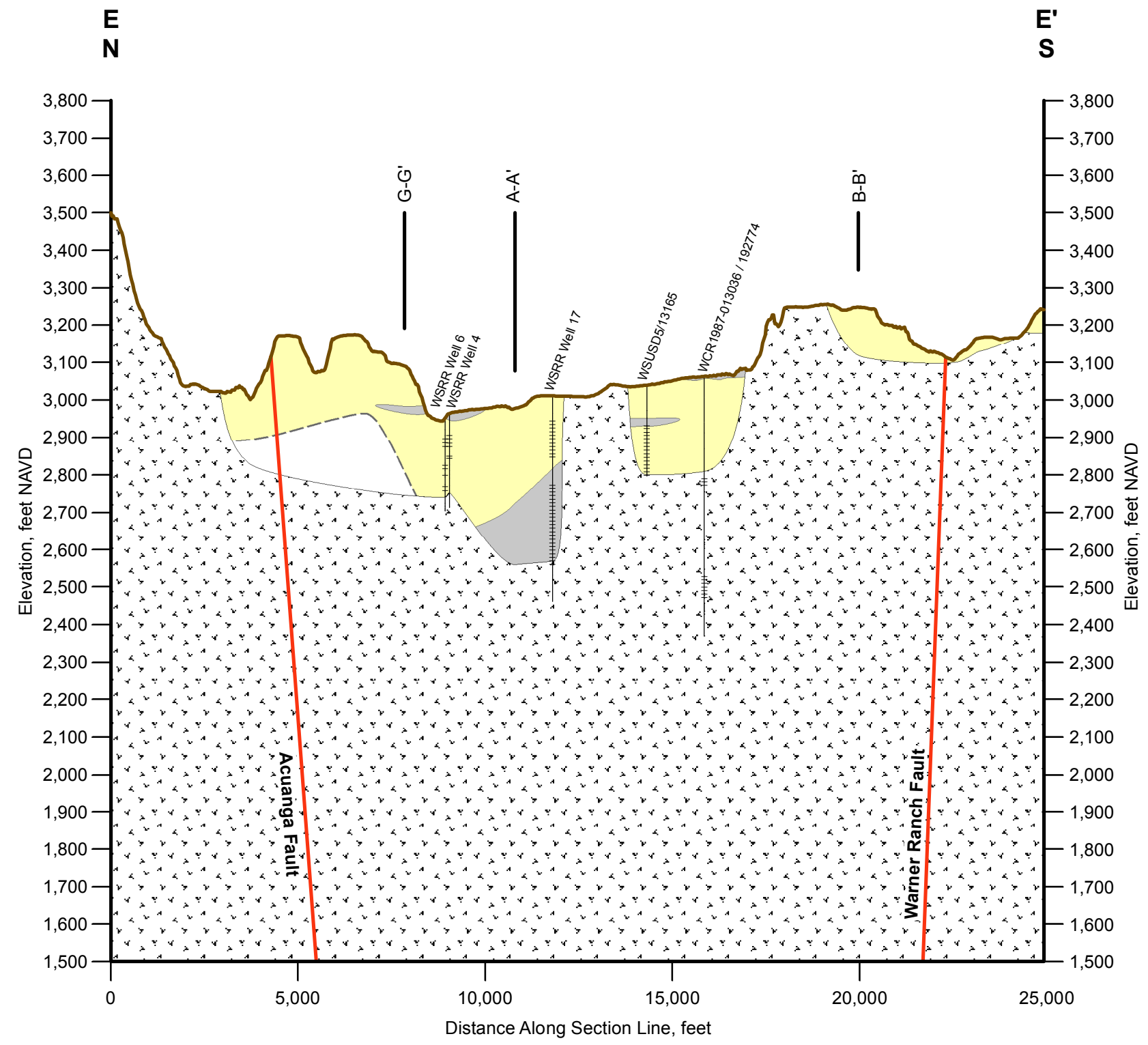


Figure 9
Cross Section D-D'



- Well Screen
- Total Drilled Depth
- Short Normal Geophysical Log
- Fault
- Sand and Gravel
- Silt and Clay
- Bedrock
- No Information

Notes:
 Cross section only extended to depth of available information.
NAVD 88: North American Vertical Datum of 1988.

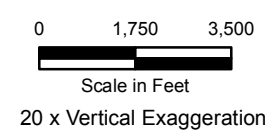
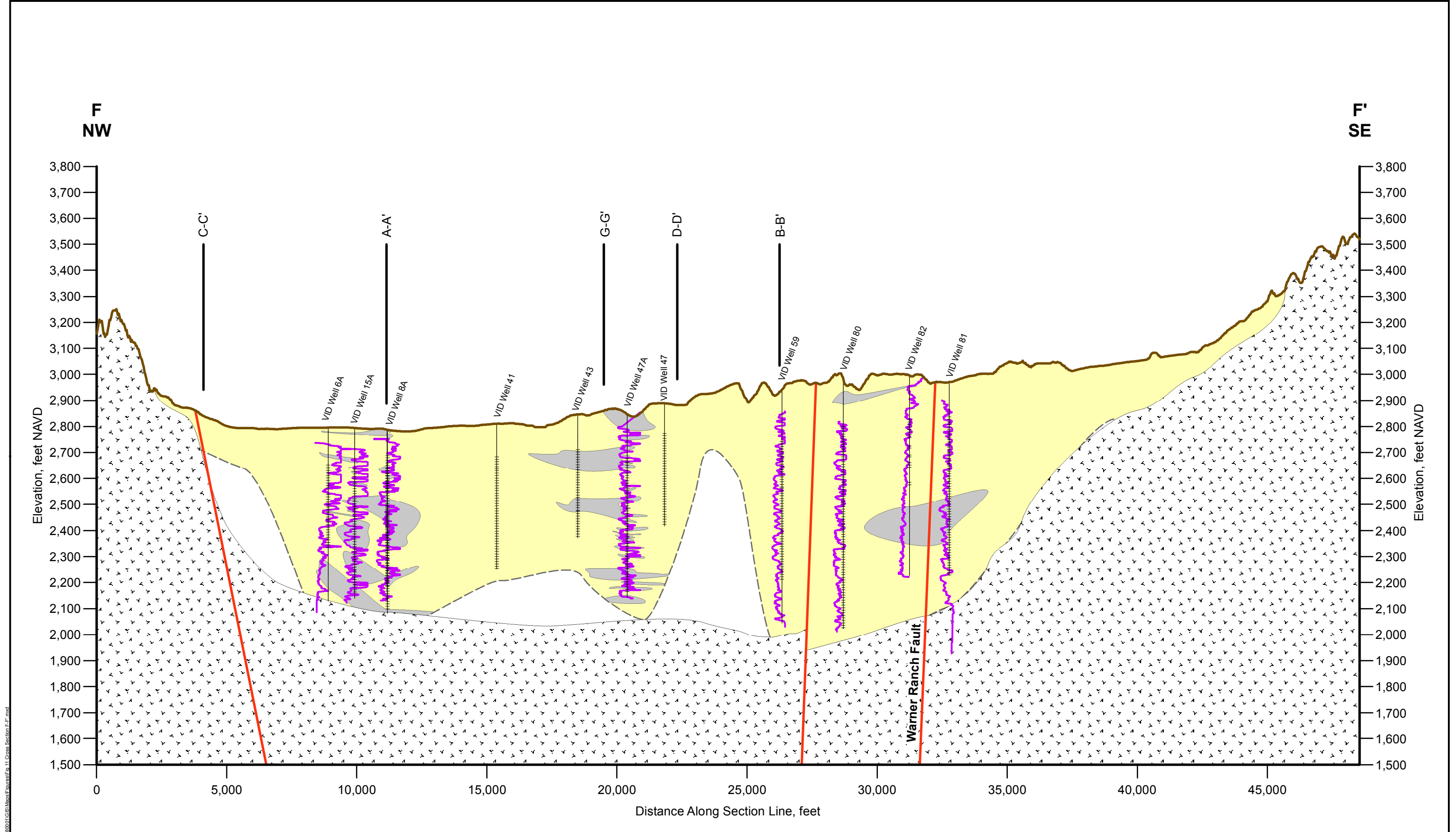


Figure 10
Cross Section E-E'

Path: T:\Projects\VD Warner Basin 800\GIS\Maps\Figures\Fig 10 Cross Section E-E'.mxd



Path: T:\Projects\VID Warner Basin 600\GIS\Maps\Figures\Fig 11 Cross Section F-F.mxd

- Well Screen
- Total Drilled Depth
- Short Normal Geophysical Log
- Fault
- Sand and Gravel
- Silt and Clay
- Bedrock
- No Information

Notes:
 Cross section only extended to depth of available information.
NAVD 88: North American Vertical Datum of 1988.

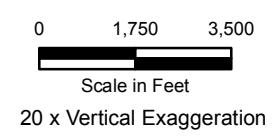
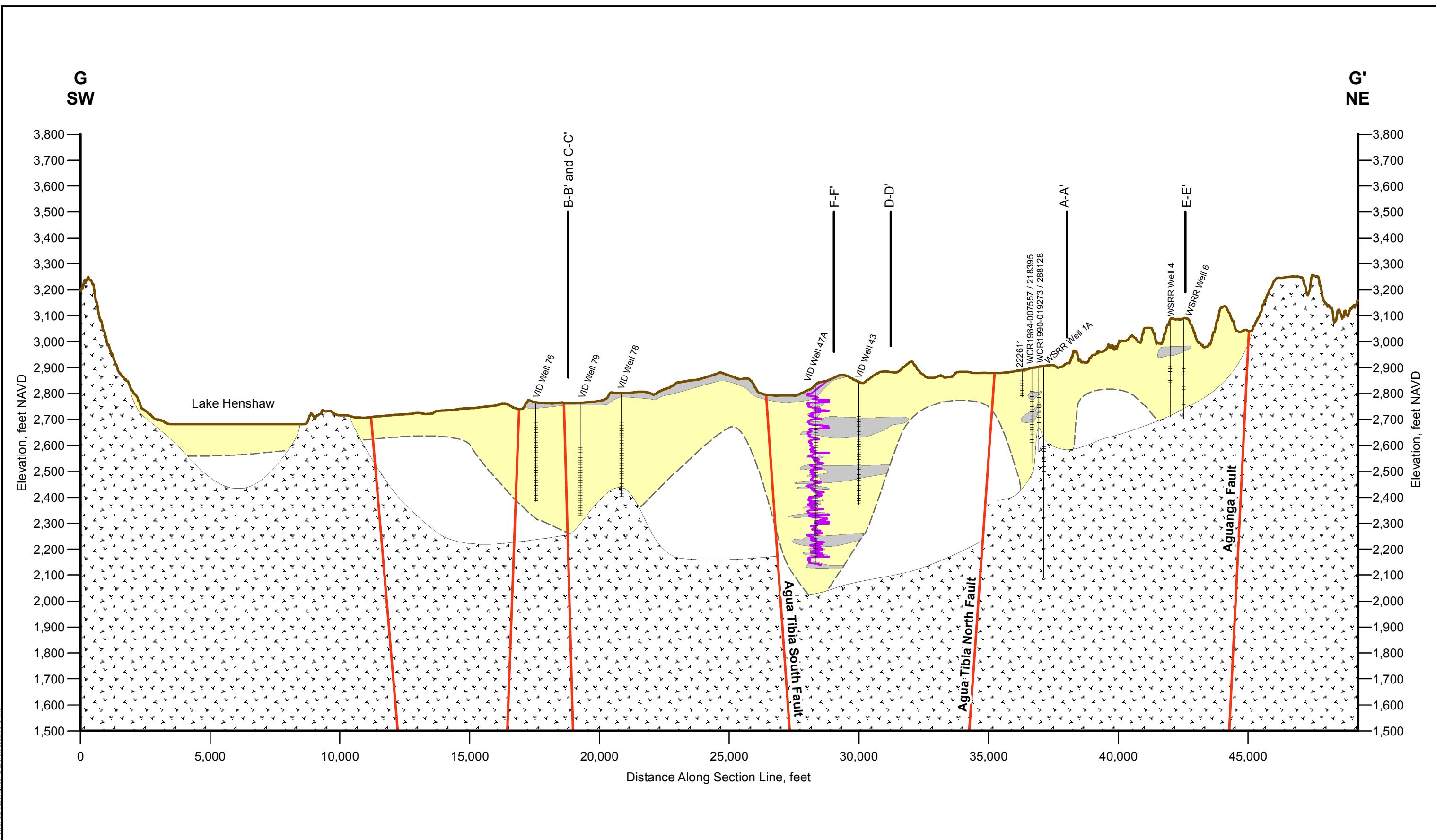


Figure 11
Cross Section F-F'



Path: T:\Projects\VID_Warner Basin_600\GIS\Maps\Figures\Fig_12_Cross Section G-G'.mxd

- Well Screen
- Total Drilled Depth
- Short Normal Geophysical Log
- Fault
- Sand and Gravel
- Silt and Clay
- Bedrock
- No Information

Notes:
 Cross section only extended to depth of available information.
 NAVD 88: North American Vertical Datum of 1988.

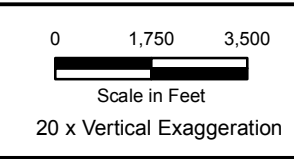
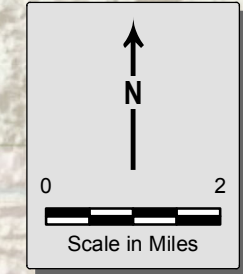
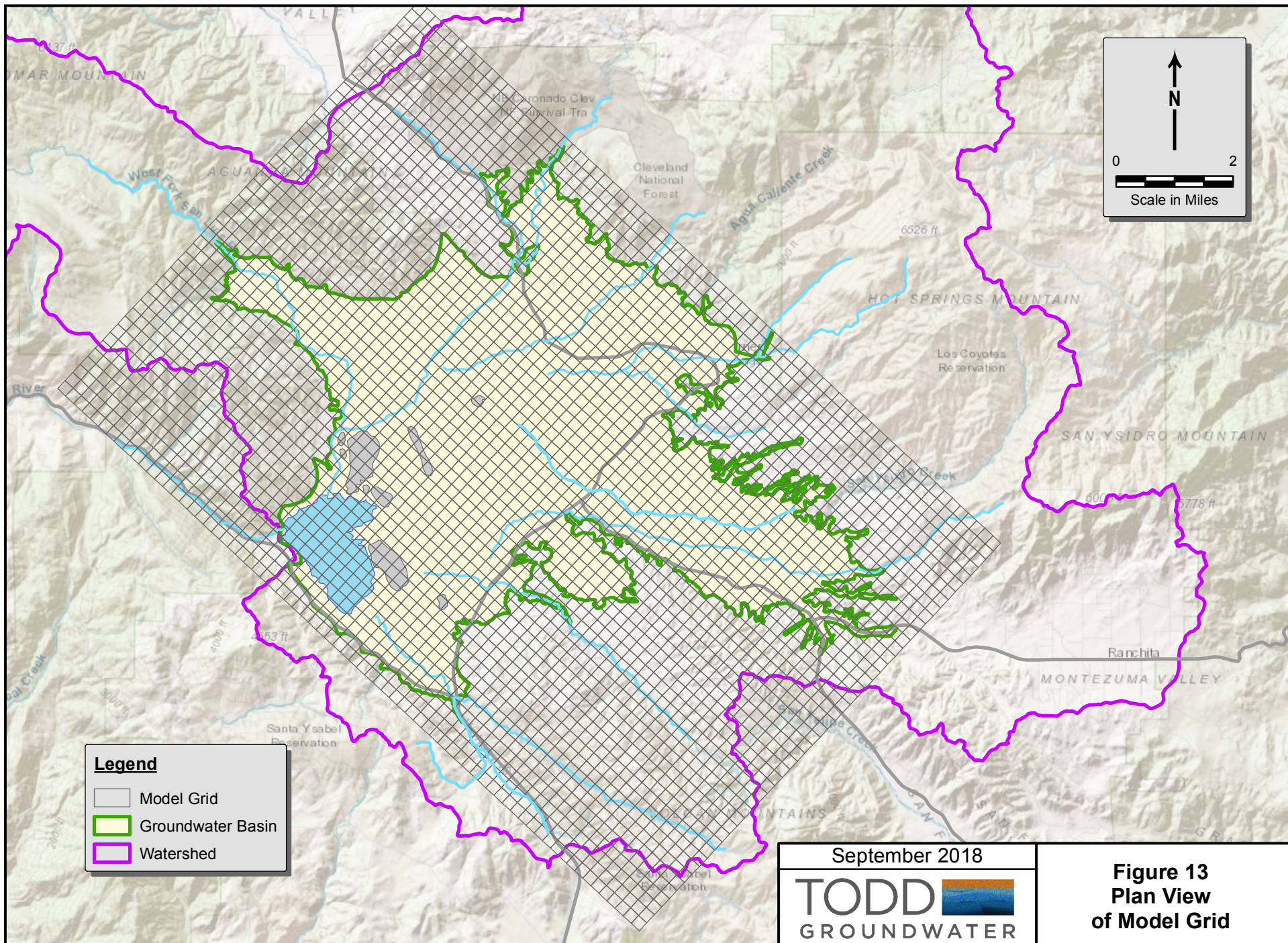


Figure 12
Cross Section G-G'



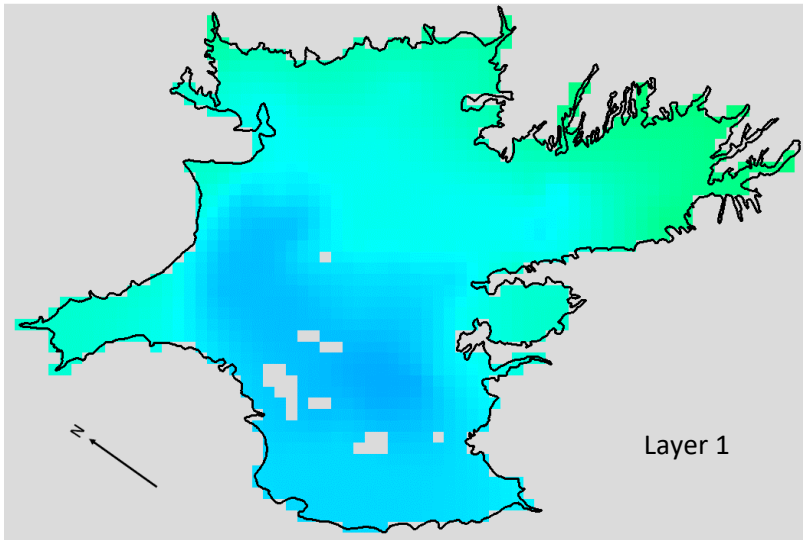
Legend

- Model Grid
- Groundwater Basin
- Watershed

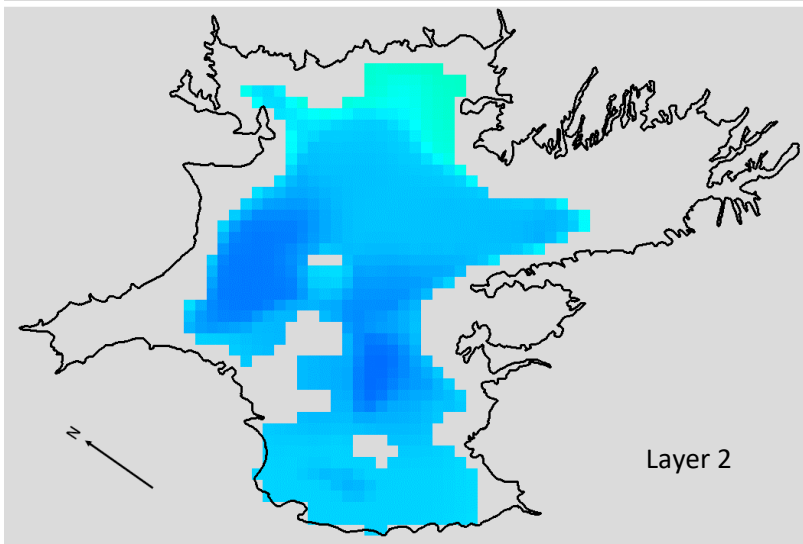
September 2018

TODD 
GROUNDWATER

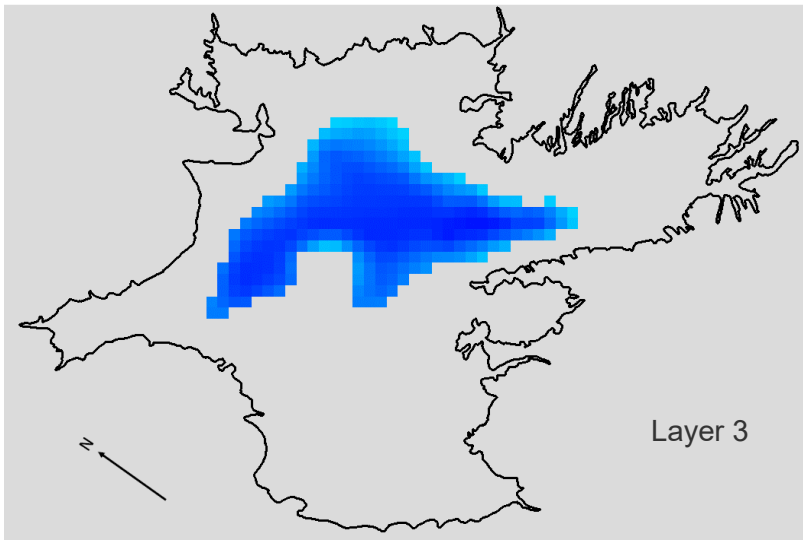
Figure 13
Plan View
of Model Grid



Layer 1



Layer 2



Layer 3

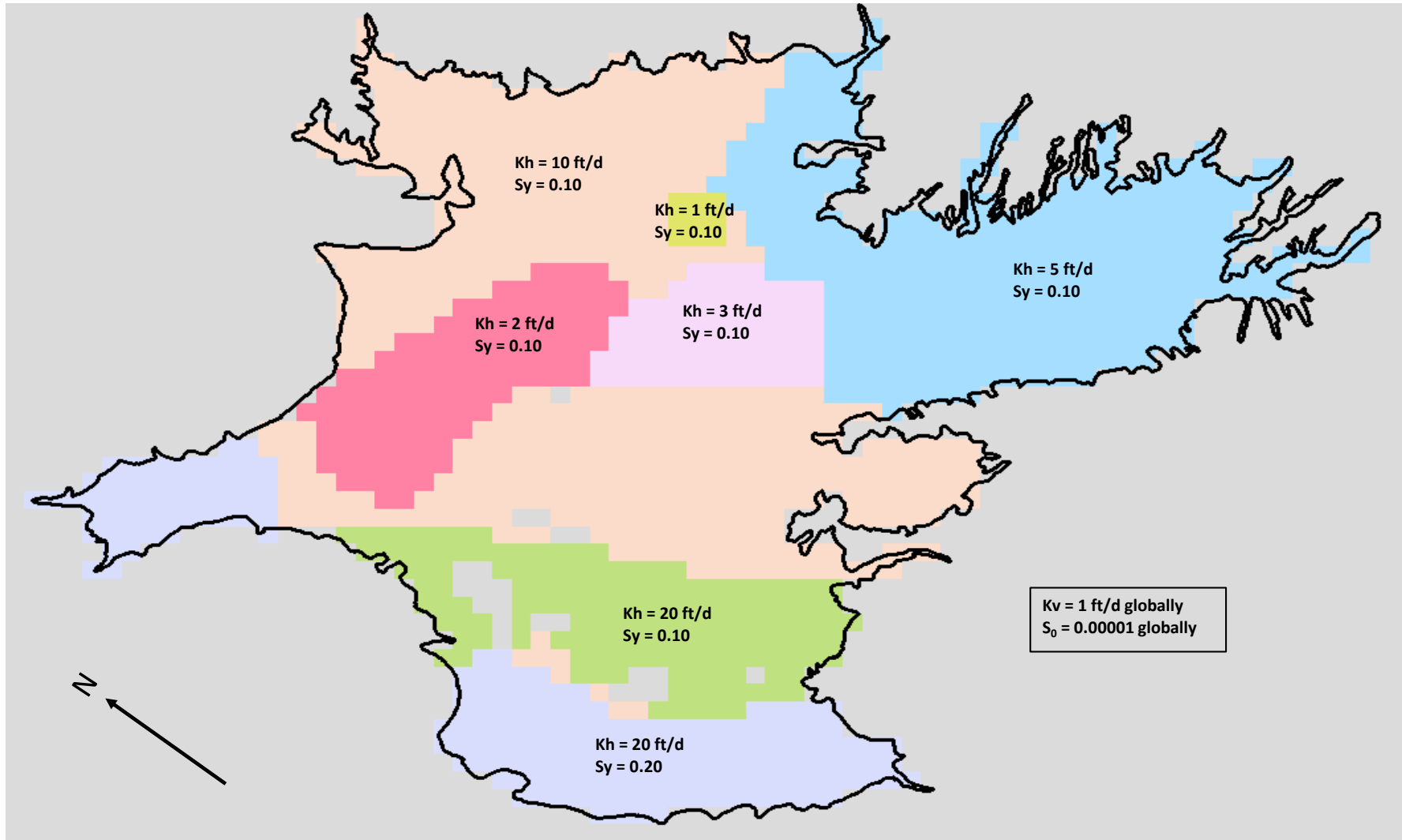
Layer Bottom Elevation (feet NAVD88)



September 2018



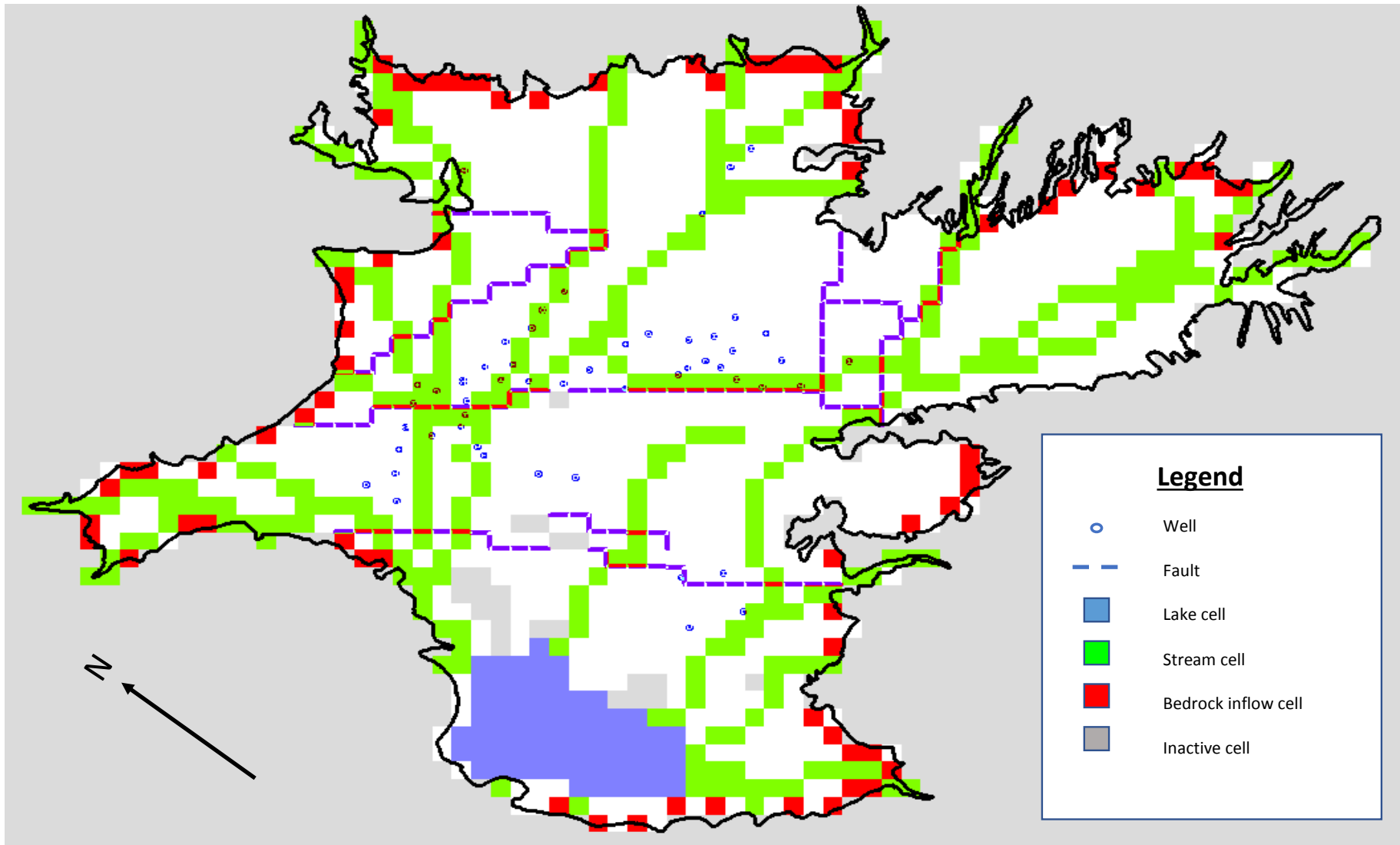
**Figure 14
Model Layer
Extents and
Elevations**



September 2018

TODD 
GROUNDWATER

Figure 15
Aquifer
Parameter Zones

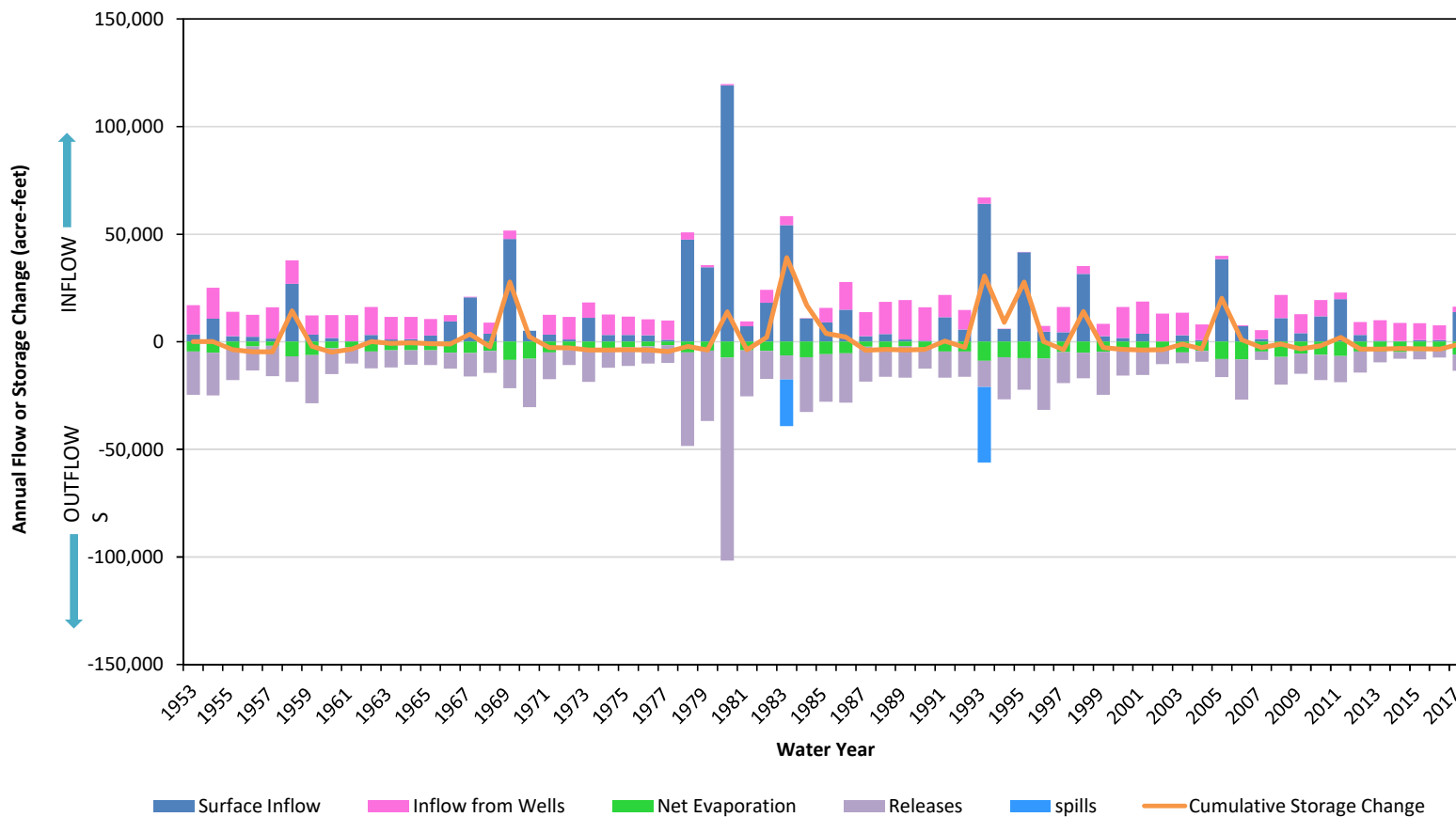


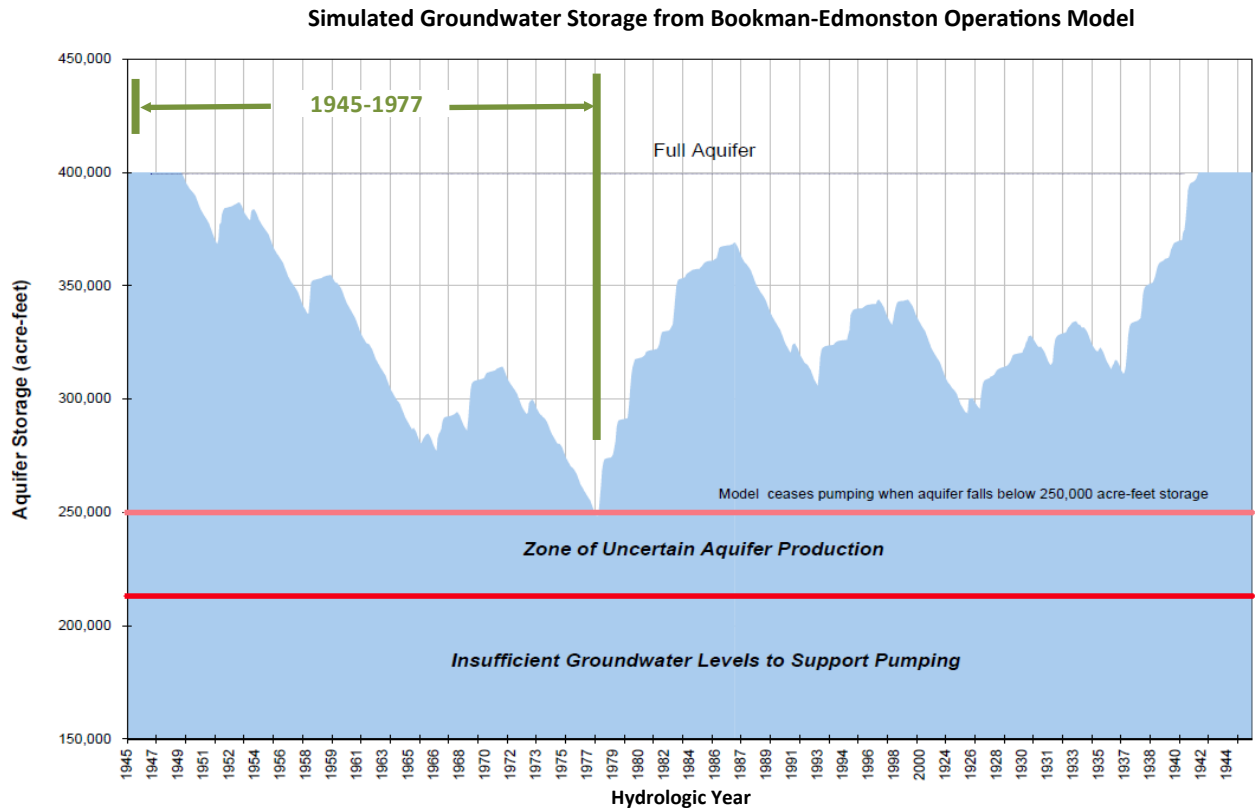
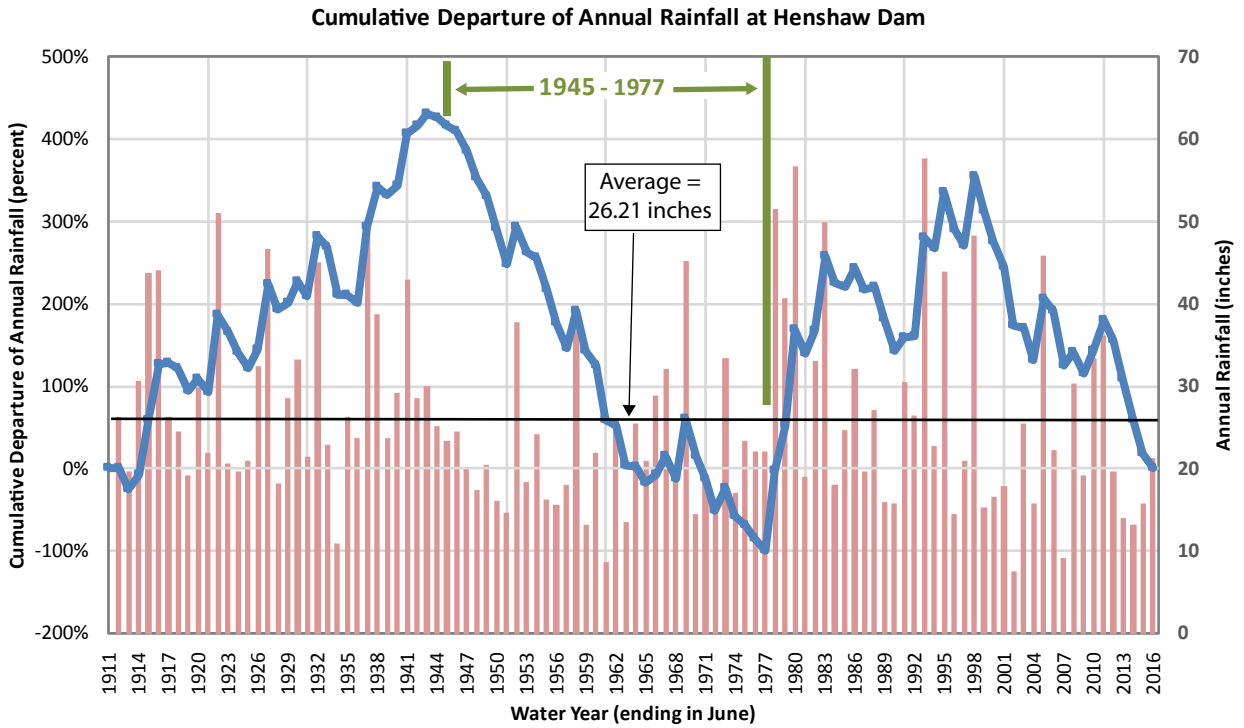
September 2018

TODD
GROUNDWATER

Figure 16
Boundary Conditions
in Groundwater Model

Lake Henshaw Historical Annual Water Balance



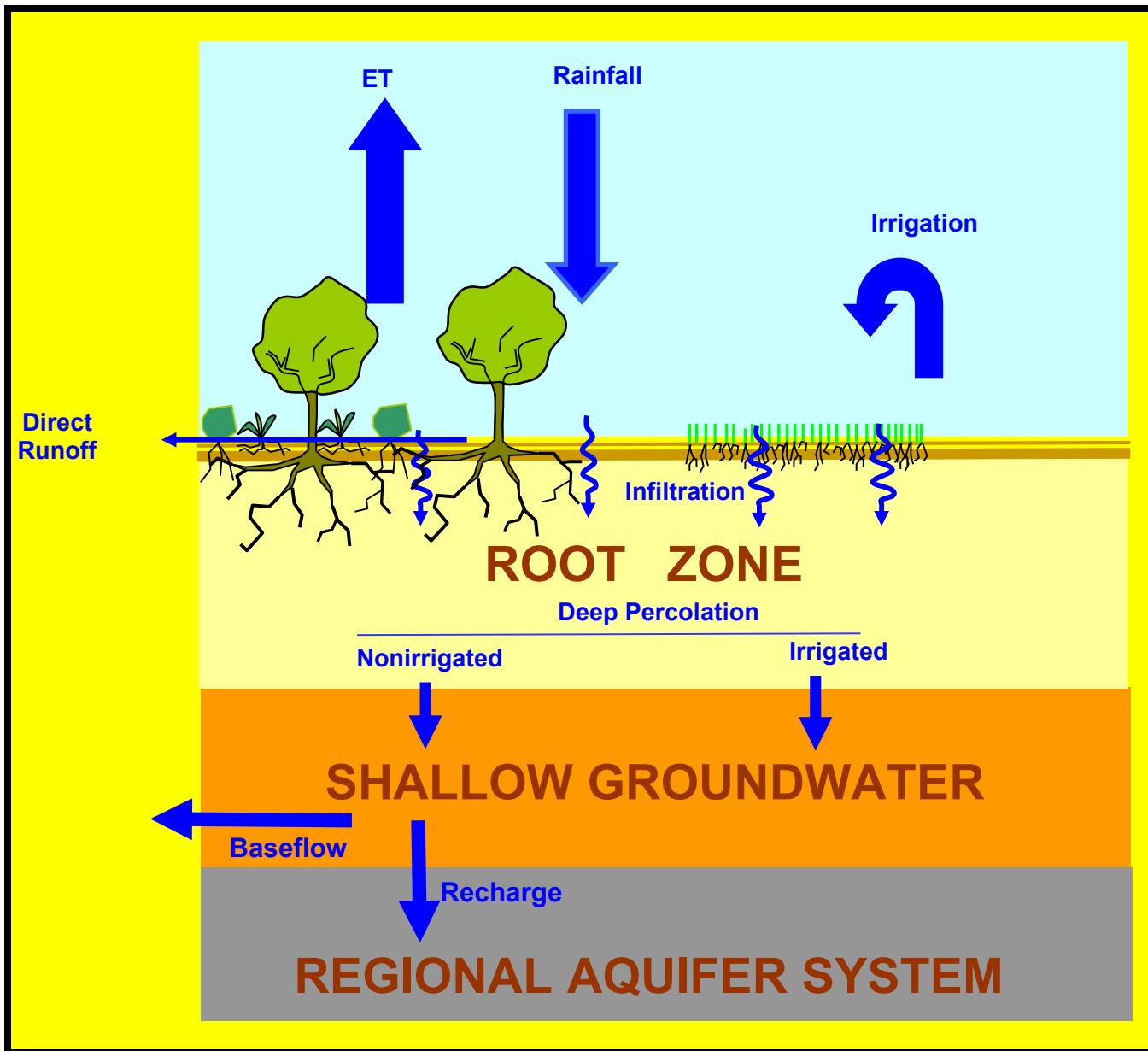


Reproduced from Bookman-Edmonston (2002) Figure 4-8

September 2018

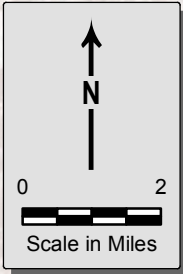
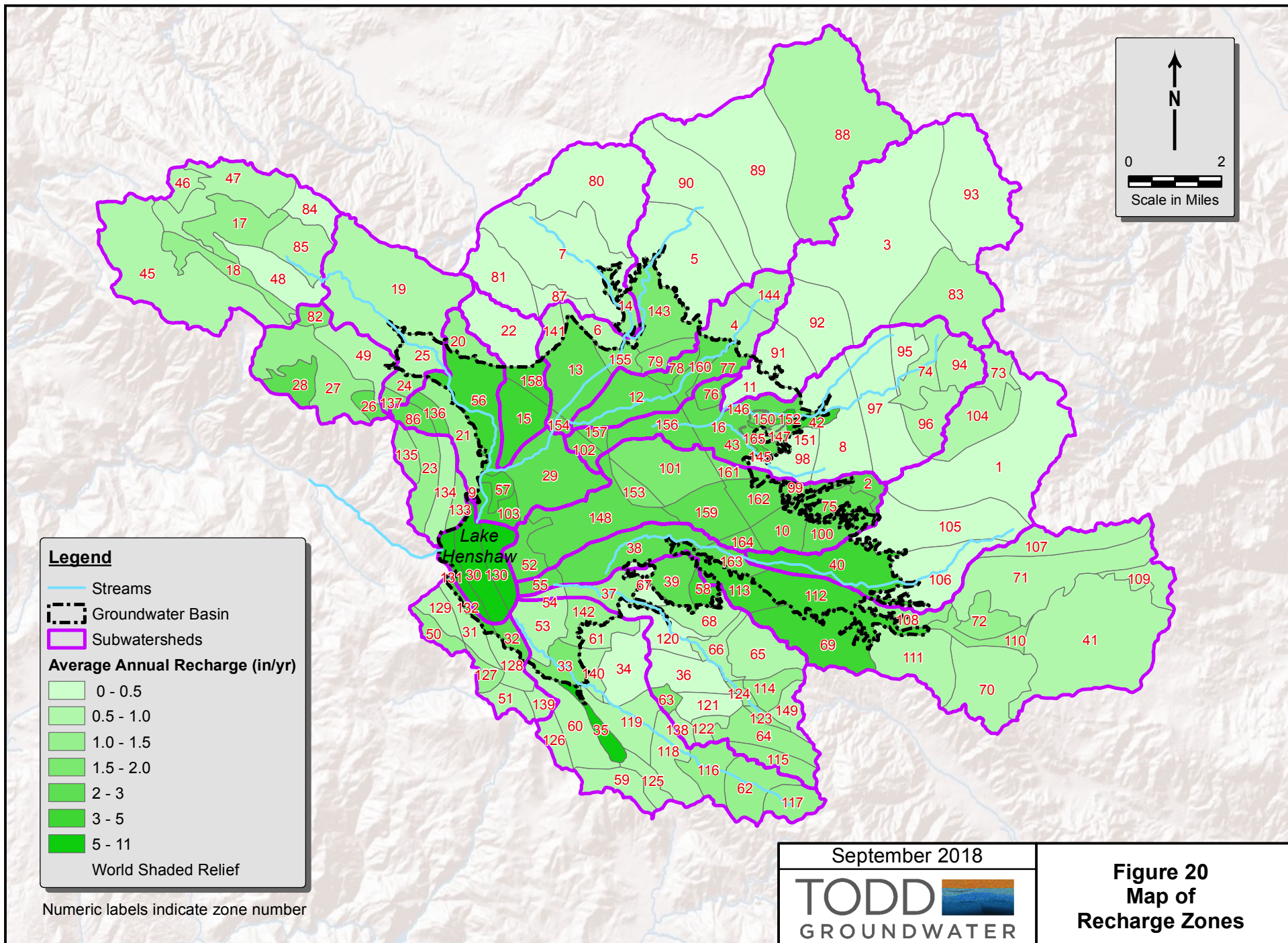
TODD **GROUNDWATER**

Figure 18
1945 - 1977
Design Drought



September 2018

Figure 19
Rainfall-Runoff-
Recharge
Processes



Legend

- Streams
- Groundwater Basin
- Subwatersheds

Average Annual Recharge (in/yr)

- 0 - 0.5
- 0.5 - 1.0
- 1.0 - 1.5
- 1.5 - 2.0
- 2 - 3
- 3 - 5
- 5 - 11

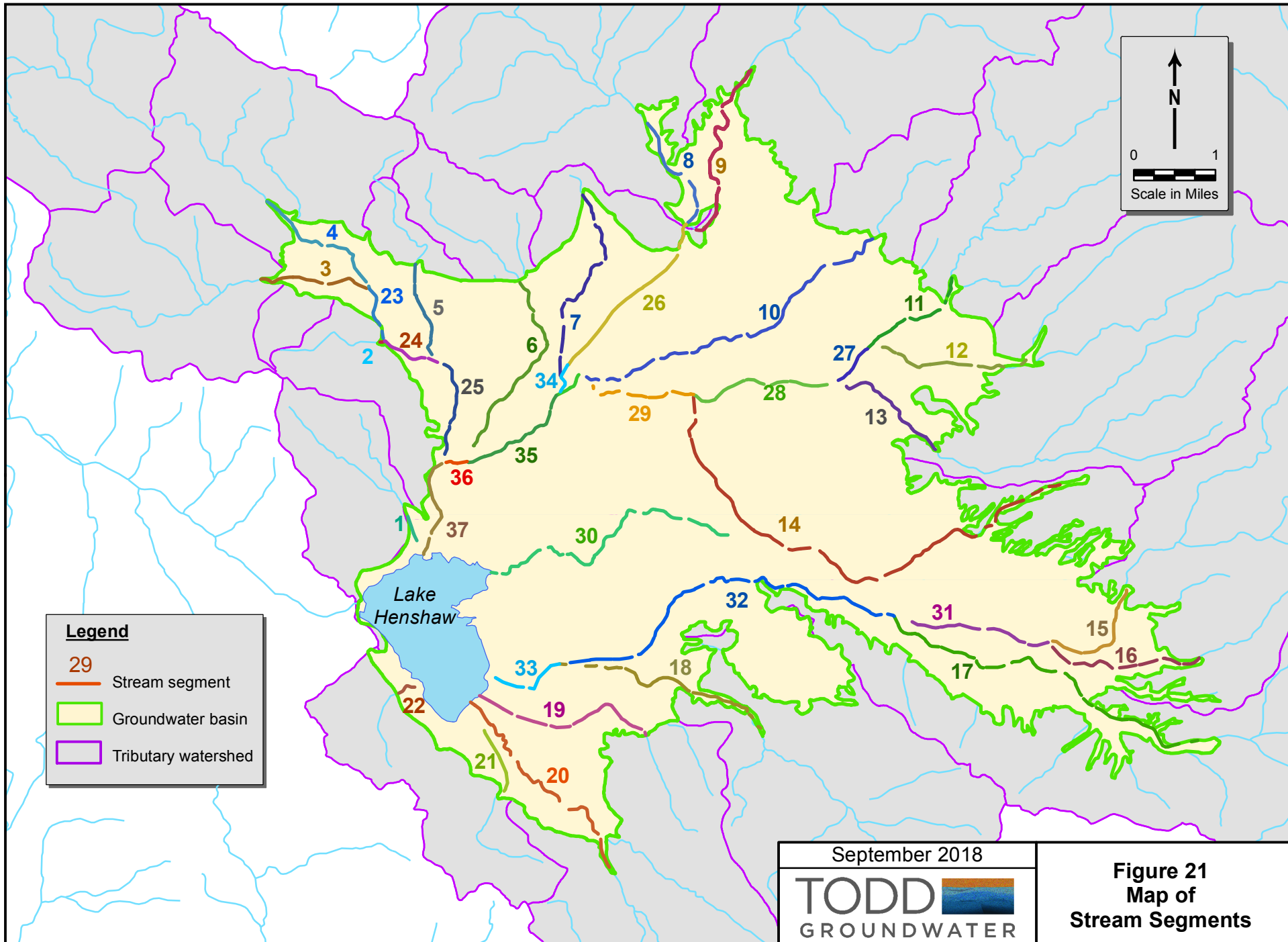
World Shaded Relief

Numeric labels indicate zone number

September 2018

TODD
GROUNDWATER

Figure 20
Map of
Recharge Zones



Legend

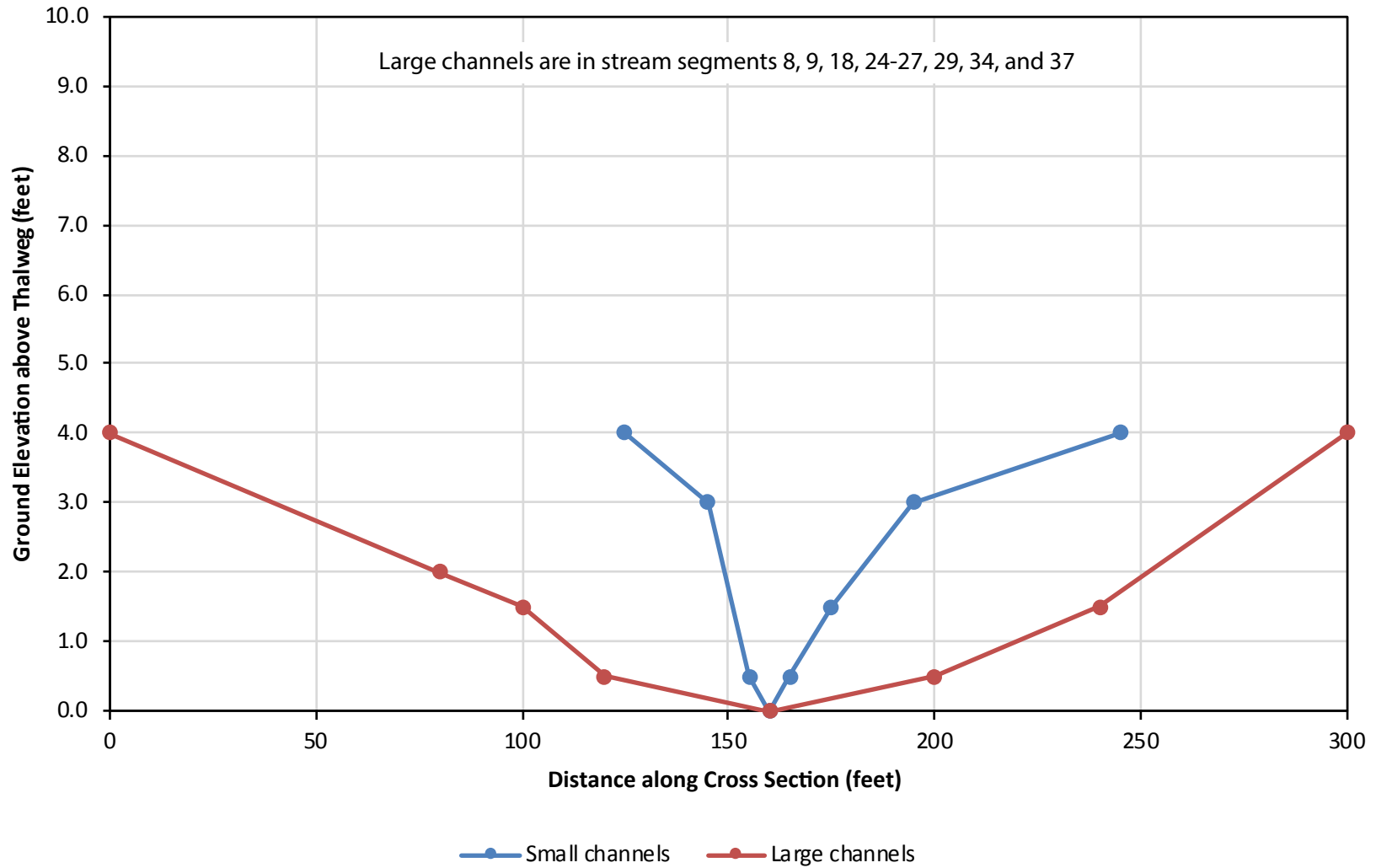
- 29 Stream segment
- Groundwater basin
- Tributary watershed

September 2018

TODD 
GROUNDWATER

Figure 21
Map of
Stream Segments

Channel Cross Section



September 2018



Figure 22
Stream Channel
Cross Sections

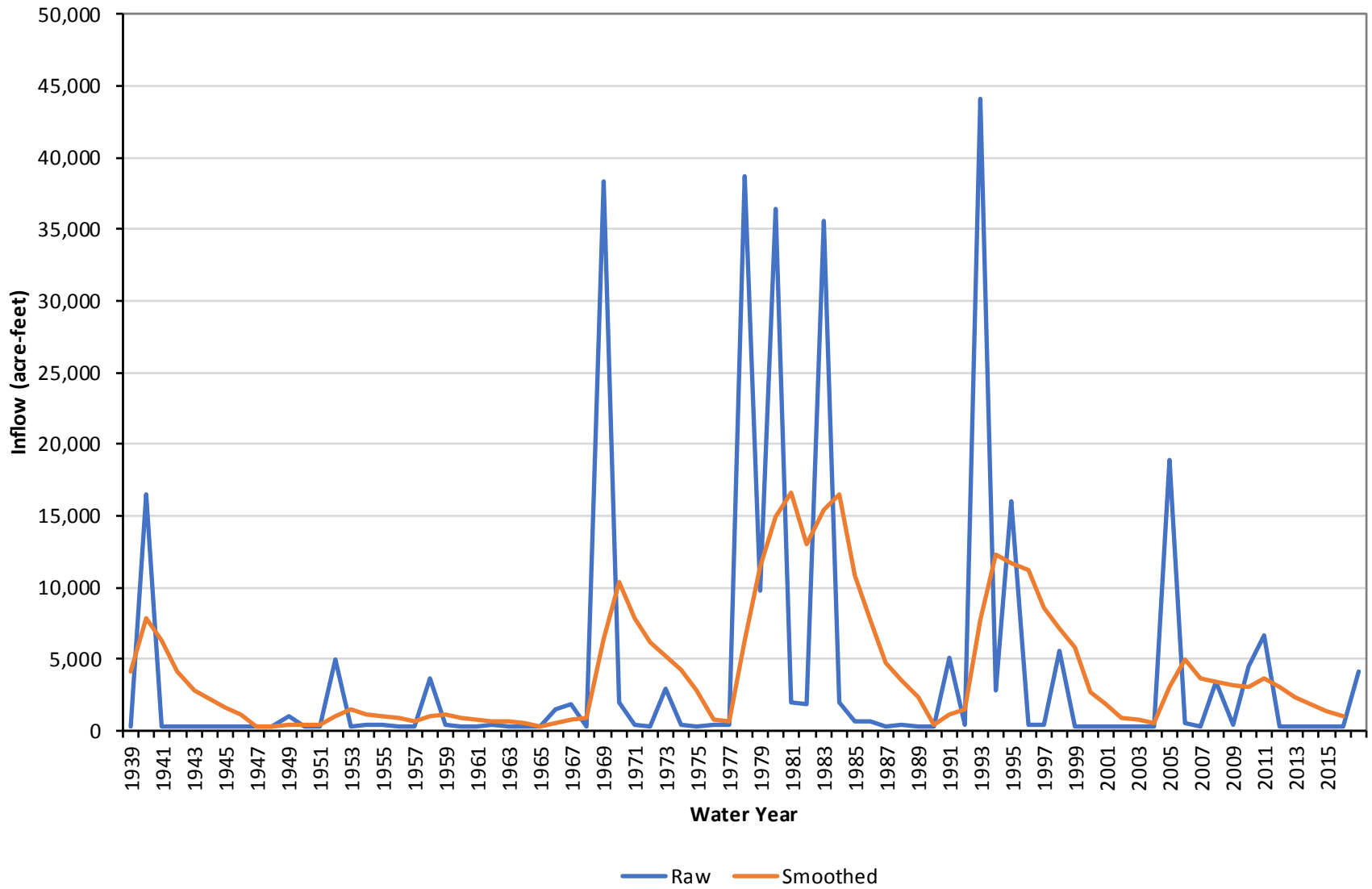
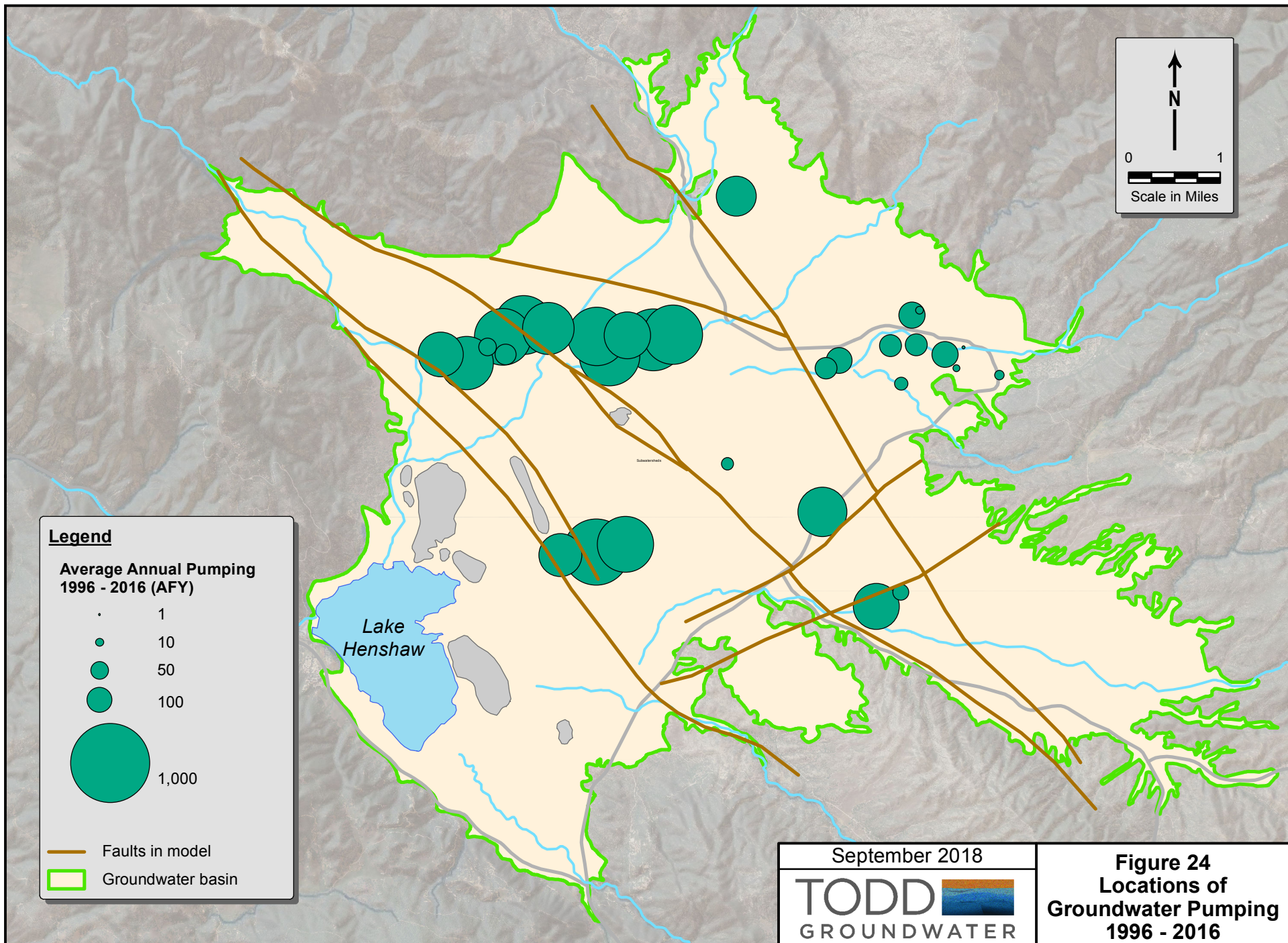


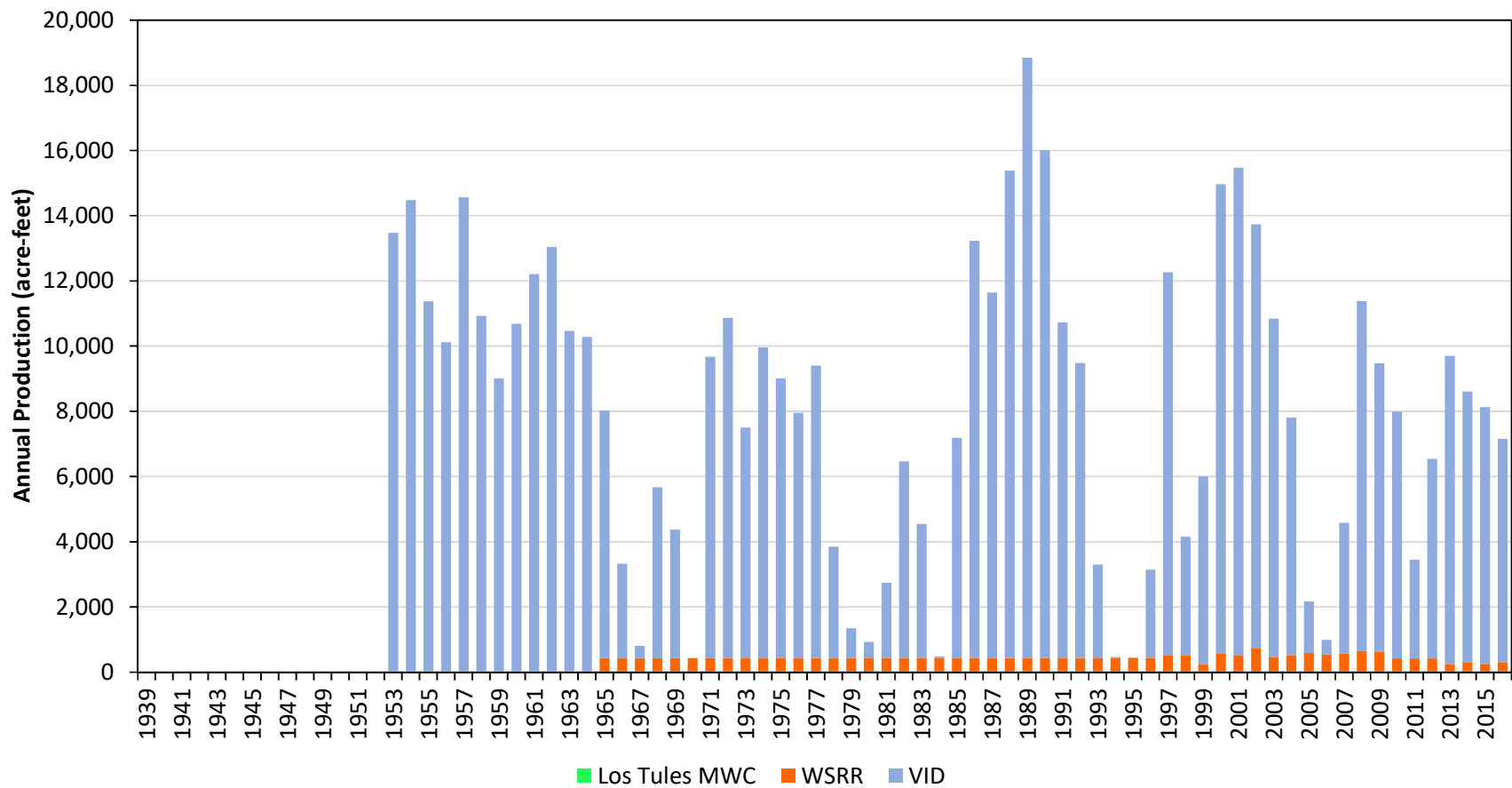
Figure 23
Total Bedrock
Inflow to Basin

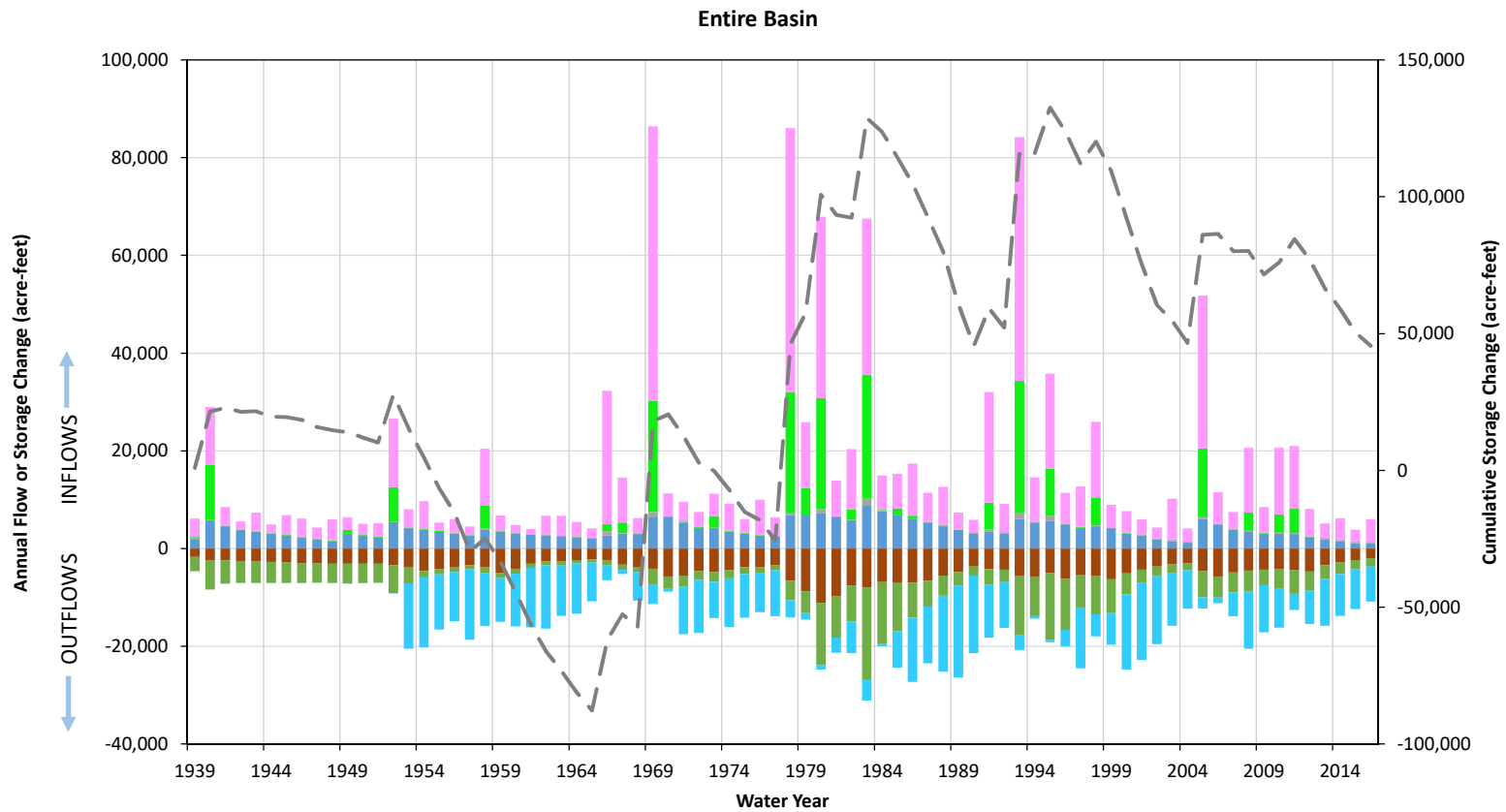


September 2018

TODD
GROUNDWATER

Figure 24
Locations of
Groundwater Pumping
1996 - 2016



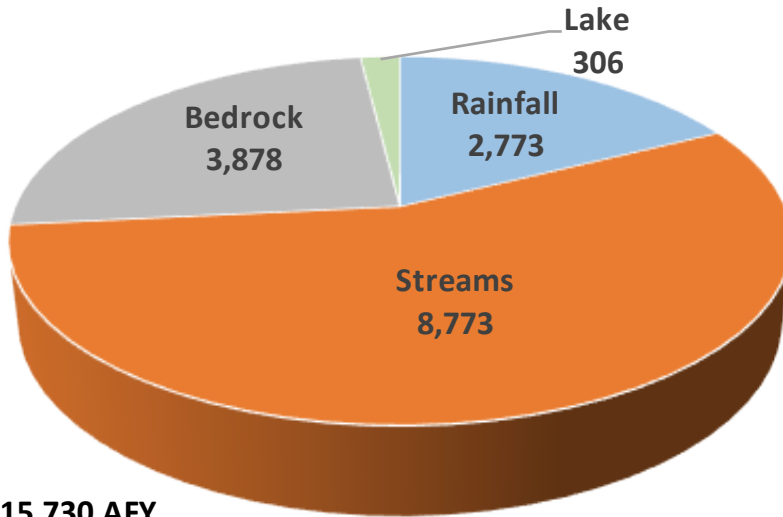


- | | | | |
|----------------|------------|-------------------|---------------------------|
| Bedrock inflow | From lake | Rainfall Recharge | From streams |
| To Lake | To streams | Well pumping | Cumulative Storage Change |

September 2018

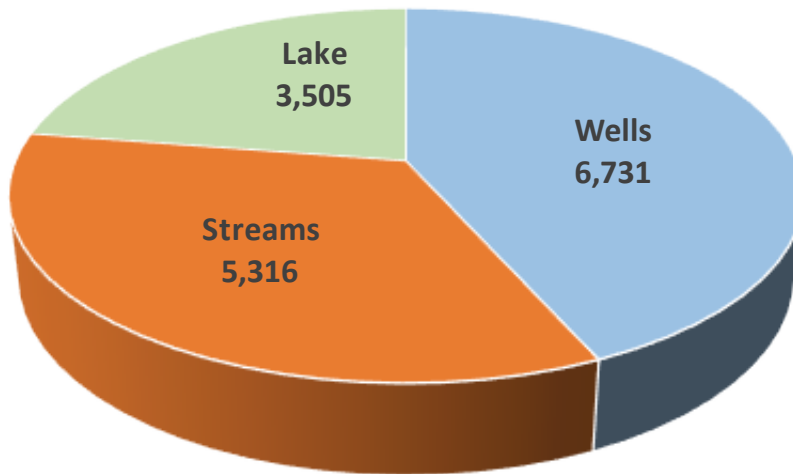
Figure 26
Annual Basin-Wide
Groundwater Balances,
1939-2016

Basin-wide Inflows



Total = 15,730 AFY

Basin-wide Outflows



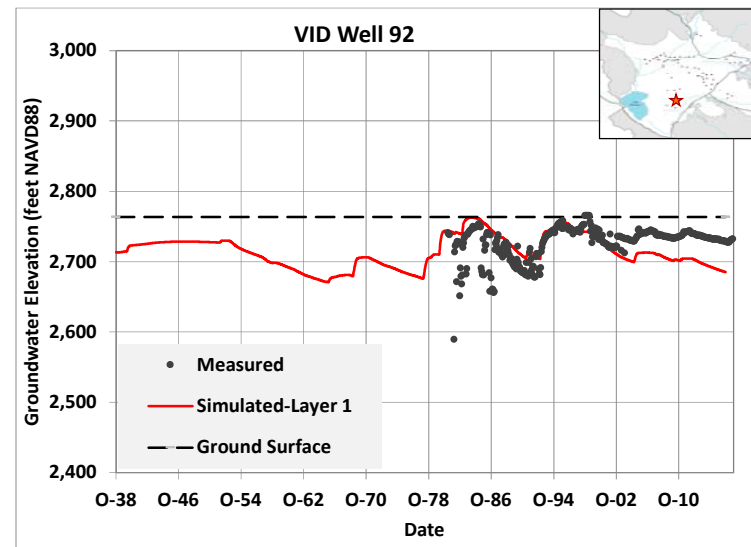
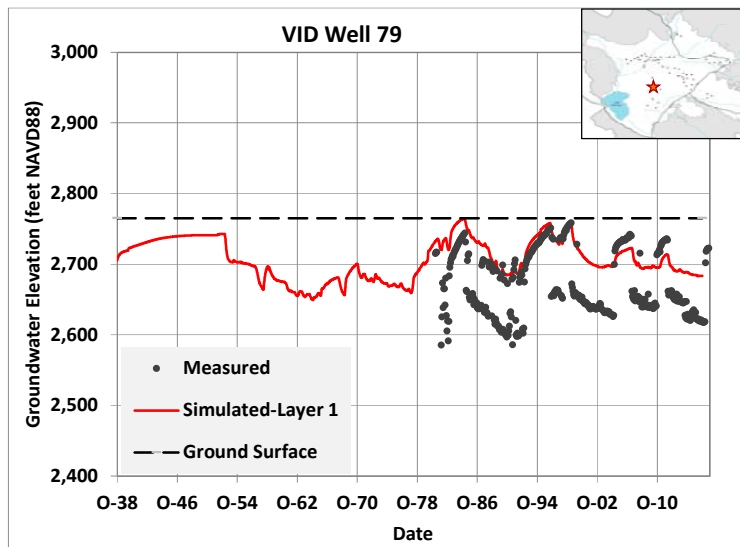
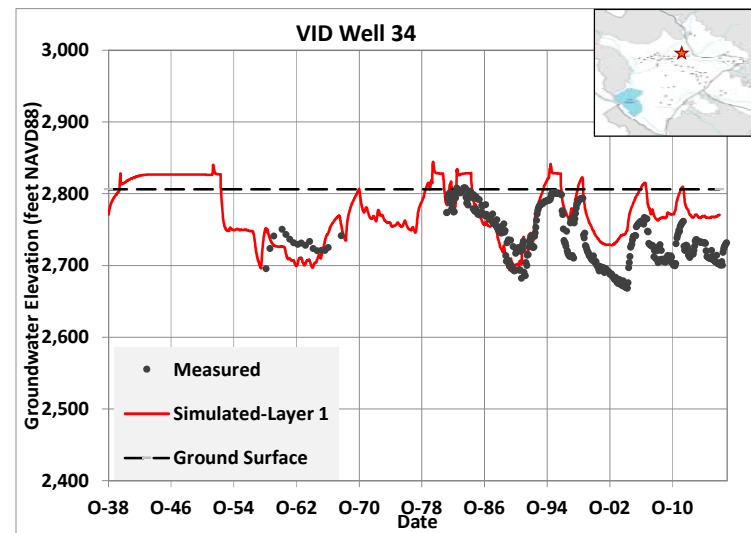
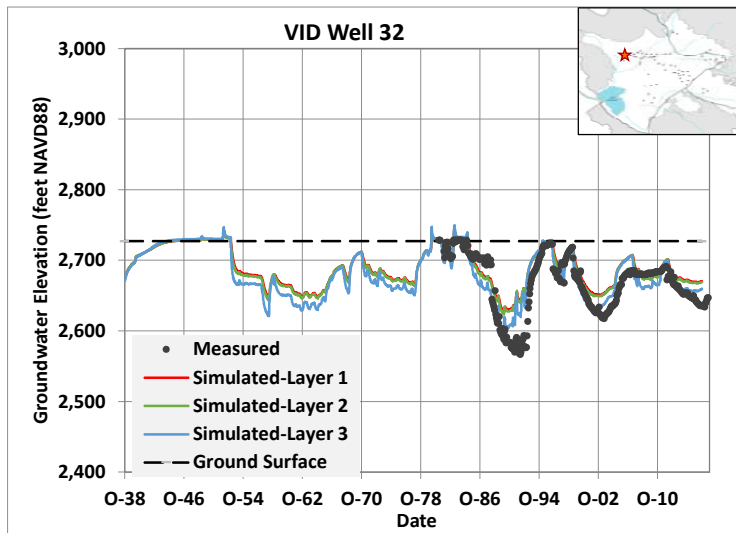
Total = 15,260 AFY

Note: the difference between total inflows and total outflows reflects a net increase in simulated Basin storage from 1939 to 206, probably as a result of underestimating groundwater levels in 1939.

September 2018



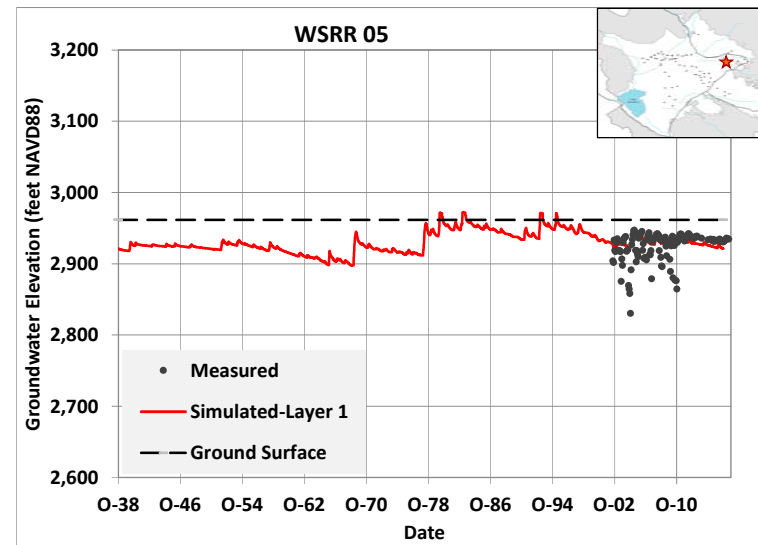
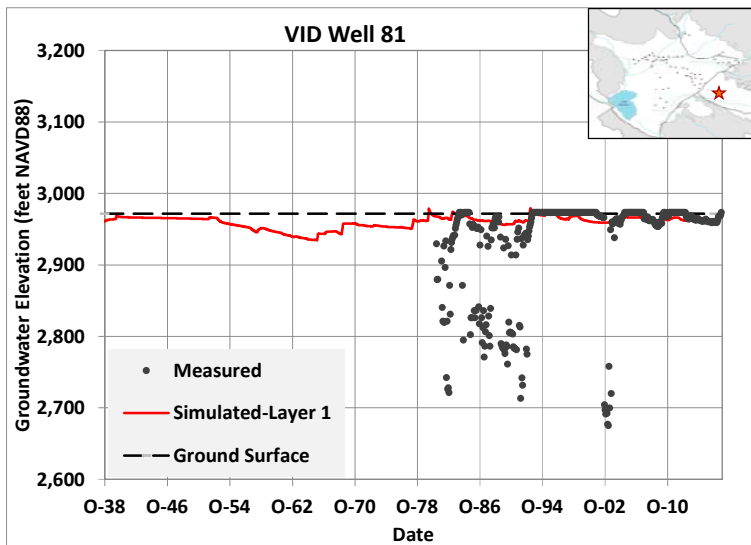
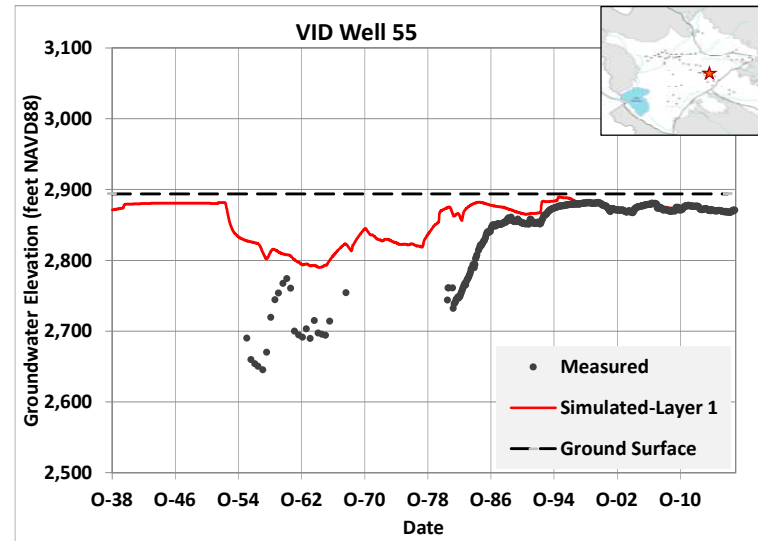
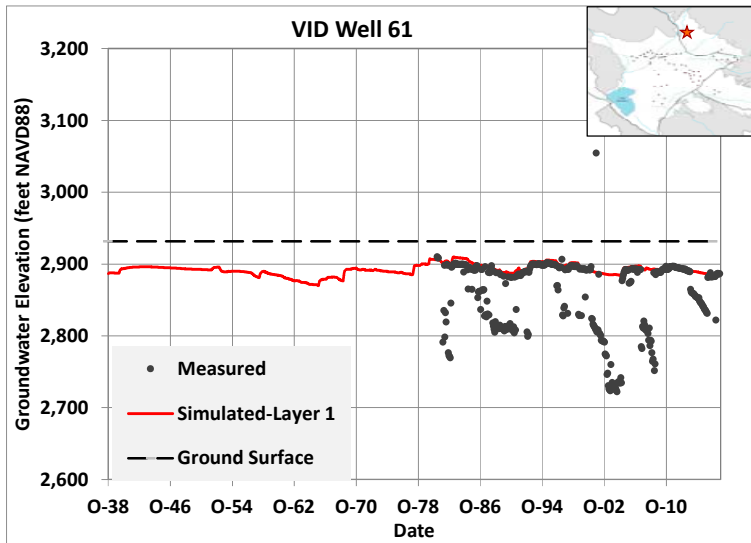
Figure 27
Average Annual
Groundwater Balance
1939 - 2016

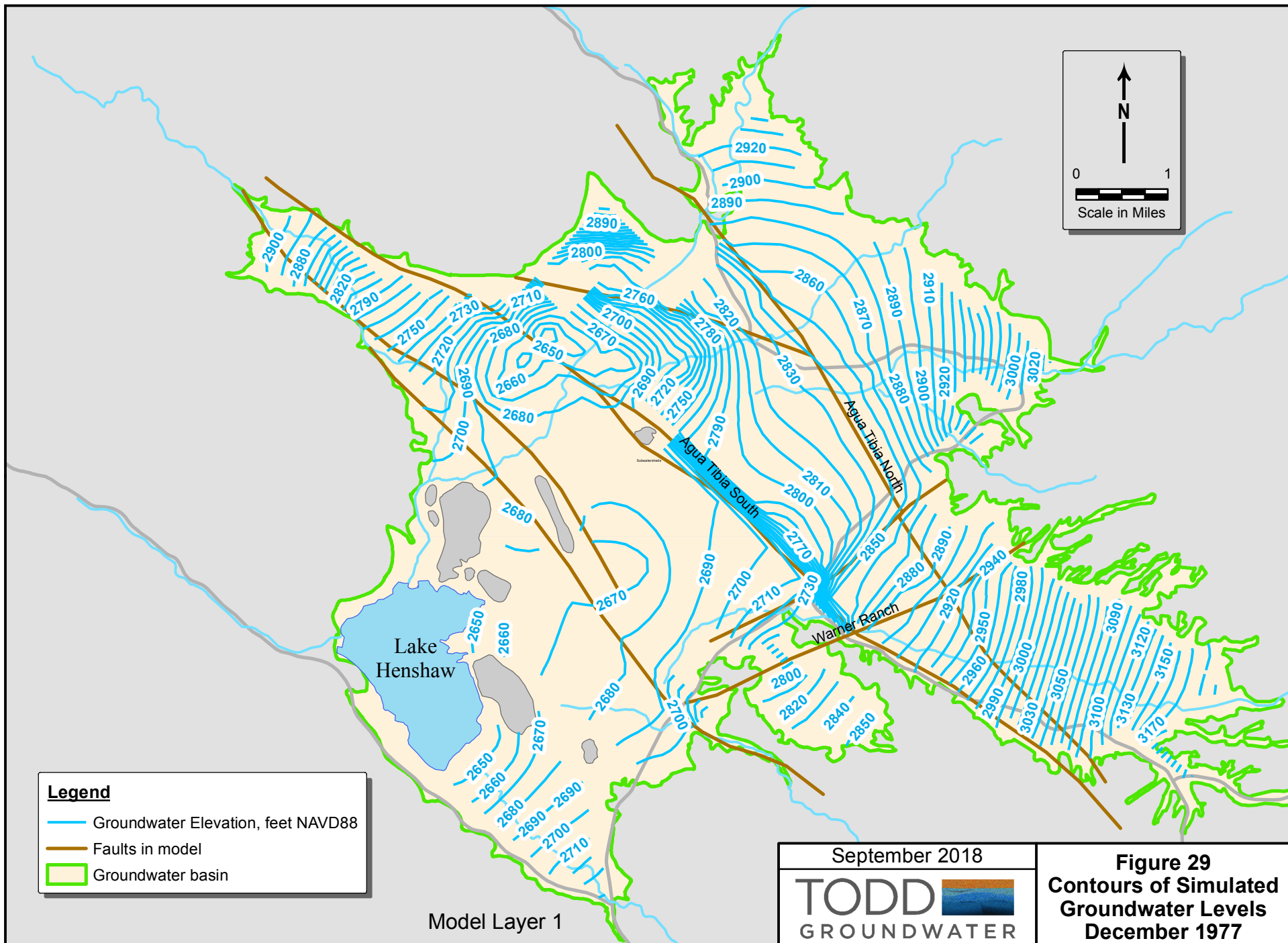


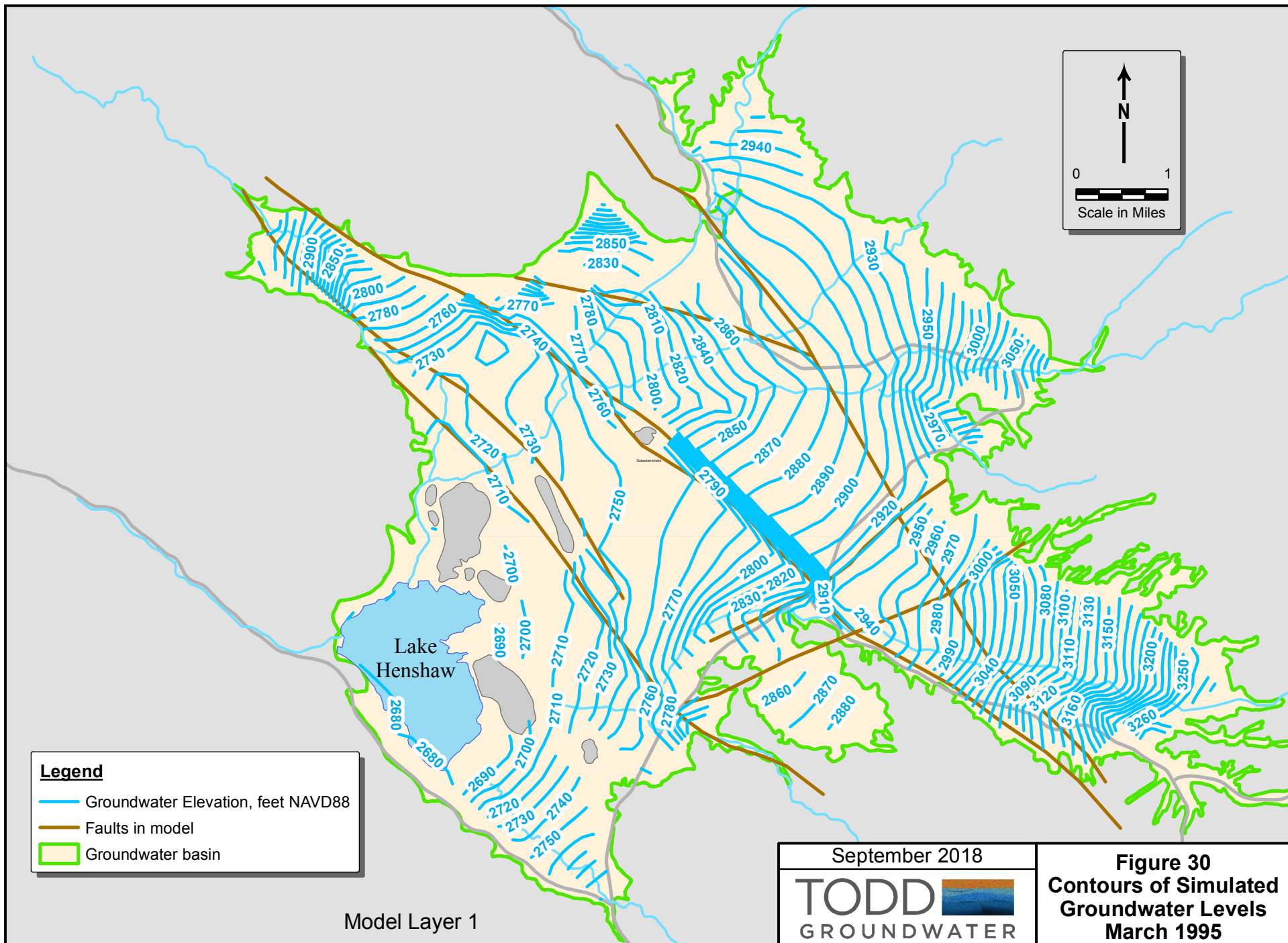
September 2018



Figure 28a
Hydrographs of Measured
and Simulated Groundwater
Levels







Legend

- Groundwater Elevation, feet NAVD88
- Faults in model
- Groundwater basin

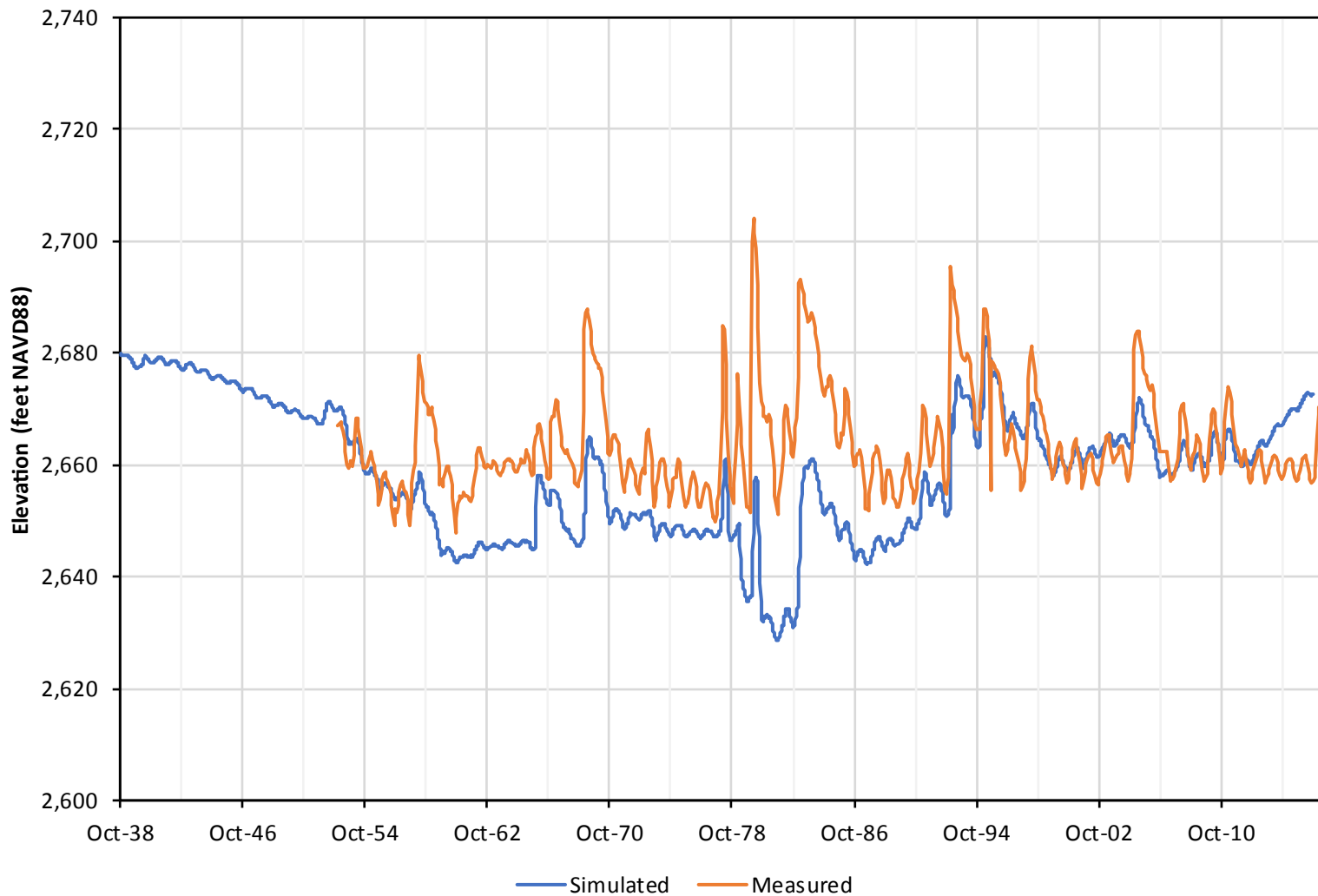
Model Layer 1

September 2018

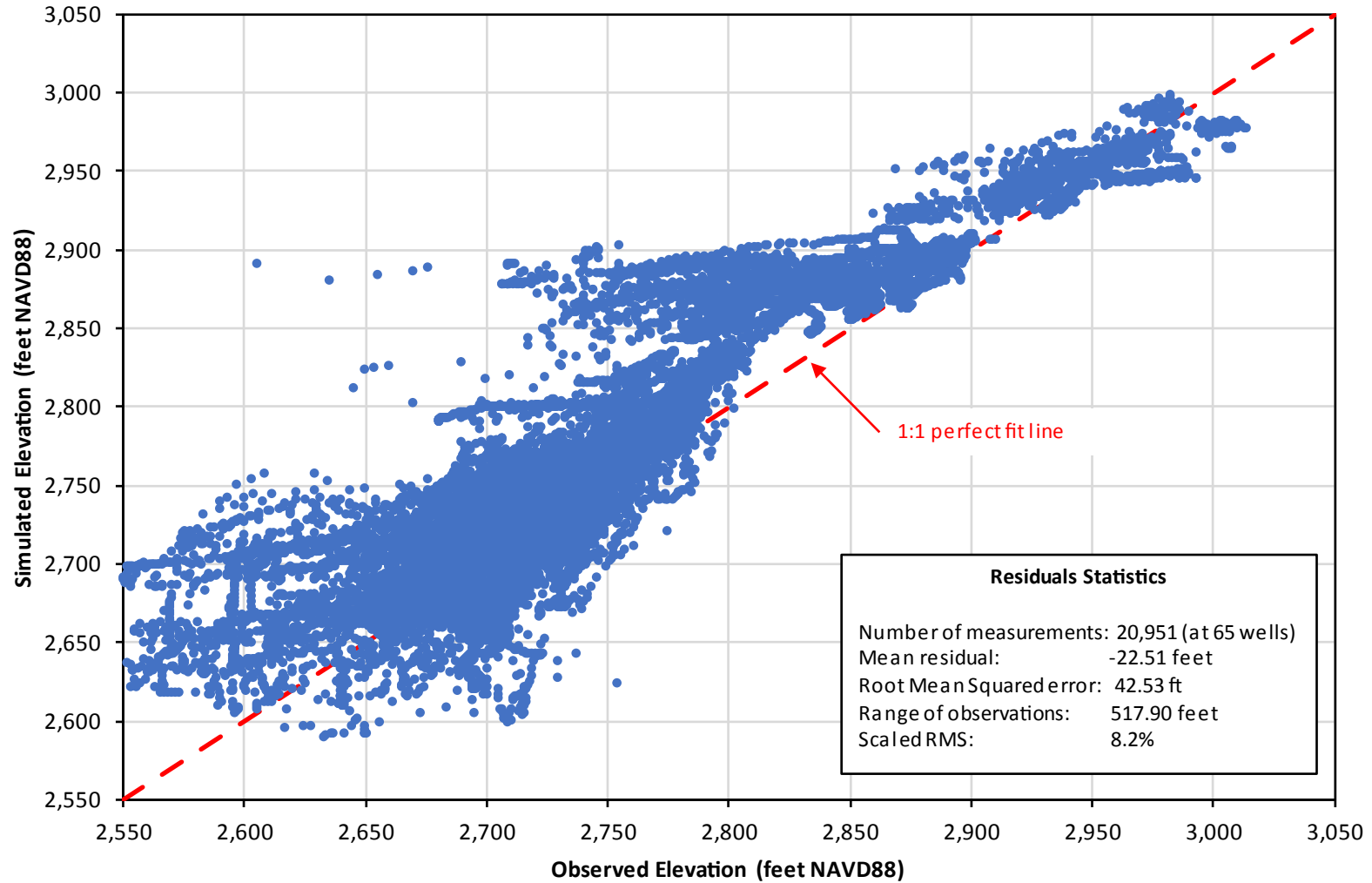
TODD **GROUNDWATER**

Figure 30
Contours of Simulated
Groundwater Levels
March 1995

Lake Henshaw Surface Elevation



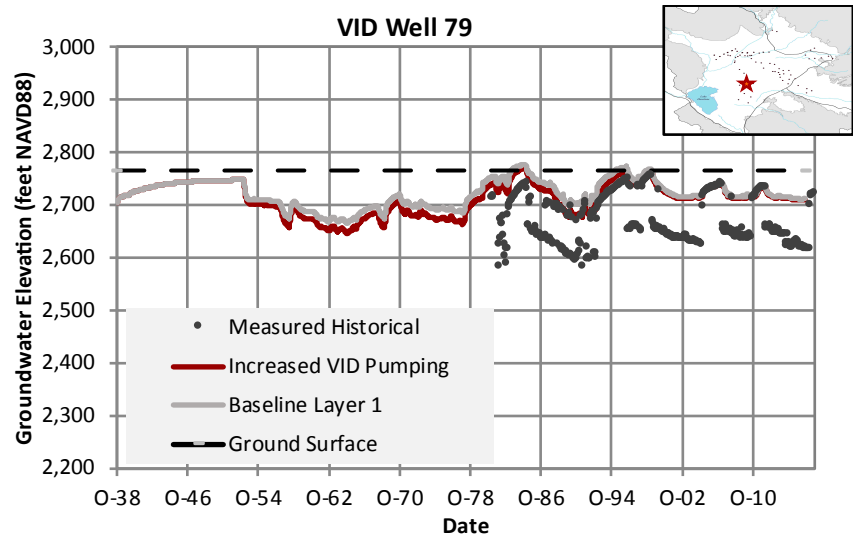
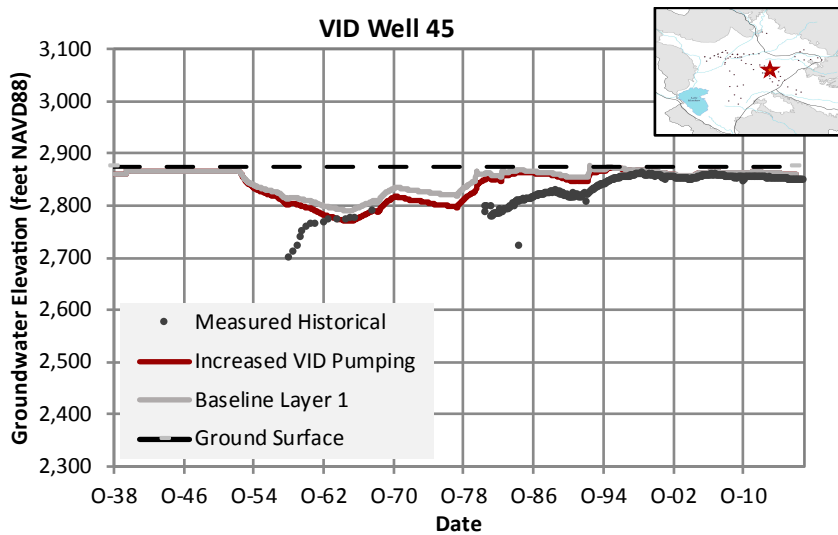
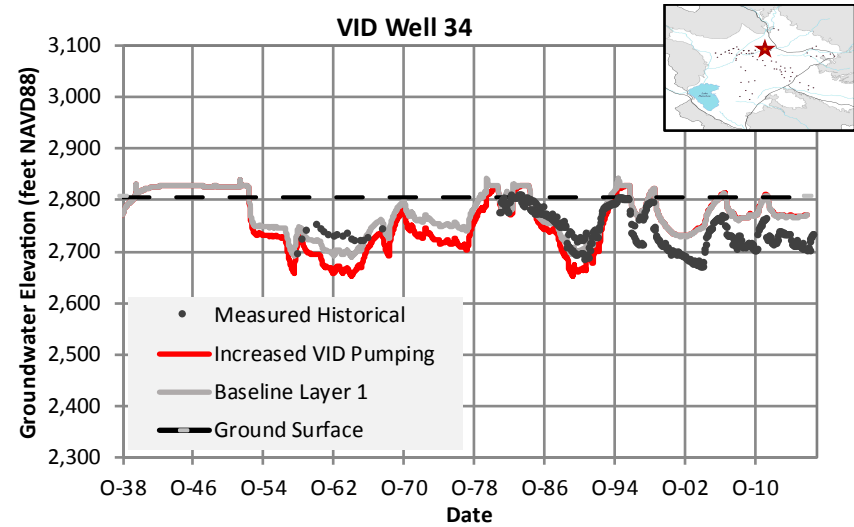
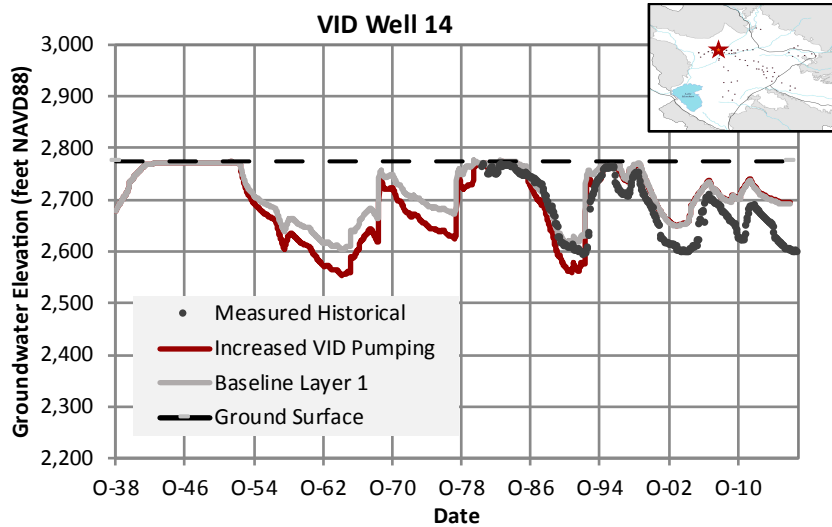
Simulated vs. Observed Water Levels

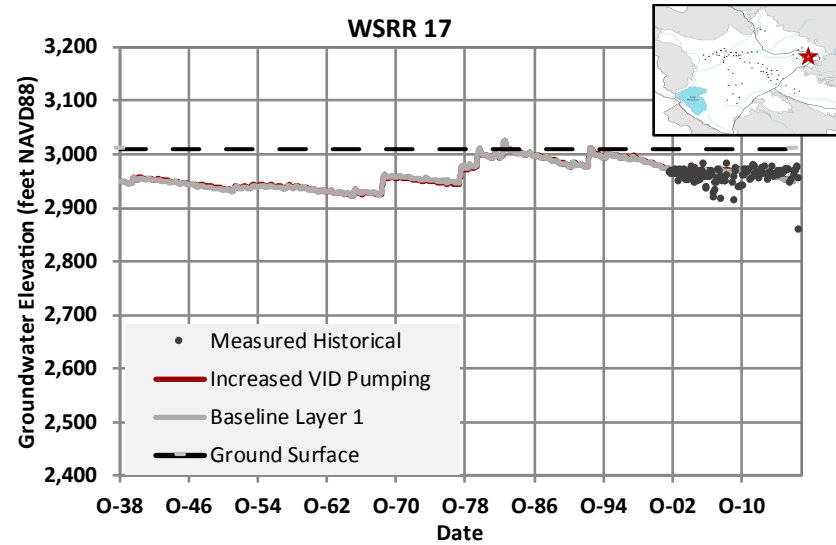
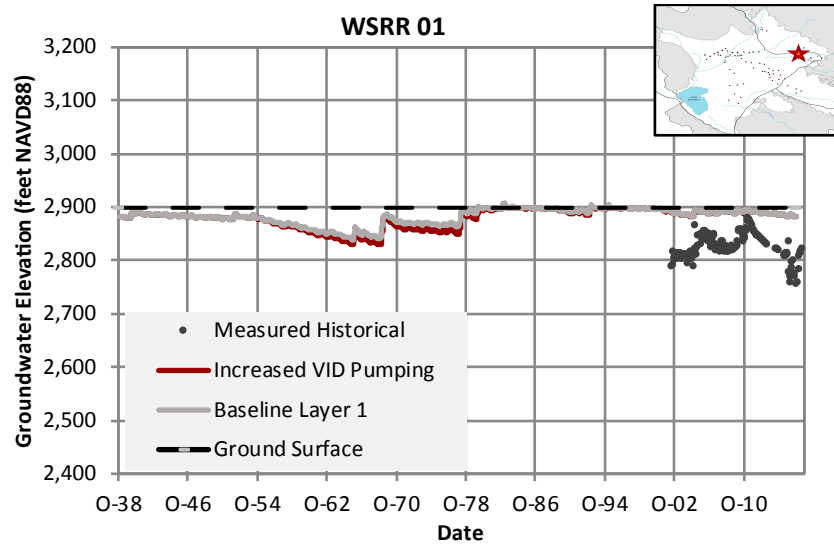
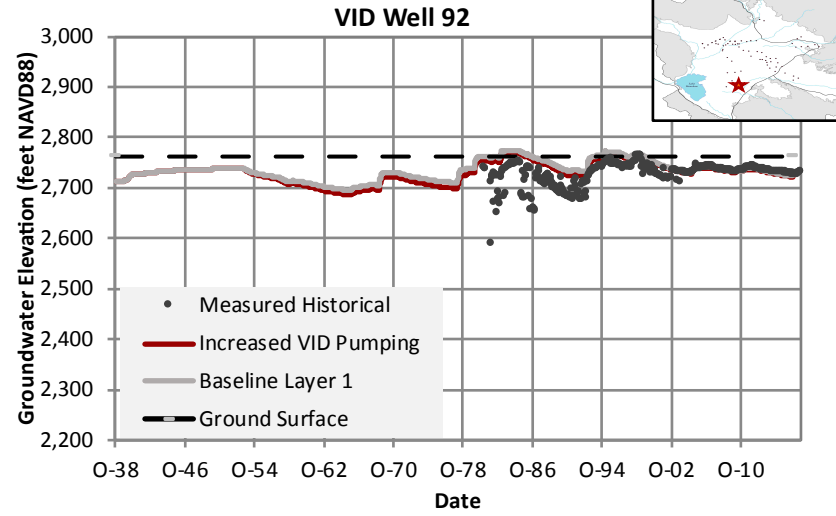
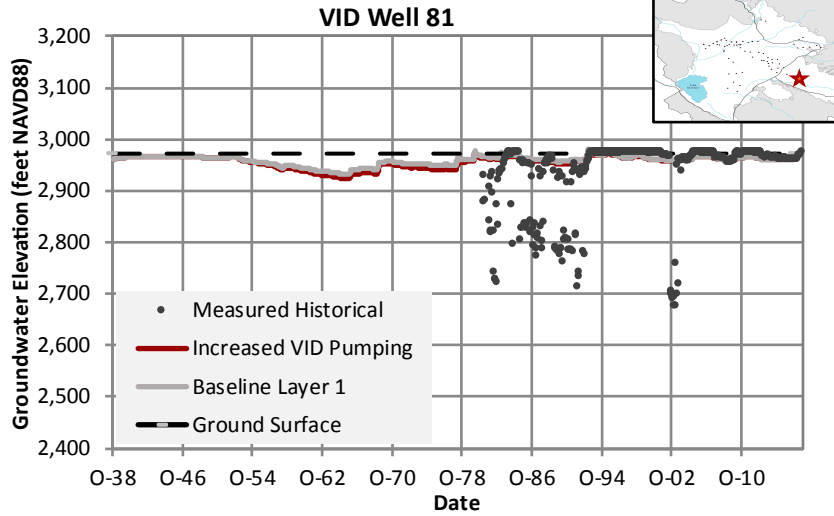


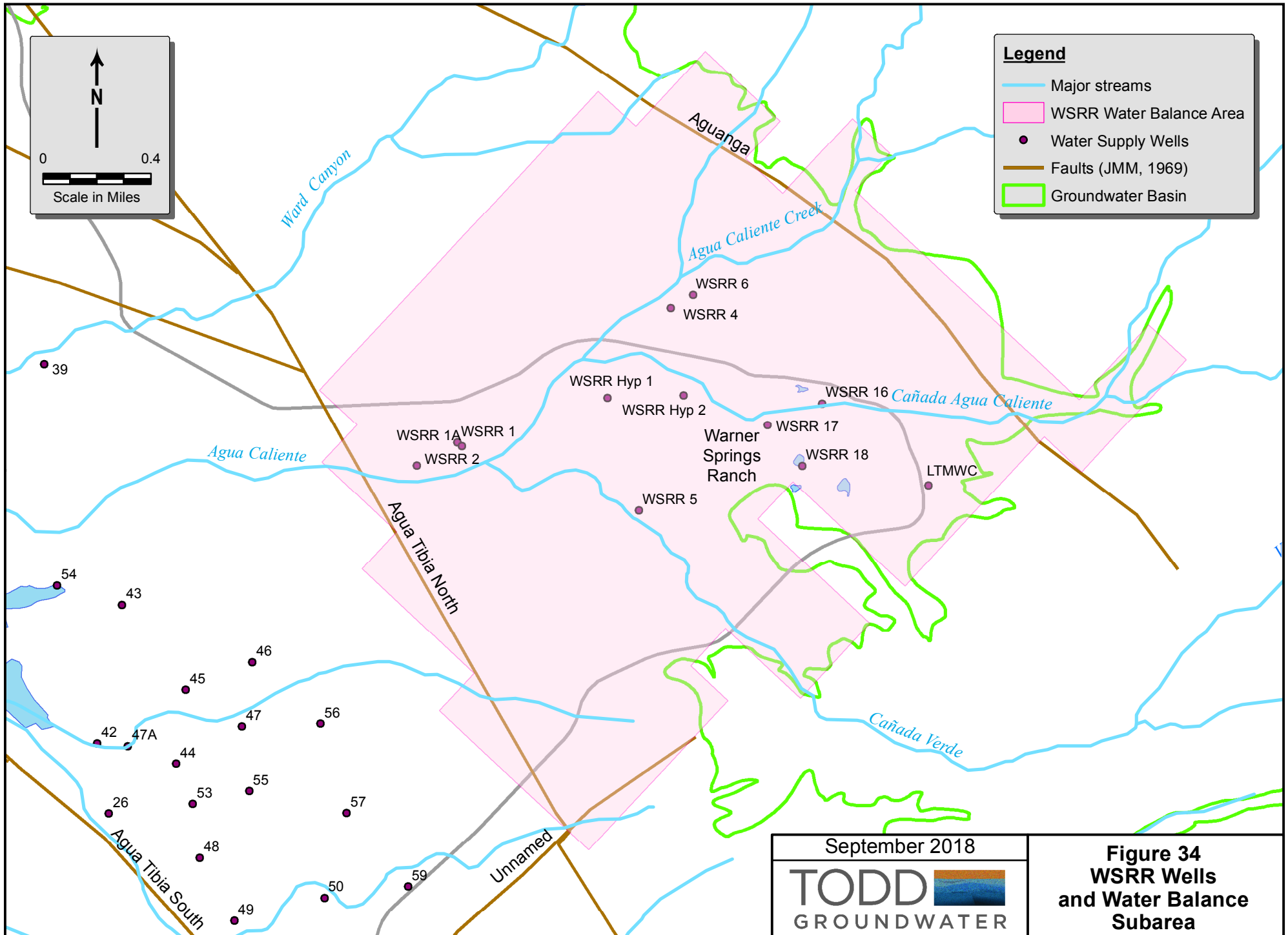
September 2018

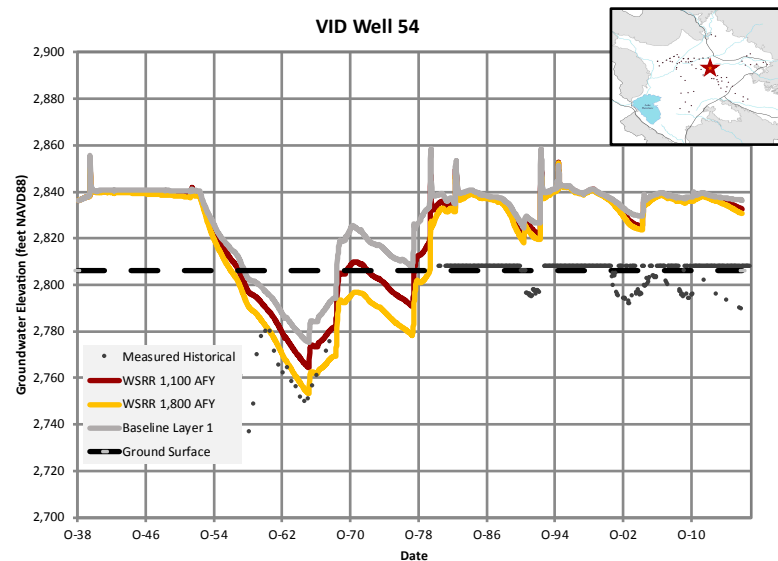
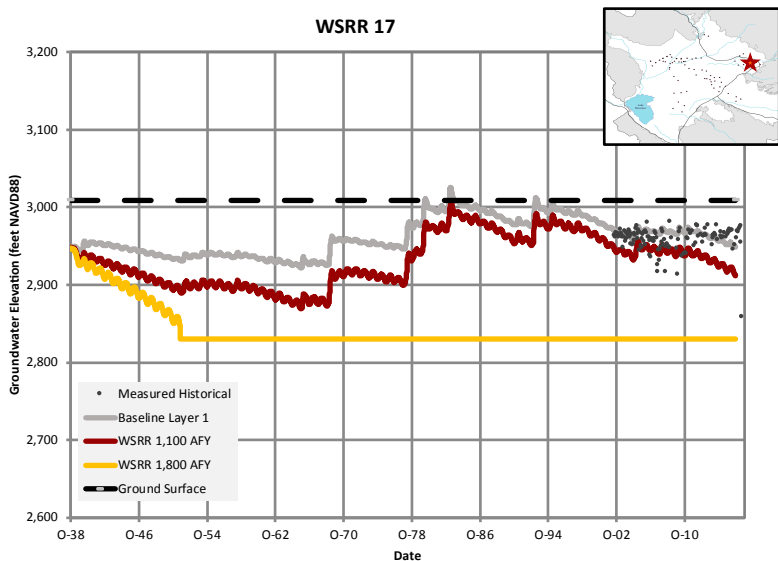
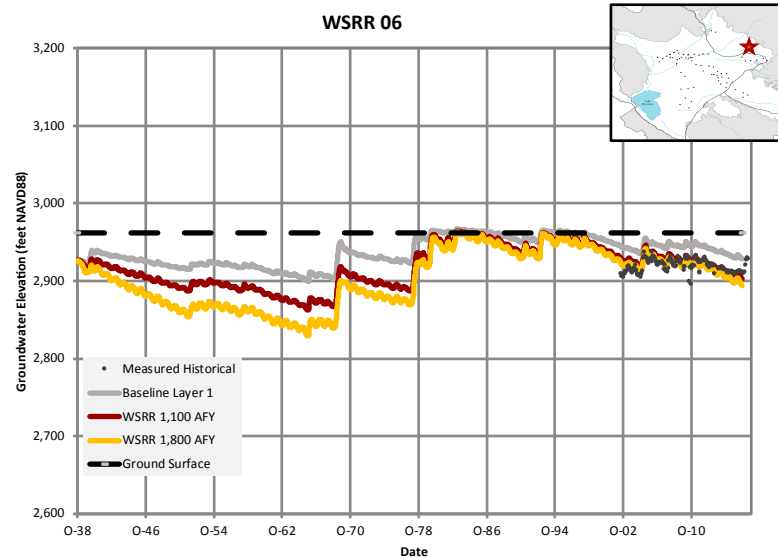
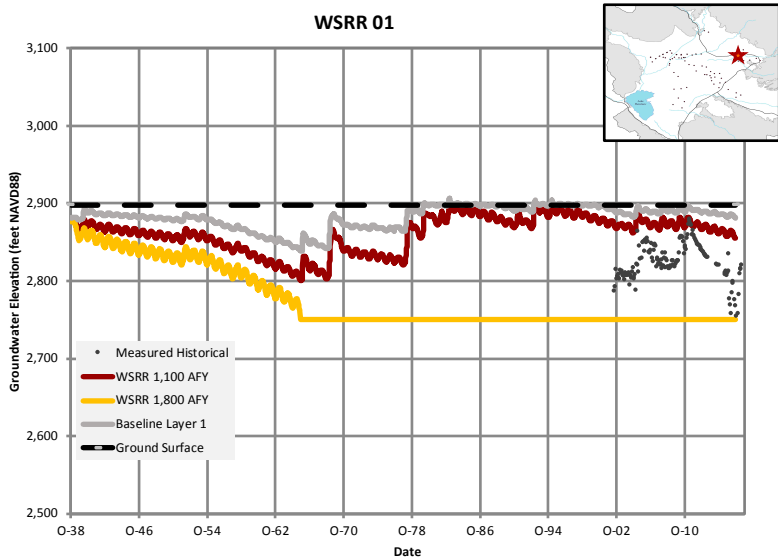


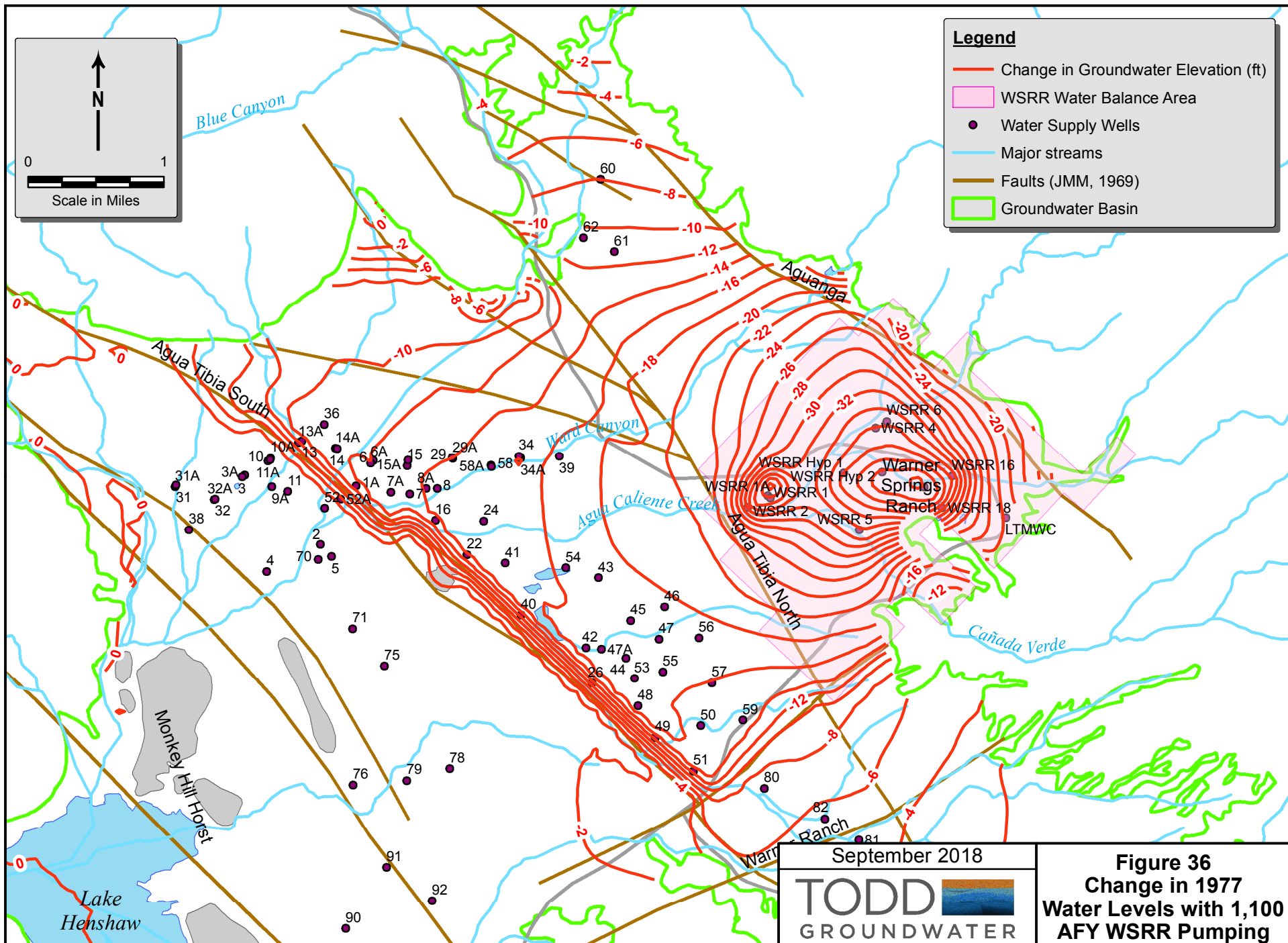
Figure 32
Scatterplot of
Simulated and
Observed Water Levels



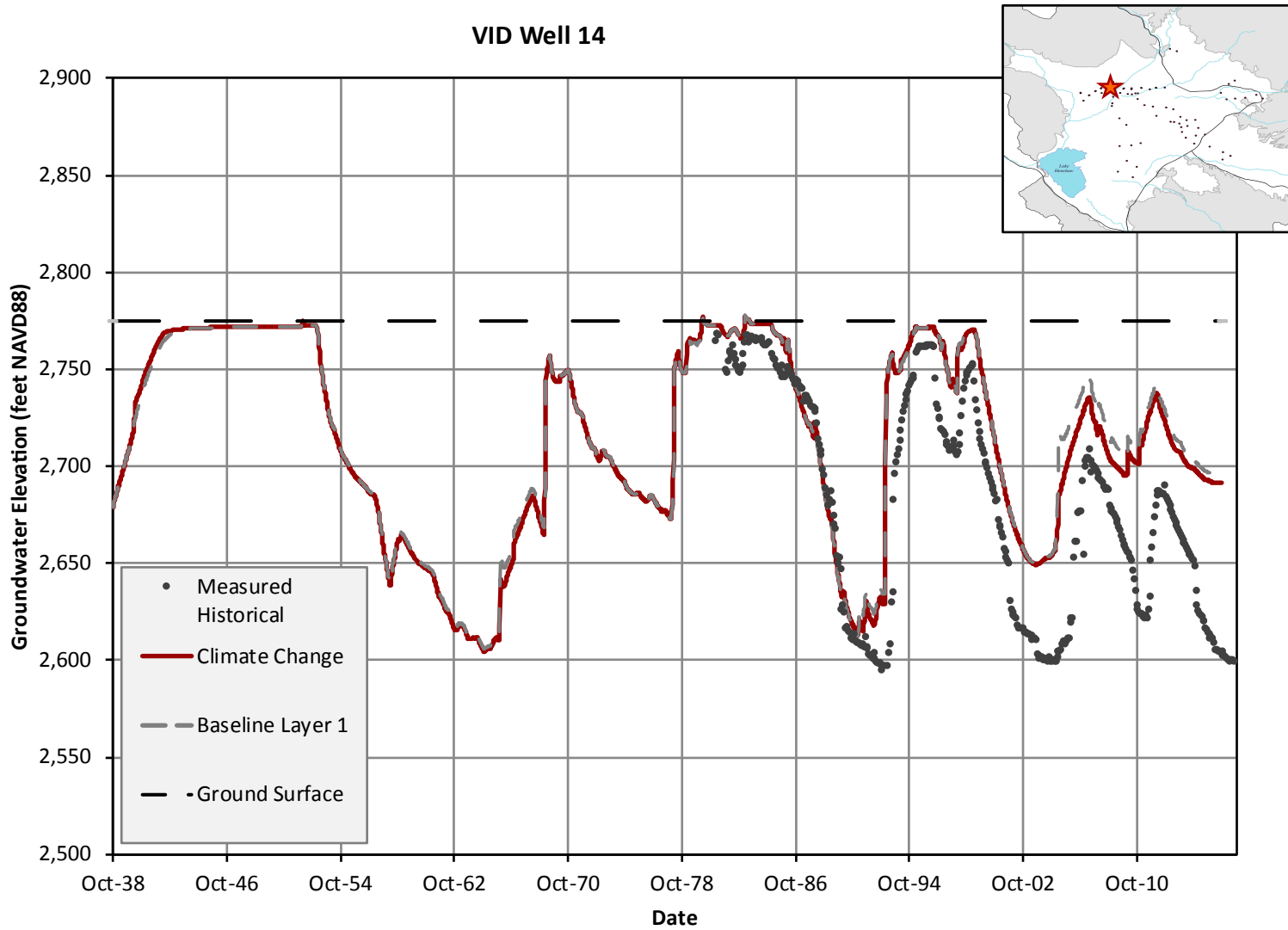


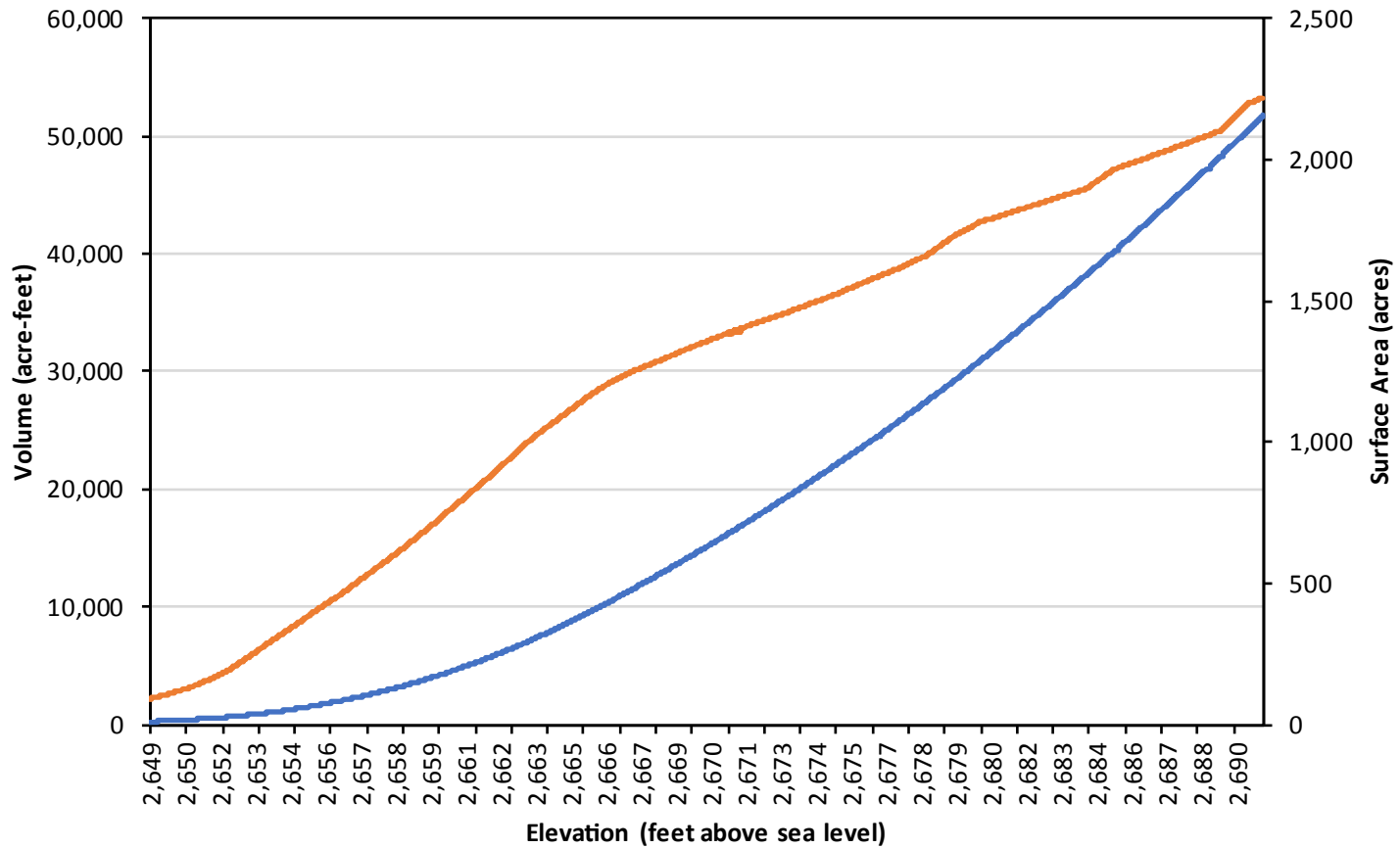






VID Well 14





— Volume — Area

Appendix A. Comparison of Basin Boundary Delineations

This appendix documents a new delineation of the boundary of the Warner Valley Groundwater Basin (Basin) in northwestern San Diego County. This delineation was used in the groundwater modeling and yield analysis described in the main report.

Evaluation of Previous Basin Boundaries

Four previous Basin boundary delineations were compared and evaluated with respect to consistency with detailed geologic mapping and suitability for managing groundwater in the Basin. The four previous delineations are shown in **Figure A-1**. Findings regarding each of the previous delineations are as follows:

Current DWR Bulletin 118 Boundary

The California Department of Water Resources (DWR) has statewide authority to delineate groundwater Basin boundaries for regulatory purposes. Official boundaries of all basins in California were historically published in DWR's Bulletin 118 series. Now the current boundaries are maintained on-line at <https://water.ca.gov/Programs/Groundwater-Management/Bulletin-118>. The origin of DWR's delineation of the Basin (Basin 9-08) is unknown, but the smooth boundary line suggests that it was based on a small-scale regional geologic map. The Basin is intended to include unconsolidated deposits, as distinct from the granitic rocks that form the bedrock surrounding the Basin. Inexplicably, however, the Basin does not include the area around Lake Henshaw between Monkey Hill Horst and the Elsinore Fault. Major previous hydrogeologic studies have all considered the fault to be the western boundary of the Basin and Lake Henshaw to be the natural outflow point for groundwater in the Basin (Scheliga, 1963; James M. Montgomery Consulting Engineers, Inc. (JMM), 1969; Bookman-Edmonston, 2002). This Basin boundary delineation is unsuitable for detailed analysis and groundwater management because it omits a large part of the connected groundwater system.

San Diego County Boundary

This delineation was obtained as a geographic information system (GIS) shapefile downloaded from the Regional GIS Data Warehouse maintained by the San Diego Association of Governments and SanGIS (<http://www.sangis.org/download/index.html>). Metadata for the shapefile do not indicate the source of the delineation. This delineation deviates substantially from the other delineations to include areas with groundwater users. For example, it extends north along State Highway 79 to include Holcomb Village, to the east along County Road 22 to include Ranchita (which Bulletin 118 considers a separate groundwater basin), and to the south along State Highway 79 to include irrigated cropland near Carrista Creek. San Diego County staff have informally reported that this delineation was done for planning and resource management purposes and was not intended to substitute for or supersede the Bulletin 118 boundary (Trey Driscoll, Dudek, personal communication, October 5, 2017). This delineation is unsuitable for detailed analysis because it departs too dramatically from the geologic boundaries of the Basin.

John Scheliga Boundary

John Scheliga's master's thesis includes a geologic map figure and another figure on which the Basin boundary is indicated. His mapping units consisted of alluvium, residuum, Pauba Formation, Temecula Formation, and various types of older igneous rocks. He completed his own mapping of surficial geology at a scale of 1:24,000 in 45 days of field work. Conceptually, the Basin boundary was the extent of the aforementioned unconsolidated deposits. There were two problems with transcribing his Basin boundary into a digital format:

- His Basin boundary line was sometimes inconsistent in following fingers of alluvium up small tributary canyons.
- When the geologic map and Basin boundary figure image files were georeferenced using the same control points (five road points and one stream point), his boundary line did not exactly overlie the geologic contact it was intended to follow.

Scheliga's mapping units and scale of mapping are appropriate for delineating the groundwater Basin, provided that the boundary line mapping and georeferencing inconsistencies are resolved.

James M. Montgomery Consulting Engineers, Inc. Boundary

Geologic mapping shown in the JMM report also appears to be original. The report does not cite previous mapping but uses the same mapping units as Scheliga. The level of detail in the mapping is comparable to Scheliga's, and the mapping is generally similar. However, it differs in detail in some locations, which suggests that it was independently mapped by JMM staff. For example, **Figure A-2** shows a small section of the two maps near Warner Springs; the upper map is Scheliga's and the lower map is JMM's. The Basin boundaries delineated by the two authors are shown on both maps. The upper map shows that Scheliga mapped a northwest-trending finger of granite relatively far out into the alluvial valley floor area (near the word "Warner"). The map also shows how Scheliga's Basin boundary line (digitized from a separate report figure) does not exactly align with the mapped contact between unconsolidated materials and bedrock. The lower map shows the same area mapped by JMM. In that map, the granite does not extend as far to the northwest, and transitions to Pauba Formation gravels, instead. The discrepancy appears to be a real difference in interpretation by two different geologists.

The JMM map scale and level of detail are appropriate for delineating the groundwater Basin boundary. However, differences from Scheliga's mapping would need to be resolved, such as the degree to which fingers of alluvium are traced up small tributary canyons and the granite-versus-Pauba discrepancy mentioned above.

Todd Basin Boundary Delineation

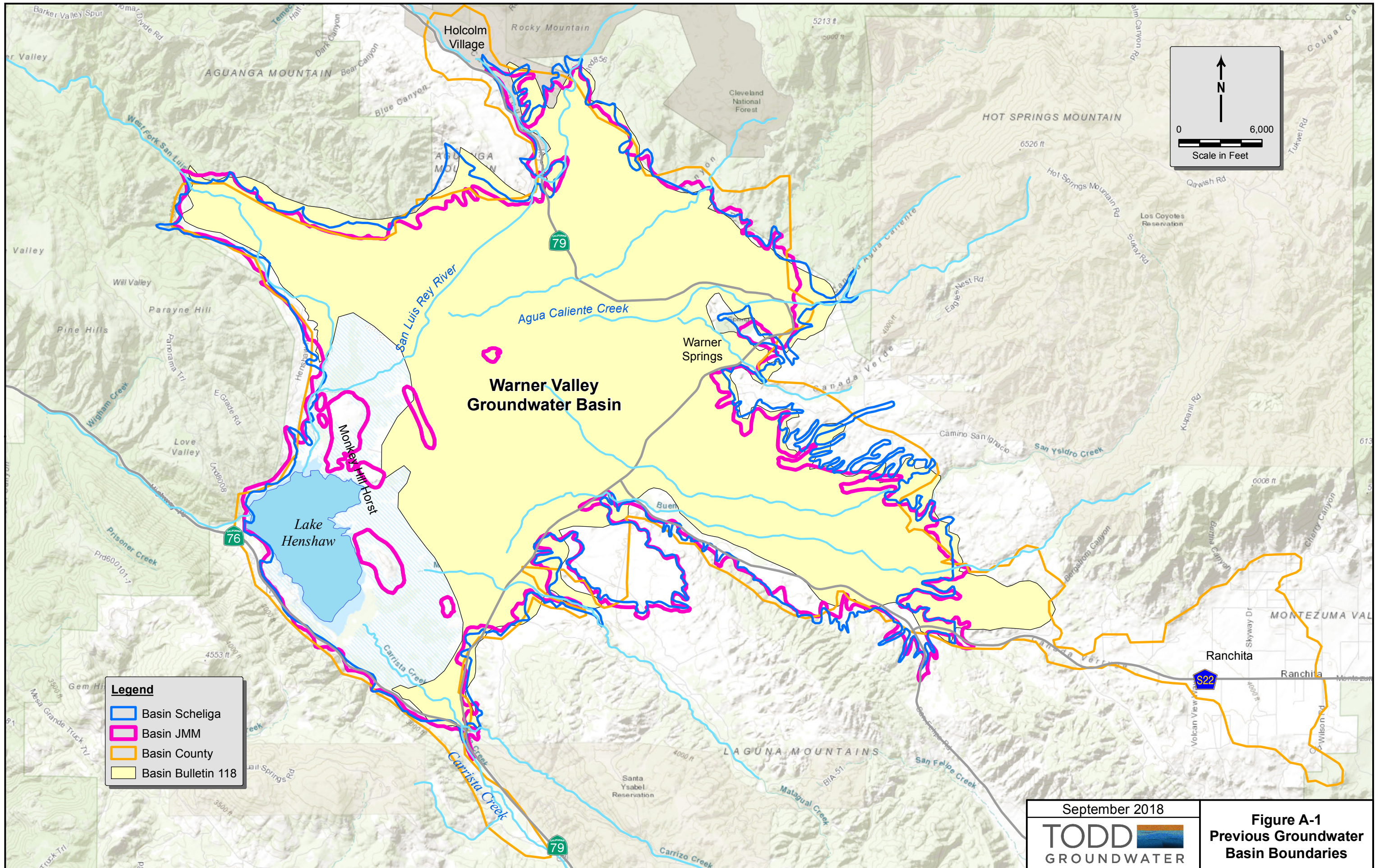
Todd Groundwater constructed a new Basin boundary delineation for this study using the following data sources, assumptions and procedures:

- Scheliga's geologic map was used as the primary basis for delineation. A scanned paper copy was georeferenced in ArcGIS Desktop 10.5 software using five control points along

roads and one control point on a stream. With the “projective transformation” option, the root-mean-square error of the georeferencing was 1 foot.

- The contact between unconsolidated deposits (alluvium, residuum, Pauba Formation and Temecula Formation) and granitic bedrock was digitized using a Bezier curve tool at a screen scale of 1:12,000. Fingers of alluvium extending up small tributary canyons were included in the Basin.
- Where there appeared to be real differences in geologic interpretation between Scheliga and JMM, the new boundary follows the map showing the greater extent of unconsolidated deposits.
- Isolated “islands” of exposed bedrock in the interior part of the Basin were included in the Basin, on the assumption that wells located in those areas would probably pull water from the surrounding unconsolidated deposits and thus should be included in Basin groundwater management.

The new delineation honors detailed geologic mapping and is inclusive in locations where the geology is uncertain. The Todd boundary is shown in **Figure A-3** and encompasses a Basin area of 48.0 square miles.



Legend

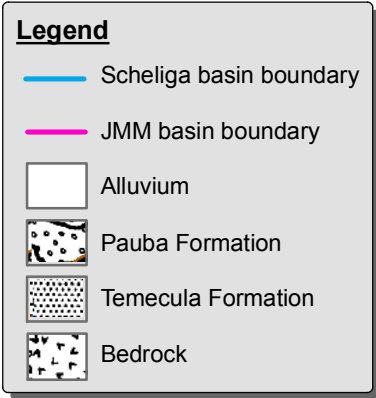
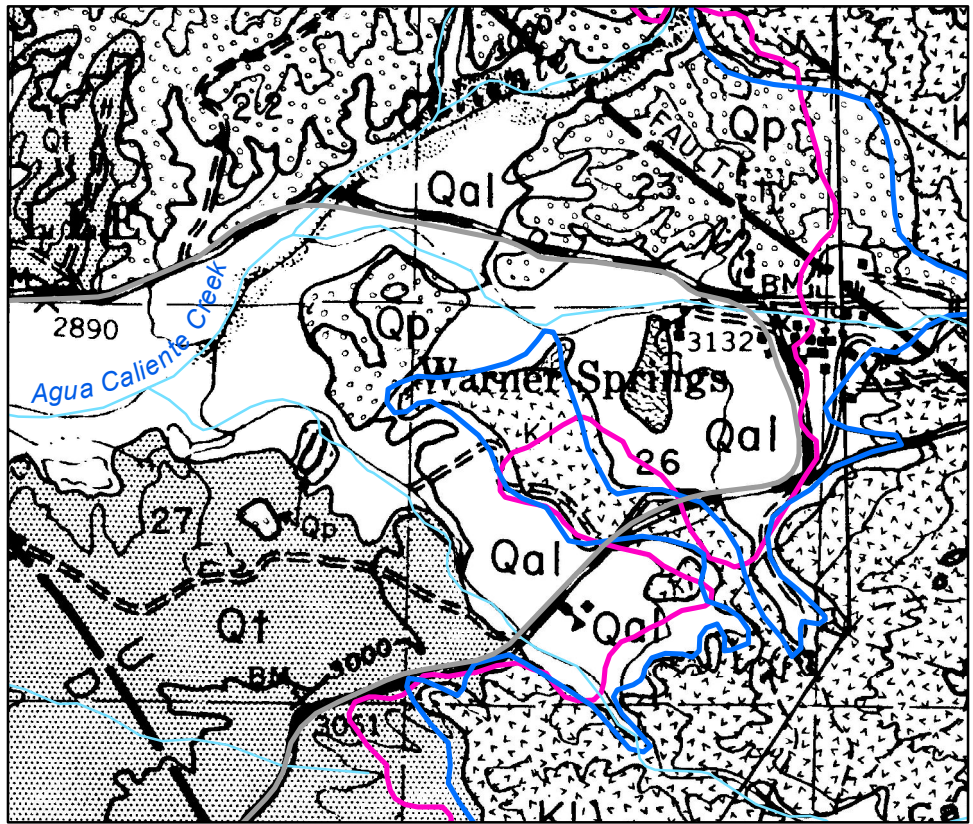
- Basin Scheliga
- Basin JMM
- Basin County
- Basin Bulletin 118

September 2018

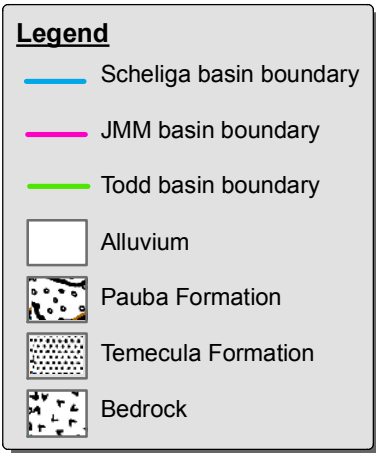
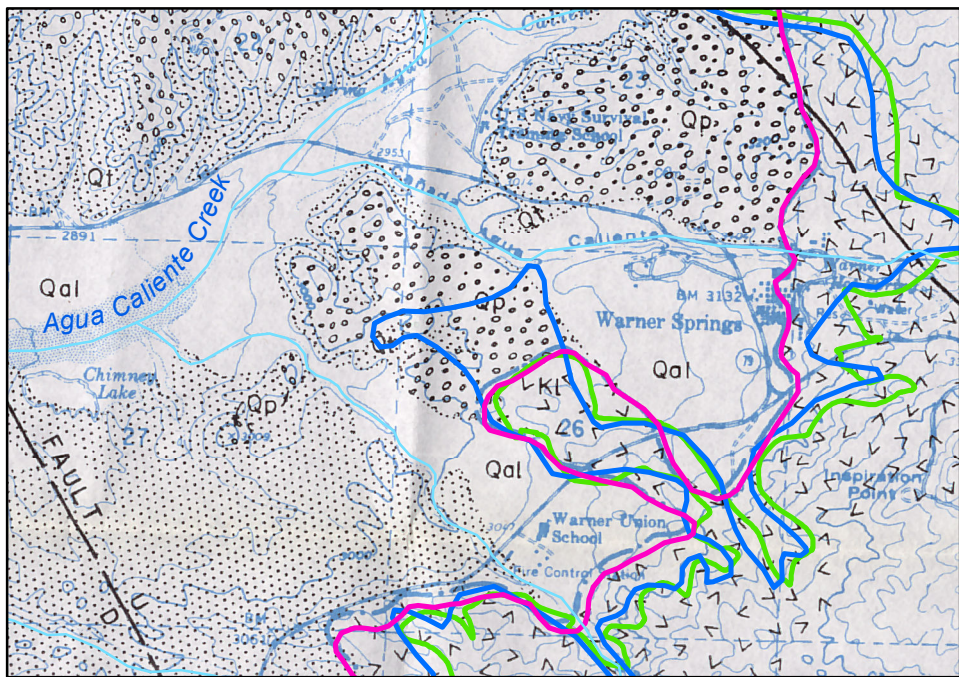
TODD **GROUNDWATER**

Figure A-1
Previous Groundwater
Basin Boundaries

A. Geologic Map of Scheliga (1963)



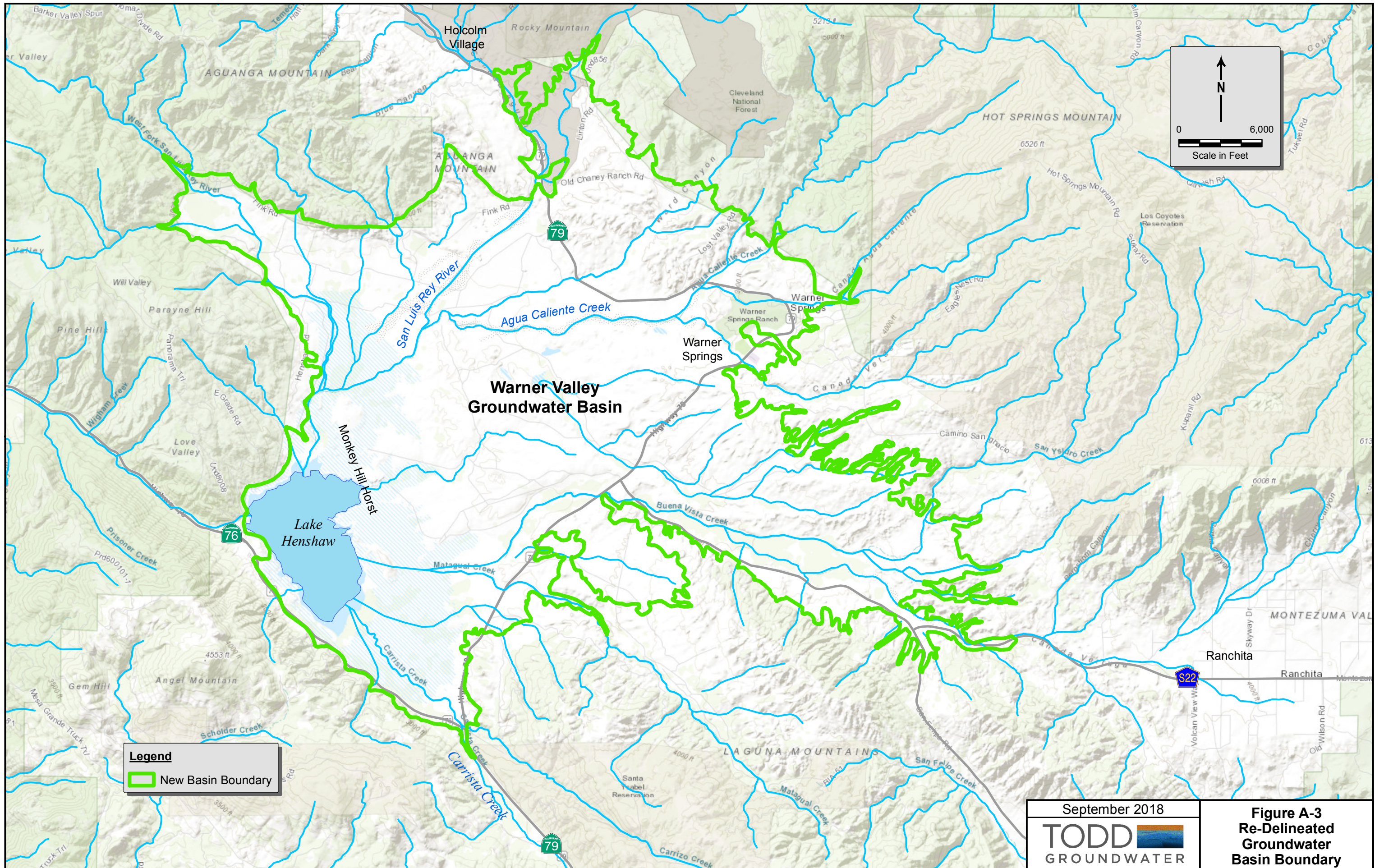
B. Geologic Map of James M. Montgomery Consulting Engineers, Inc. (1969)




September 2018



Figure A-2
Comparison of
Geologic Maps



Legend
 New Basin Boundary

September 2018
TODD 
 GROUNDWATER

Figure A-3
 Re-Delineated
 Groundwater
 Basin Boundary

Appendix B. Documentation of Rainfall-Runoff-Recharge Model

The rainfall-runoff-recharge model is a Fortran computer program that simulates hydrologic processes that contribute to dispersed recharge in a groundwater basin and its tributary watersheds. The program was developed over many years by Todd Groundwater, and it continues to evolve to reflect the needs of specific applications. It is freely available upon request.

The hydrologic processes simulated by the model include rainfall, interception, direct runoff, infiltration, soil moisture storage in the root zone, evapotranspiration (ET) by plants, irrigation, deep percolation from the root zone to a conceptual shallow groundwater zone, and partitioning of shallow groundwater into stream base flow and recharge of a deeper, regional groundwater system. In addition to natural landscape hydrology, the program addresses agricultural land uses (irrigation) and urban hydrology (connected and disconnected impervious runoff; water and sewer pipe leaks). The model is intended to represent surface hydrologic processes of importance to groundwater at a level of spatial and temporal detail and with conceptual rigor appropriate for estimating recharge, groundwater pumping for irrigation and stream flow for groundwater models simulating periods of years to decades. It is more rigorous than estimating recharge by monthly soil moisture balance and runoff by the rational method. Conversely, it is less complex and parameterized than watershed models such as PRMS or HSPF, but it is more capable of simulating urban and agricultural settings. The description in this appendix focuses on aspects of the model most relevant to the Warner Basin study.

The rainfall-runoff-recharge model simulates the same period as the groundwater model, but on a daily time step. The simulation is completed separately for recharge zones delineated to represent areas of relatively uniform rainfall, ET, soil and land use characteristics. A map of the 165 recharge zones delineated for the Warner Basin study is shown in **Figure 20** of the main report.

Rainfall

The model requires a continuous, complete time series of daily rainfall for at least one station. A time series for the Lake Henshaw station for water years 1939-2016 was developed by filling missing data with values from gages at Warner Springs, Palomar Observatory or Escondido. For each of those gages, twelve monthly ratios of rainfall to Lake Henshaw rainfall were developed from the period of overlapping record and applied to convert values from the correlation gage to estimated values at Lake Henshaw.

The rainfall contour (isohyetal) map selected for use in the model was obtained from California Polytechnic Institute and originally derived from the California Department of Water Resources (DWRs) on-line "California Atlas" geodatabase. It was one of four isohyetal maps that differed substantially from one another. The maps and selection process are documented in **Appendix C**. Average annual rainfall at each recharge zone was assigned based on the contoured rainfall value at the zone centroid, rounded to the nearest half-inch. Daily rainfall at

each zone was estimated by multiplying daily rainfall at the Lake Henshaw gage by the ratio of average annual rainfall at the zone to average annual rainfall at the gage.

Average annual rainfall at recharge zones in the West Fork San Luis Rey River and Agua Caliente Creek watersheds were adjusted downward during model calibration to bring simulated annual discharge at gaging stations on those creeks more in line with measured discharge.

Interception

Interception is rainfall that lands on plant leaves and stems and does not reach the ground. That water generally evaporates quickly. In the rainfall-runoff-recharge model, interception was applied to each day's rainfall and was set equal to the smaller of the rainfall amount and a fixed interception capacity that varied by vegetation type: 0.0-inch for impervious surfaces, 0.02-inch for golf course and pasture, 0.04-inch for natural grassland, and 0.08-inch for natural shrubs and trees. These values are consistent with field studies of interception in other areas (Viessman and others, 1977). Throughfall is the amount of rainfall that reaches the ground surface after subtracting losses to interception.

Runoff

Most rainfall reaching the ground surface (throughfall) infiltrates into the soil, but direct runoff occurs when throughfall exceeds a certain threshold. The threshold at which runoff commences and the percent of additional rainfall that runs off are significantly influenced by a number of variables, including soil texture, soil compaction, leaf litter, ground slope, and antecedent moisture. These factors can be highly variable within a recharge zone, and data are not normally available for them. Also, the intercept and slope of the rainfall-runoff relationship depends on the time increment of analysis. Most analytical equations for infiltration and runoff apply to spatial scales of a few square meters over periods of minutes to hours (Viessman and others, 1977). They are suitable for detailed analysis of individual storm events. The curve number approach to estimating runoff also applies to single, large storm events. It is not suitable for continuous simulation of runoff over the complete range of rainfall intensities (Van Mullen and others, 2002). The approach used in the recharge model is similar but less complex than the approach used in popular watershed models such as HSPF (Bicknell and others, 1997).

In the recharge model, daily infiltration is simulated as a three-segment linear function of throughfall, and throughfall in excess of infiltration is assumed to become runoff. The general shape of the relationship of daily infiltration to daily throughfall is shown in **Figure B-1** (upper graph). Below a specified runoff threshold, all daily throughfall is assumed to infiltrate. Above that amount, a fixed percentage of throughfall is assumed to infiltrate, which is the slope of the second segment of the infiltration function. Finally, an upper limit is imposed that represents the maximum infiltration capacity of the soil.

The runoff threshold, the percentage of excess throughfall that infiltrates, and the maximum daily infiltration capacity were assumed to vary by land use and were among the variables adjusted for model calibration. For the Warner Basin model, runoff parameters were calibrated to match gaged stream flow at the West Fork San Luis Rey River and Agua Caliente Creek gages. Early results indicated a need for a relatively high runoff threshold to decrease the number and

magnitude of simulated peak flow events at the gages. Also, instead of varying the runoff threshold by vegetation type, it was varied by depth to bedrock. Shallow and exposed bedrock areas in the tributary watersheds were expected to generate more runoff than areas with deeper soils. The runoff thresholds in the final calibration were 1.2 inches, 1.4 inches, 1.6 inches and 1.8 inches for soil depths of less than 16 inches, 29-30 inches, 56 inches, and greater than 60 inches, respectively. Those were the soil depth categories in the Natural Resources Conservation Service soil survey. For those same soil depth categories, the slopes of the infiltration line were 0.86, 0.91, 0.93 and 0.95. The slopes represent the percentage of excess throughflow that infiltrates. The values were obtained entirely by calibration to the gaged stream flow hydrographs. The maximum daily infiltration was set to 3 inches per day (in/d) for recharge zones in the Basin and 4 in/d for zones in the tributary watersheds. These values were selected during calibration to better match peak flows during large storm events and are reasonable in terms of soil permeability.

The above parameter values are for soils that are relatively dry. Infiltration rates decrease as soils become more saturated. This phenomenon led to the development of the Antecedent Runoff Condition adjustment factor for rainfall-runoff equations (Rawls and others, 1993). However, application of the concept has been focused on individual storm events. For the purpose of the recharge model, the adjustment provides a means of simulating empirical observations that a given amount of rainfall produces less runoff at the beginning of the rainy season when soils are relatively dry than at the end of the rainy season when soils are relatively wet. This effect is included in the recharge model as a multiplier that decreases the estimated infiltration as soil saturation increases. This multiplier is applied to the runoff threshold, the infiltration slope and the maximum infiltration rate. The multiplier decreases from 1.0 when the soil is dry to a user-selected value between 1.0 and 0.60 when the soil is fully saturated (lower graph in **Figure B-1**). A low value has the effect of decreasing infiltration (and potential groundwater recharge) toward the end of the rainy season or in very wet years, and also to increase simulated peak runoff during large storm events. The multiplier under saturated conditions was assumed to be 0.95 for the Warner Basin model.

Evapotranspiration

The model also requires a continuous, complete time series of daily reference evapotranspiration (ET_0). The nearest station with measured data is the California Irrigation Management Information System (CIMIS) station in Escondido. That station is in CIMIS climate zone 9 (55.1 inches per year [in/yr] ET_0), whereas Warner Basin is in CIMIS zone 16 (62.5 in/yr). Initially, daily ET_0 at the Escondido station was multiplied by the ratio of the annual zonal ET_0 values to obtain daily ET_0 for all recharge zones. During model calibration, annual ET_0 in the Warner Basin was assumed to equal the value for zone 18 (71.6 in/yr), which is slightly farther inland on the CIMIS map. This increased overall abstraction of rainfall, but simulated stream flow was not very sensitive to ET_0 .

Evapotranspiration (ET) varies by vegetation type and growth stage. ET_0 is the amount of water evapotranspired from a broad expanse of turf mowed to a height of 4-6 inches with ample irrigation. ET_0 is multiplied by a crop coefficient to obtain the actual ET of a different crop or vegetation type at a particular point in its growth and development. Although primarily used for

agricultural crops, crop coefficients can also be applied to urban landscape plants and natural vegetation. On lands overlying Warner Basin, the primary vegetation is annual grassland, and in the tributary watersheds it is natural shrubs and trees. Both of these were assigned a crop coefficient of 1.0 in all months of the year. Annual grassland is similar to the vegetation used to define ET_0 except that it is not irrigated. By assuming a coefficient of 1.0 at all times, simulated root zone moisture dries out in summer slightly faster than if a value less than 1.0 were assumed. However, that difference has no effect on rainfall recharge, which occurs under wet conditions in winter. The xeric shrubs and trees on the mountain slopes of the tributary watersheds have leaves and needles that transpire less water per area than a blade of grass—which would indicate a crop coefficient less than 1.0—but they are much taller. The additional height is associated with greater leaf area per square meter of ground and with increased wind exposure. During calibration, it was necessary to increase evapotranspiration losses in order to match the annual volumes of water passing the stream gages and entering Lake Henshaw. Accordingly, the crop coefficient of 1.0 for trees and shrubs was retained as reasonable.

Irrigation

There are two small irrigated areas in the Basin. One is the golf course at Warner Springs Ranch Resort (WSRR) and the other is a field of pasture or alfalfa in the Carrista Creek watershed south of Lake Henshaw. The rainfall-runoff-recharge model simulates irrigation by assuming that an irrigation event occurs whenever soil moisture drops below a user-specified percent of maximum. The amount of applied water equals the accumulated moisture deficit divided by the irrigation efficiency. If irrigation efficiency is less than 100 percent, the irrigation event overfills the storage capacity of the root zone and the excess becomes deep percolation. An irrigation efficiency of 90 percent was assumed for the golf course and pasture. This refers to the percentage of applied water that becomes deep percolation. There are other losses such as sprinkler spray evaporation that result in an overall applied water efficiency of less than 90 percent. Although this procedure produces an estimate of irrigation pumping, the amount of WSRR pumping for golf course irrigation in the groundwater model was obtained from metered production at the wells.

Deep Percolation Beneath the Root Zone

Whenever simulated soil moisture storage exceeds the storage capacity of the root zone—whether by rainfall infiltration or irrigation—the excess becomes deep percolation, which moves downward to the shallow groundwater zone. Root zone soil moisture storage capacity is the product of root depth and the available water capacity (AWC) of the soil. Based on published soil surveys, AWC ranges from 0.07 to 0.14 inch per inch and averages 0.104 inch per inch. Root depth is much more uncertain because it is not uniform over the land surface, it varies by plant type and size, and is influenced by soil type and bedrock depth. For many types of plants rooting depth is somewhat facultative, meaning that roots will grow deeper in highly drained soils with low AWC than in loamy soils with high AWC. Also, soil moisture storage capacity has a strong influence on simulated deep percolation. Consequently, root depth was a prominent calibration variable in the joint calibration of the rainfall-runoff-recharge model and groundwater model. The initial estimates of root depth produced too much annual flow at

stream gages and total inflow (surface water and groundwater) to Lake Henshaw on a long-term average annual basis. In the final calibration, the root depths of annual grasses, natural shrubs and natural trees were 84, 180 and 240 inches, respectively, except in the West Fork San Luis Rey River watershed where a better simulation of gaged stream flow was obtained with depths of 60, 108 and 120 inches.

Shallow Groundwater, Base Flow and Deep Recharge

Deep percolation beneath the root zone accrues to a shallow groundwater storage zone. The existence of such a zone is based more on patterns of stream flow in tributary watershed areas than on geology. In the rainfall-runoff-recharge model, the shallow groundwater zone serves to attenuate pulses of deep percolation from rainfall and irrigation events and partition deep percolation into stream base flow and deep recharge. The gradual, logarithmic recession of stream flow following periods of wet weather observed in many upland streams is consistent with a body of water draining to the stream according to a first-order rate law. In the model, daily outflow of shallow groundwater to streams is calculated using the following empirical fitting equation:

$$q_b = (stor_{t-1} + 1)^a - 1$$

Where,

q_b = one-dimensional flow from shallow groundwater to stream (inches)

$stor_{t-1}$ = one-dimensional shallow groundwater storage on previous day (inches)

a = empirical exponent

The exponent is obtained by calibration to replicate the total volume and observed rate of recession of stream flow in gaged watersheds. The balance between the exponent and the deep recharge flux determines how shallow groundwater outflow is partitioned between base flow and regional recharge.

Adding the simulated runoff and base flow rates produces a daily time series of stream flow leaving the recharge zone. For each tributary watershed that enters the groundwater Basin, stream flow was summed for all zones within the watershed to obtain the flow in that stream where it enters the Basin. Those flows are used as input to the groundwater model.

Groundwater also flows out of the shallow groundwater zone by downward leakage to a deeper regional groundwater system. This leakage occurs at a constant rate, consistent with the hydraulics of one-dimensional unsaturated flow under a unit gradient. A relatively high rate partitions more of the shallow groundwater outflow to deep recharge, whereas a smaller value sends more outflow to streams. In tributary watersheds of the Warner Basin, a deep recharge flux rate of 0.02 in/d was used in the West Fork San Luis Rey River and Agua Caliente Creek watersheds and 0.03 in/d in all other watersheds. Deep recharge in upland tributary areas is assumed to become subsurface inflow to the groundwater Basin, as described in the main report.

Within the groundwater Basin, the terrain is relatively flat and groundwater discharge to streams is assumed to derive from the regional groundwater system, not from a shallow groundwater zone. This was implemented by specifying a small base flow exponent and large deep recharge flux rate, which effectively sent all deep percolation from the root zone downward to become deep groundwater recharge.

Stream Flow Calibration Results

Two stream gage records and Lake Henshaw operations data were available for calibrating stream flow and deep recharge. The West Fork San Luis Rey River near Warner Springs gage (U.S. Geological Survey [USGS] station 11033000) operated from 1913 to 1986. The Agua Caliente Creek near Warner Springs gage (USGS 11031500) operated from 1961 to 1987. These gages are located 1.9 and 2.4 miles downstream of the groundwater Basin boundary, respectively, so the gaged flows reflect percolation gains and losses not included in the simulated flows at the Basin boundary. **Figure B-2** shows gaged and simulated flows at the two stations for 5-year excerpts of their periods of record. Simulated daily flows generally exhibit the same qualitative characteristics of the gaged flows in terms of the frequency and magnitude of runoff events. Specific events might not match closely, but those differences could reflect actual differences between rainfall at Lake Henshaw and rainfall in the watershed. Simulated base flow is sometimes noticeably smaller or greater than observed base flow, and the discrepancy varies from year to year. Base flow is determined largely by variables that are not expected to change over time, and no combination of rainfall-runoff-recharge model parameters was able to match the observed annual variations in base flow. Emphasis was placed on matching average annual total stream discharge, which has a strong influence on estimated conjunctive yield of the groundwater Basin and Lake Henshaw. The calibrated model matched average annual discharge in Agua Caliente Creek within 1 percent, but simulated discharge for the West Fork San Luis Rey River was 30 percent too low, even with reasonable adjustments to parameters in that specific watershed. The cause of the discrepancy is unknown, but could, for example, stem from the isohyetal map underestimating the orographic effect of Palomar Mountain on rainfall.

Lake Henshaw operations records include the estimated surface inflow into the reservoir, which serves as an additional check on simulated rainfall runoff. Because those inflows reflect stream flow gains and losses across the groundwater Basin, those calibration results are discussed in the main report. The calibrated rainfall-runoff-recharge model parameters reflect joint calibration with the groundwater model. Parameters undoubtedly vary among the individual watersheds—as they do between the two gaged watersheds—but all watersheds except the West Fork San Luis Rey watershed were assumed to have the same characteristics as the Agua Caliente Creek watershed.

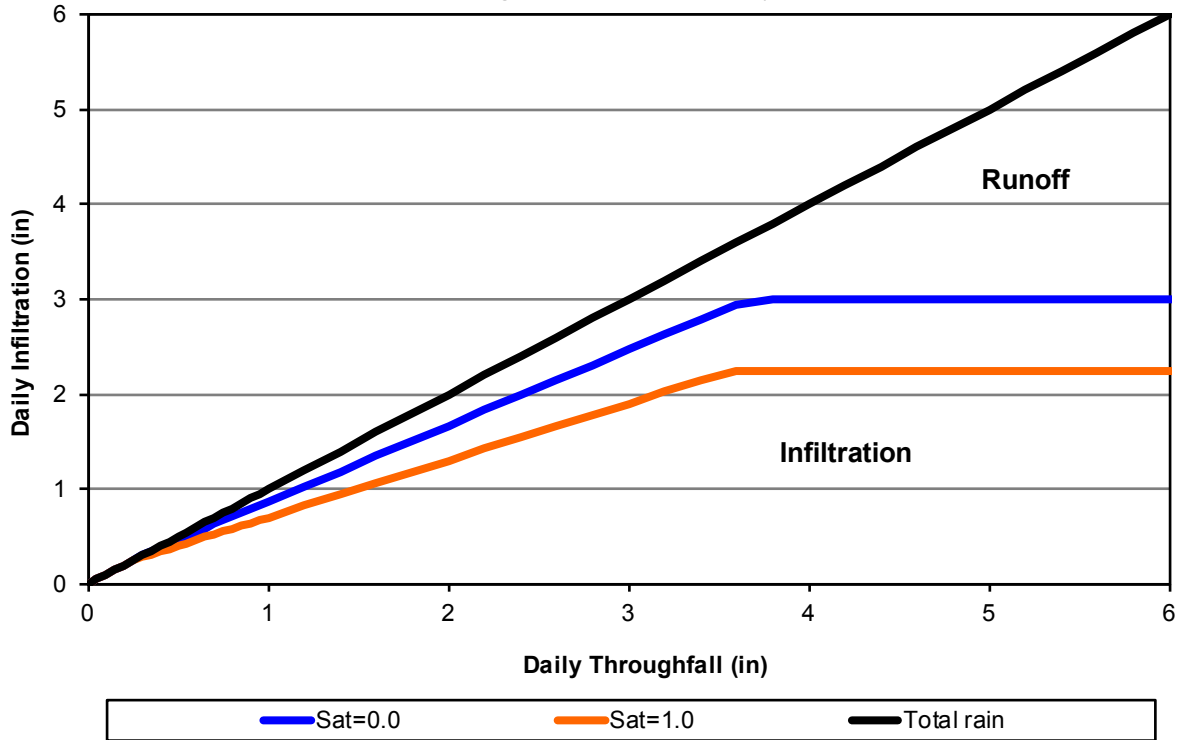
The biggest calibration issue was that the original parameter estimates produced too much stream flow at the gages and too much surface and subsurface inflow to the groundwater model, as revealed by long-term trends in simulated Lake Henshaw storage. Plausible

explanations for the discrepancy include errors in the isohyetal map, rooting depths that extend deep into weathered bedrock and bedrock fractures, plants that can absorb water at greater than the current ET_0 rate (common among desert plants), and ET of groundwater by riparian vegetation along creek channels in tributary watersheds. Some of these possibilities were implemented during calibration and resulted in parameter values that in some cases were near the limits of credibility.

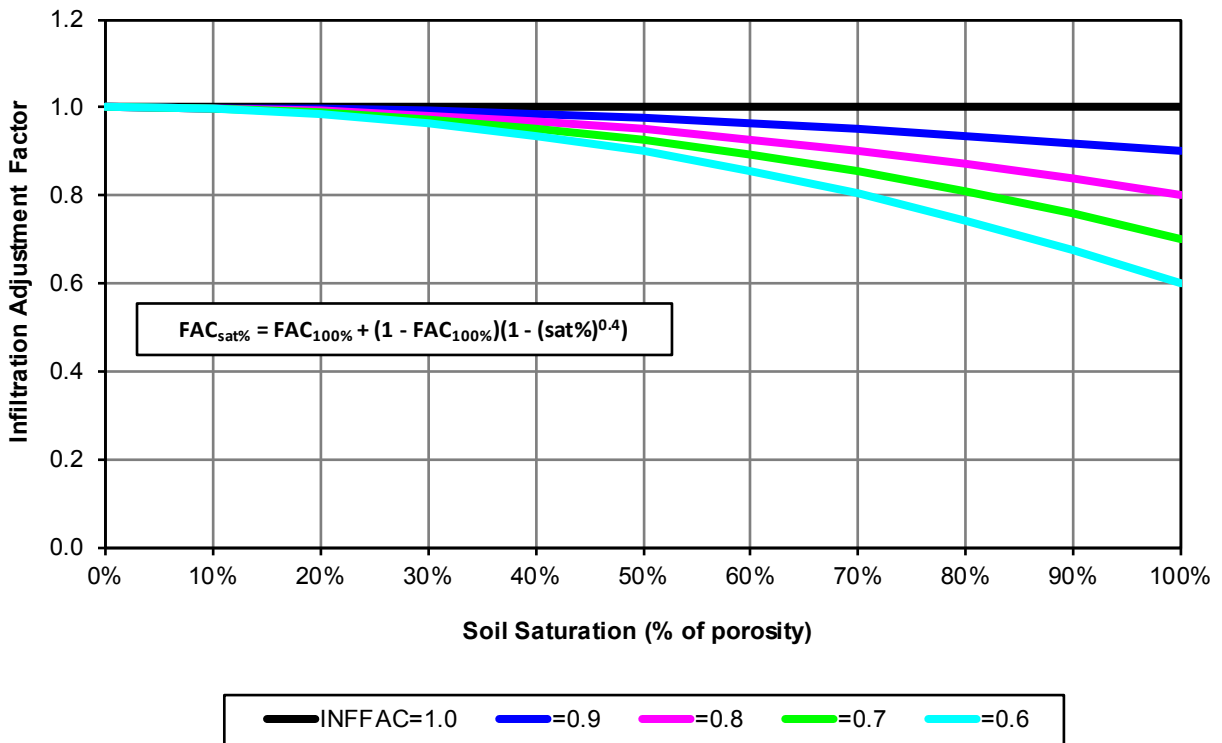
Calibration of the rainfall-runoff-recharge model provided an opportunity to test the sensitivity of simulated stream flow to various model parameters. ET_0 had little effect on simulated runoff, probably because ET_0 is small compared to rainfall during wet weather periods, when most of the runoff is generated. Average annual discharge in Agua Caliente Creek was moderately sensitive to annual rainfall. A decrease of 1 in/yr in average annual rainfall decreased simulated discharge by 12 percent. Increasing the runoff threshold for each soil depth category by 0.2-inch decreased simulated average annual discharge by 7 percent in Agua Caliente Creek and by 6 percent in West Fork San Luis Rey River.

A. Relationship of Infiltration to Throughfall

[Throughfall = rainfall - interception]



B. Effect of Soil Saturation on Infiltration



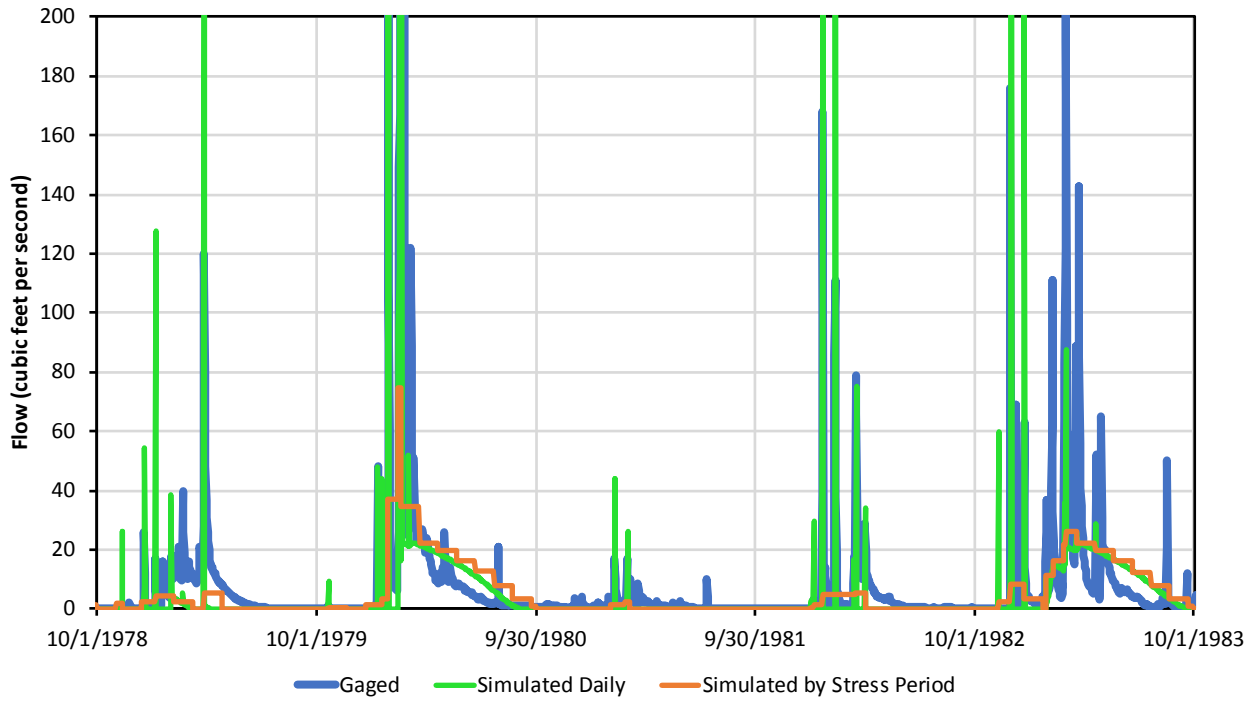
$$FAC_{sat\%} = FAC_{100\%} + (1 - FAC_{100\%})(1 - (sat\%)^{0.4})$$

September 2018

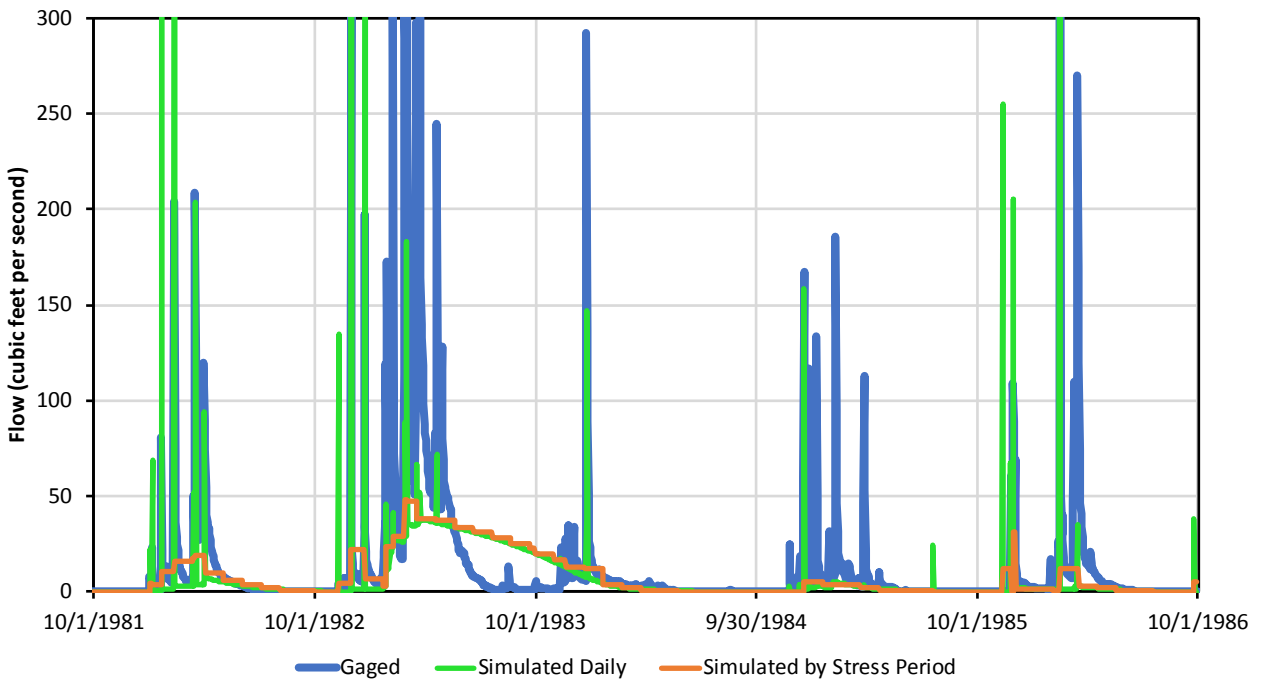
TODD
GROUNDWATER

Figure B-1
Relationship of
Infiltration to Throughfall
and Soil Saturation

Agua Caliente Creek



West Fork San Luis Rey River



September 2018



Figure B-2
Measured
and Simulated
Stream Flow

Appendix C. Comparison of Isohyetal Maps

Four maps of average annual rainfall in the Warner Valley watershed were obtained and compared. The maps are shown in **Figure C-1**, and source information and selected characteristics of the maps are listed in **Table C-1**. The maps differ substantially in their patterns of rainfall distribution across the watershed and in the total amounts of rainfall at various locations. None of the maps is considered the “correct” one; they represent different time periods of data, different methods of analysis, and different interpretations of orographic effects.

Two rain gage stations in the watershed with long periods of record are at Henshaw Dam and Warner Springs. The Warner Springs gage was discontinued in 1977, but the average ratio of Warner Springs rainfall to Henshaw Dam rainfall was calculated for water years 1939-1972 using only months with complete records for both gages. The calculated Warner/Henshaw ratio was 0.66, and this ratio was included in the criteria used to compare and evaluate the maps. A complete time series of daily rainfall at Henshaw Dam was prepared by filling periods of missing data using correlations with rainfall at Warner Springs, Palomar Mountain and Escondido. Different rainfall ratios were calculated for each month of the year based on the period of overlapping record, and the appropriate monthly factor was used to estimate missing rainfall at Lake Henshaw. Annual rainfall at Henshaw Dam averaged 23.71 inches during water years 1939-2016 and 26.14 inches during 1981-2010, which is the period represented by two of the maps.

The purpose of evaluating the rainfall (isohyetal) maps was to select one for estimating rainfall-runoff and groundwater recharge in the watershed and groundwater Basin. Higher estimates of rainfall result in higher estimates of recharge and could lead to an over-estimate of groundwater Basin yield.

Compared to the other maps, the San Diego County map has relatively low rainfall at Henshaw Dam and at the rainfall “high” just west of Lake Henshaw. The value at Warner Springs was slightly higher than in the other maps, leading to the highest Warner/Henshaw ratio (0.89 versus the value of 0.66 calculated directly from gage data). The County map includes a more pronounced orographic effect for Hot Springs Mountain than the other maps.

The PRISM map consists of a grid of 4-square-kilometer cells, which is fairly coarse at the scale of this watershed. It indicates a relatively low orographic effect for Palomar Mountain but a relatively high one for Hot Springs Mountain. The value for Henshaw Dam is about 2 inches per year (in/yr) less than indicated by gage data for 1981-2010.

The Rantz (1969) map is based on much older data than the other maps. The value at Henshaw Dam is quite high, but as a result the Warner/Henshaw ratio is the best among the four maps. The map shows no orographic effect for Hot Springs Mountain, which is probably incorrect. Conversely, the orographic effect for Palomar Mountain is the largest among the four maps, as is the value at the rainfall “high” west of Lake Henshaw.

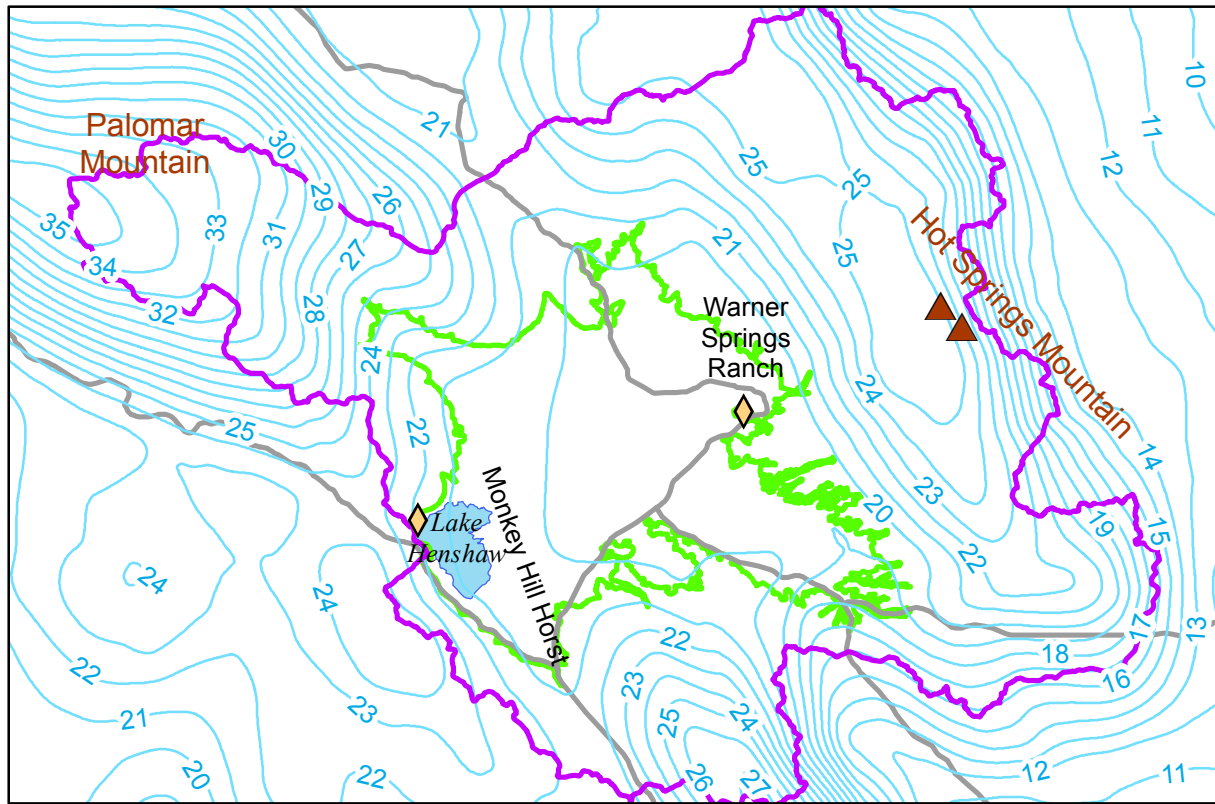
The Cal Poly Pomona map is included among many geographic information system (GIS) themes on the Geodesign program website. Its exact derivation is unknown, but it traces back to data sets included by the California Department of Water Resources (DWR) in its “California Atlas” data collection, which has since become subsumed by the California Geoportal at <http://portal.gis.ca.gov/geoportal/catalog/main/home.page> (Li, 2017). It has reasonable values for Henshaw Dam, Warner Springs and the Warner/Henshaw ratio. It features a moderate orographic effect for Palomar Mountain and a relatively large effect for Hot Springs Mountain.

Of the four maps, the Cal Poly Pomona appears to have the best overall fit to the several control locations. The second-best map for the groundwater modeling effort would probably be the San Diego County map, because the remaining two have deficiencies. The PRISM grid is too coarse for this study and the orographic effects may be too small. The Rantz map may be out of date and shows unequal treatment of orographic effects for Palomar Mountain versus Hot Springs Mountain.

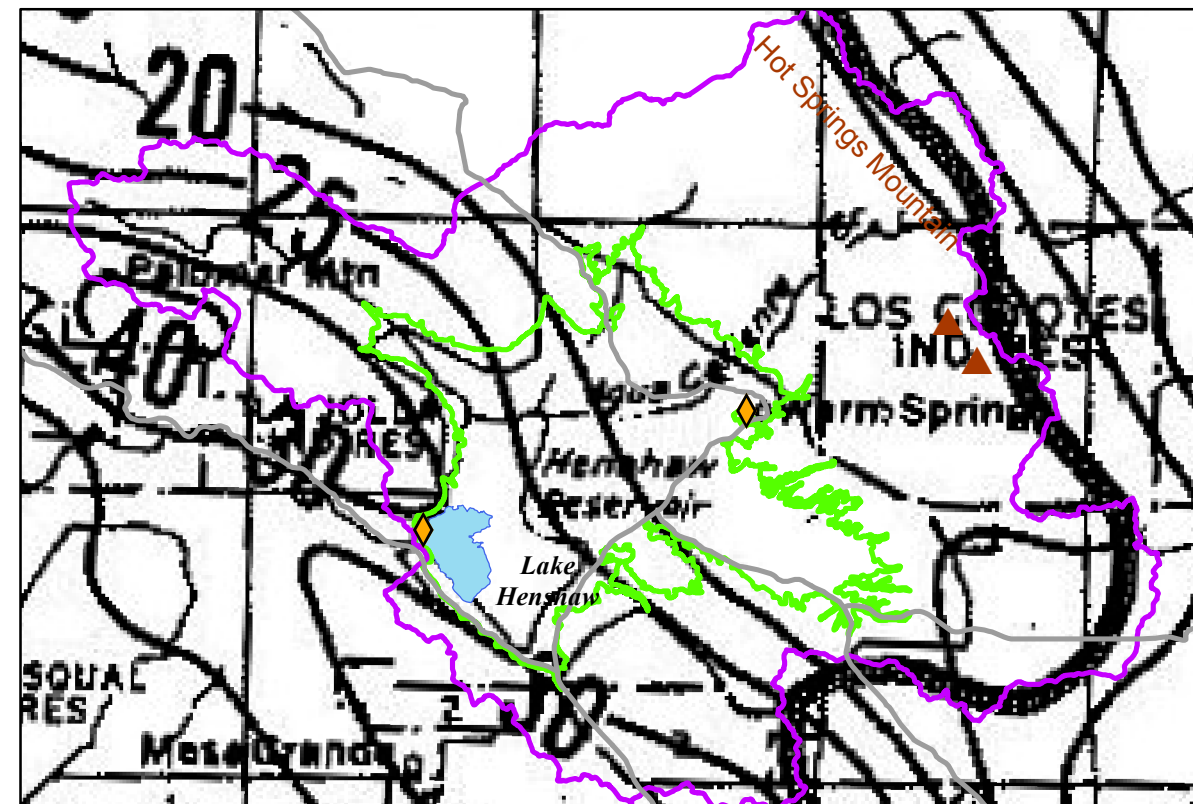
Table C-1. Comparison of Four Isohyetal Maps of Warner Valley Watershed

Attribute	County	PRISM	Rantz (1969)	Cal Poly Pomona
Source	San Diego Regional GIS Warehouse	PRISM Climate Group, Oregon State University	U.S. Geological Survey, Basic-Data Collection 1020-01 (out of print)	California State Polytechnic University, Pomona, Geodesign Program. Originally from California Department of Water Resources "Cal Atlas" data set.
Availability	http://www.sangis.org/download/index.html	http://prism.oregonstate.edu/	Georeferenced scan of paper copy	http://www.cpp.edu/~geodesign/index.shtml
Data period	1971-2001	1981-2010	1907-1960	1981-2010
Stations shown	No	No	No	No
Contour interval	1 inch	4-km grid only; no contours	2 to 10 inches	1 inch
Contouring method	"derived from the 300-foot resolution rainfall raster dataset"	Model interpolates from stations to grid cells based on "location, elevation, coastal proximity, topographic facet orientation, vertical atmospheric layer, topographic position, and orographic effectiveness of the terrain".	Manual	Unknown
Point values				
Henshaw Dam	22	24.2	29	23
Warner Springs	19.5	18.2	19	16.5
Warner/Henshaw ratio	0.89	0.75	0.66	0.72
W/H ratio from gage data	0.66	0.66	0.66	0.66
Hot Springs Mountain	25	21	17	24
Palomar Mountain	35	23-26	40	26
High west of Henshaw	24	27	30	28

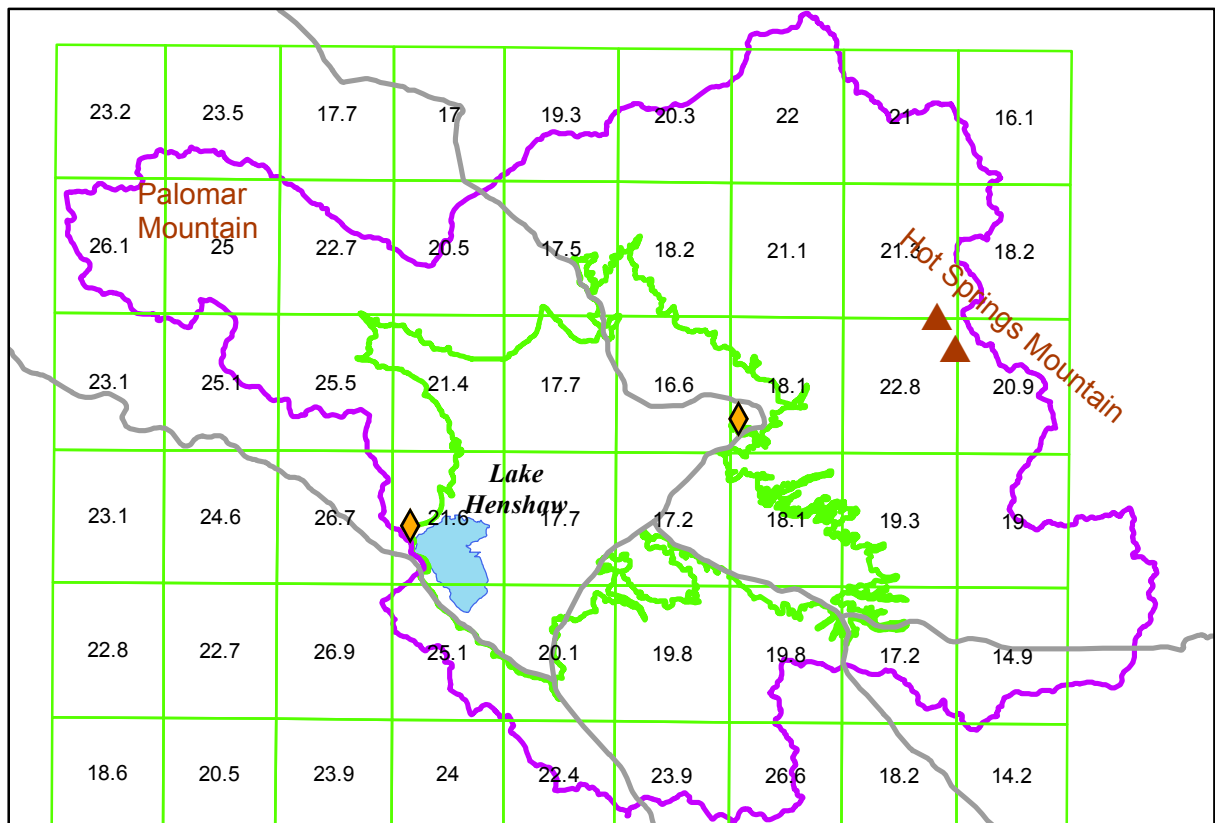
San Diego County



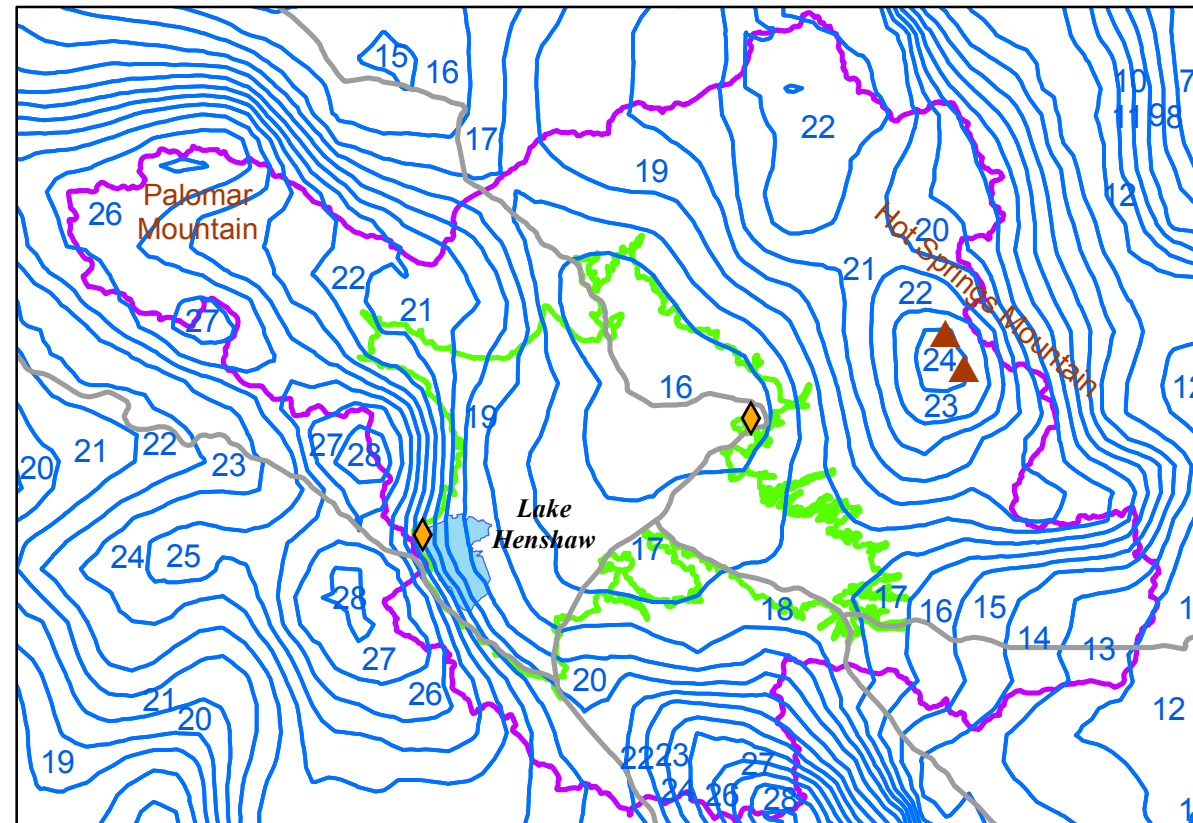
Rantz (1969)



PRISM Climate Group



Cal Poly Pomona

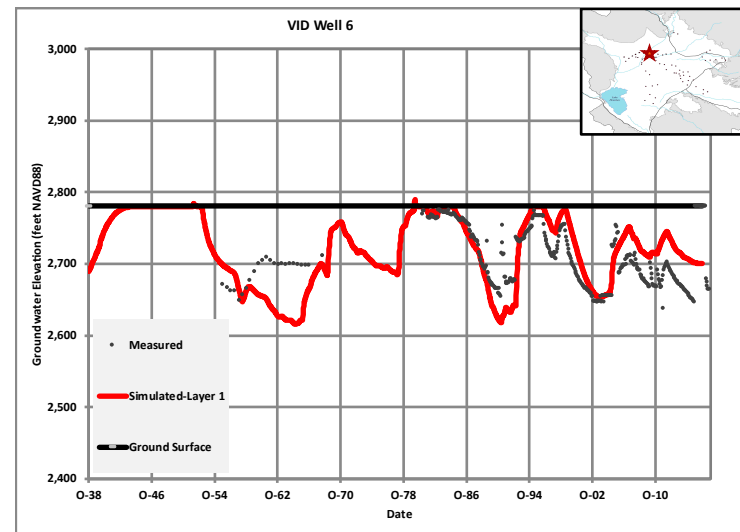
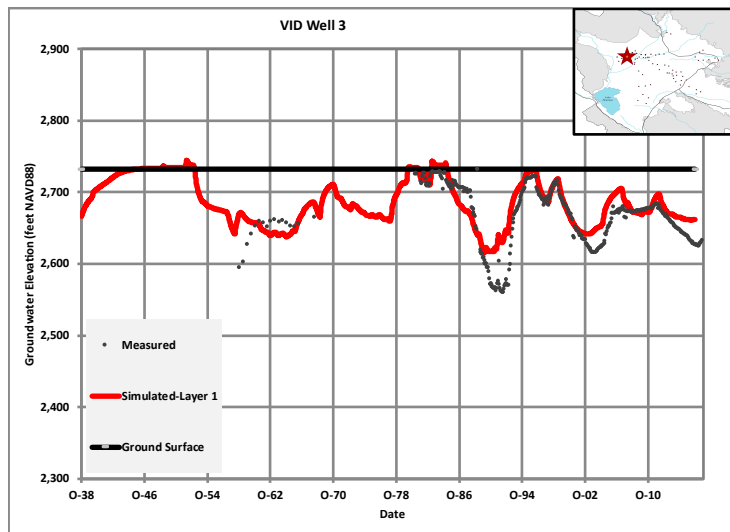
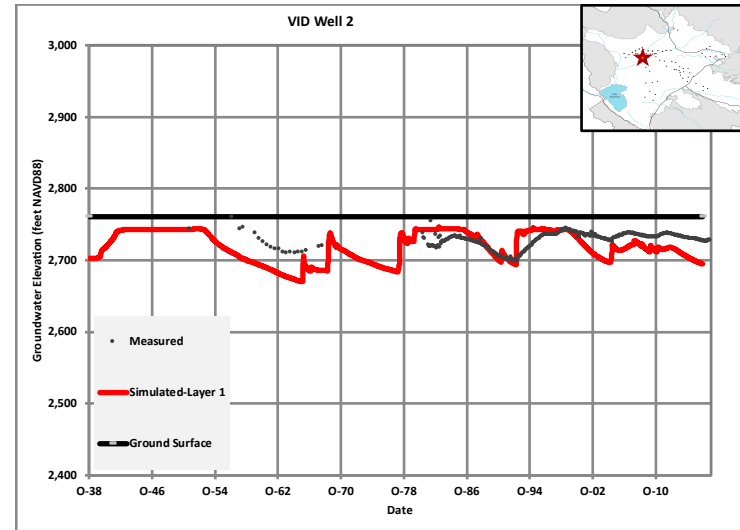
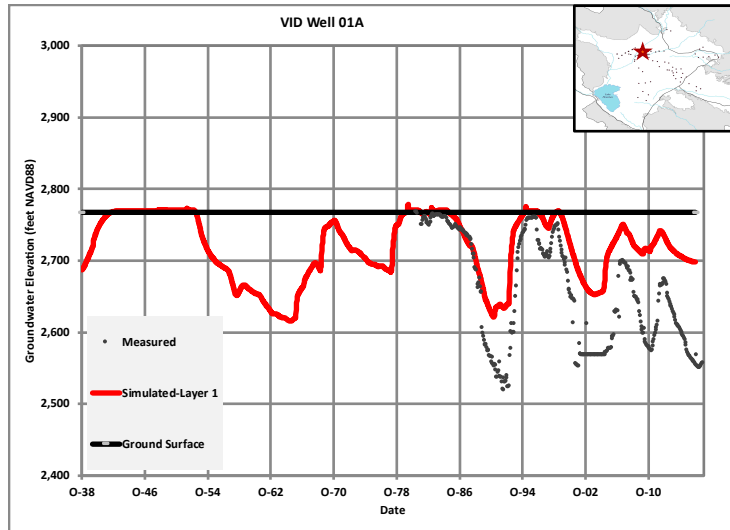


Legend

- Warner Basin Watershed
- Groundwater Basin
- Rain Gage

Figure C-1
Maps of Average Annual Precipitation
 September 2018
TODD GROUNDWATER

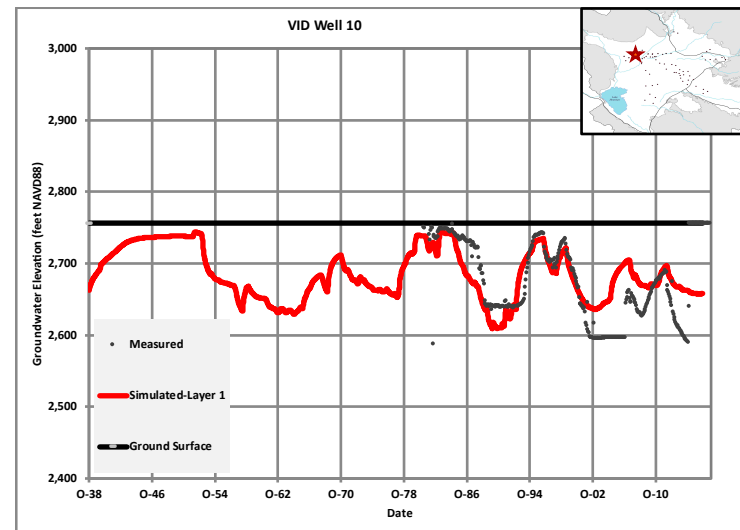
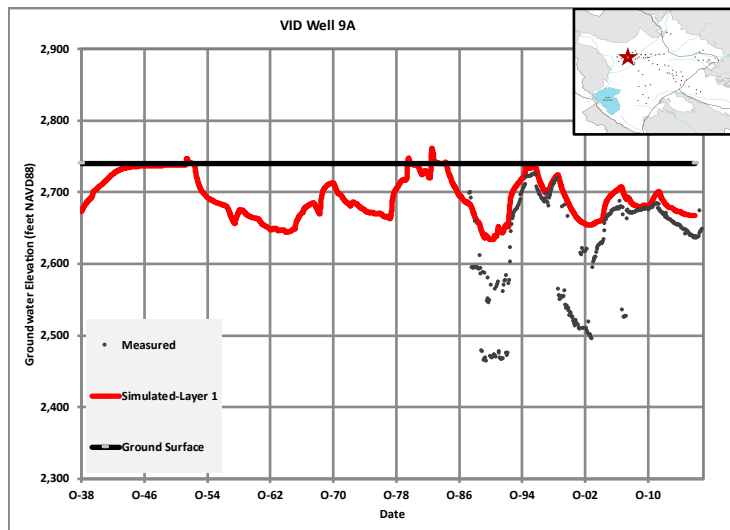
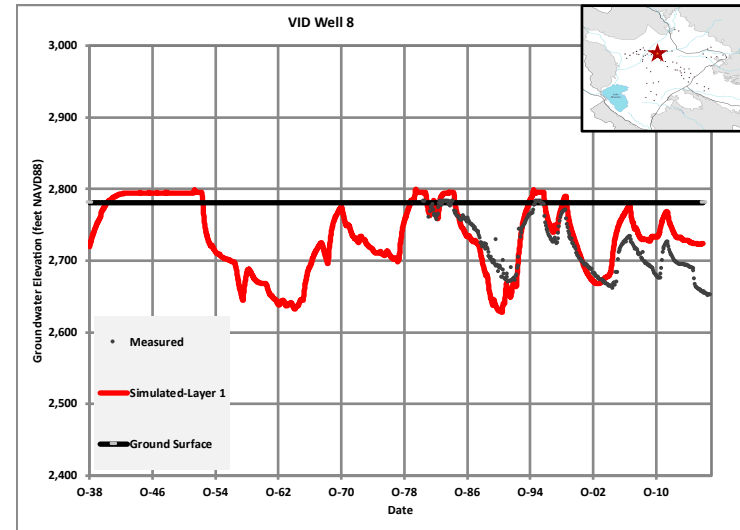
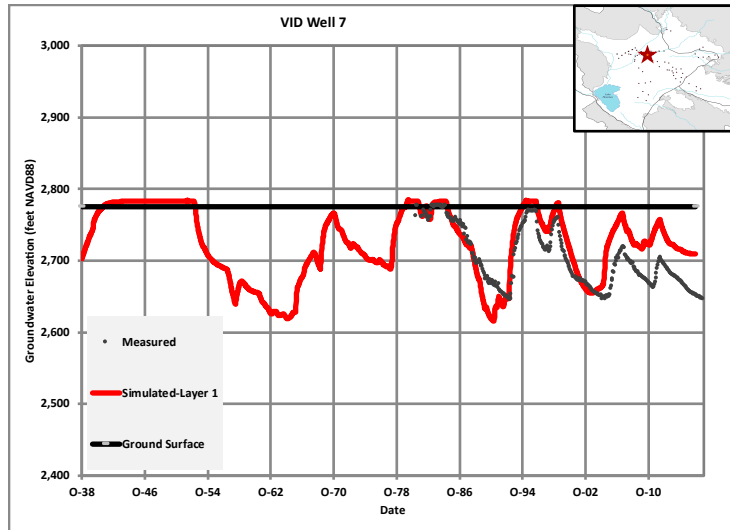
Appendix D. Calibration Hydrographs



September 2018



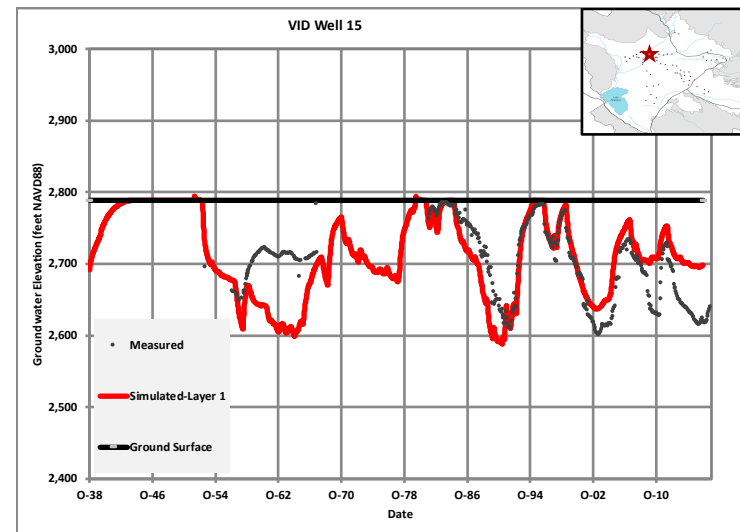
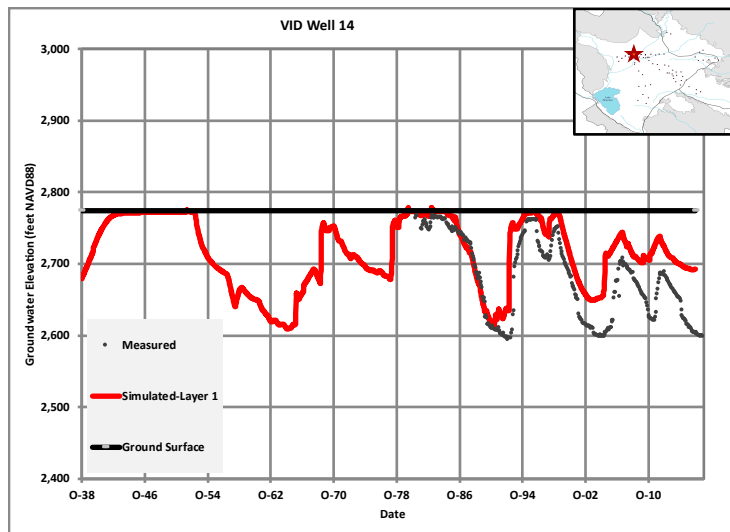
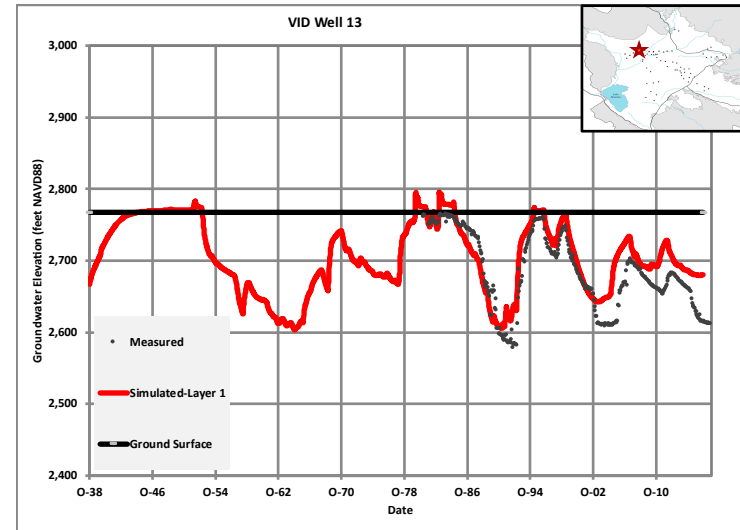
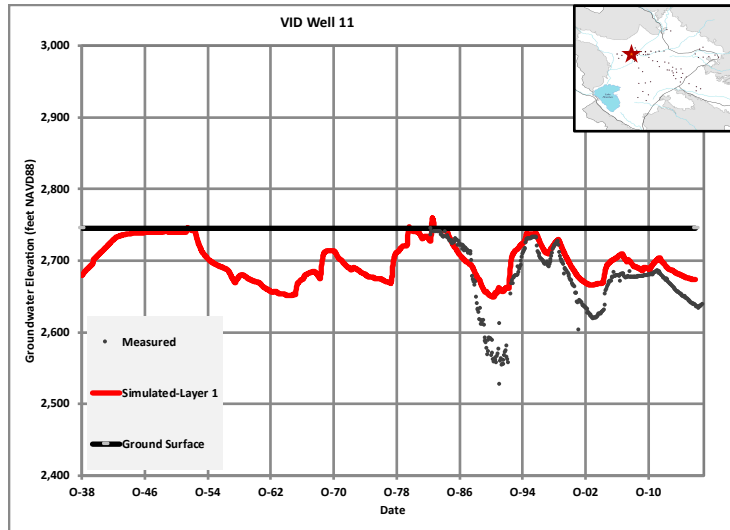
Figure D-1a
Hydrographs



September 2018



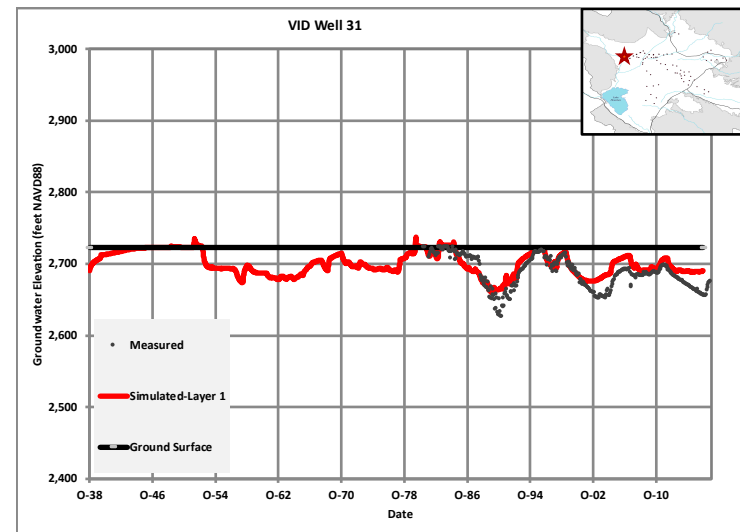
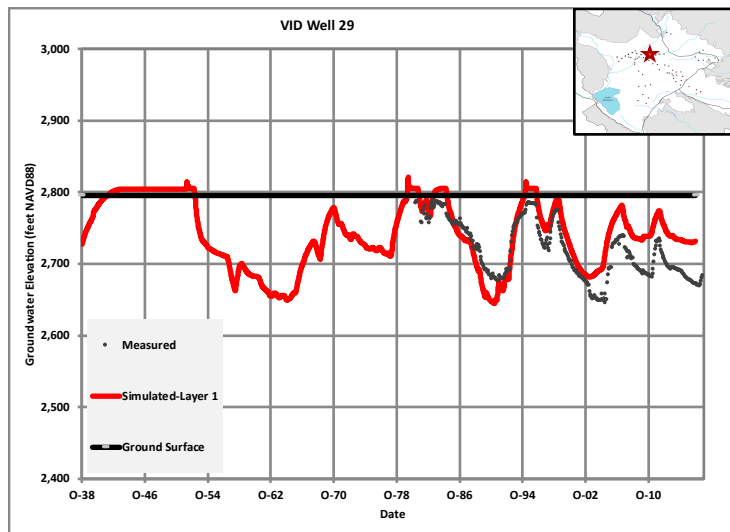
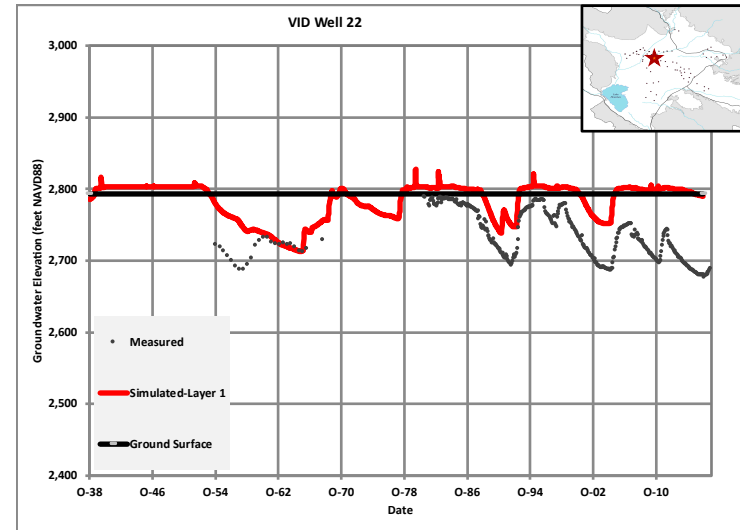
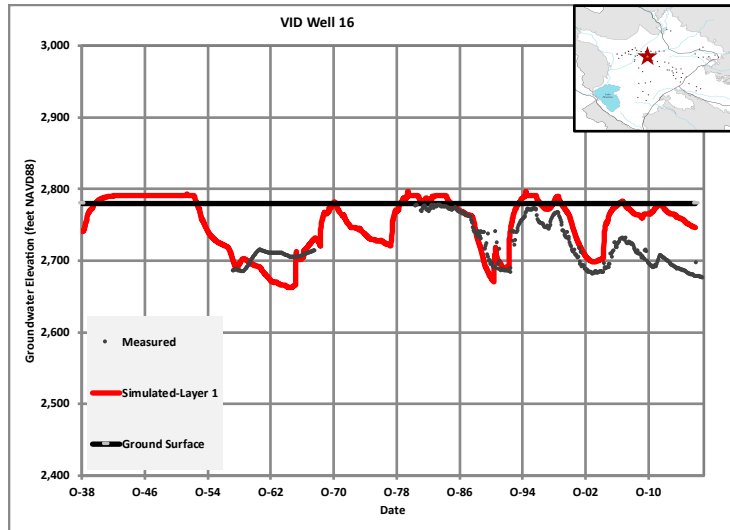
Figure D-1b
Hydrographs



September 2018



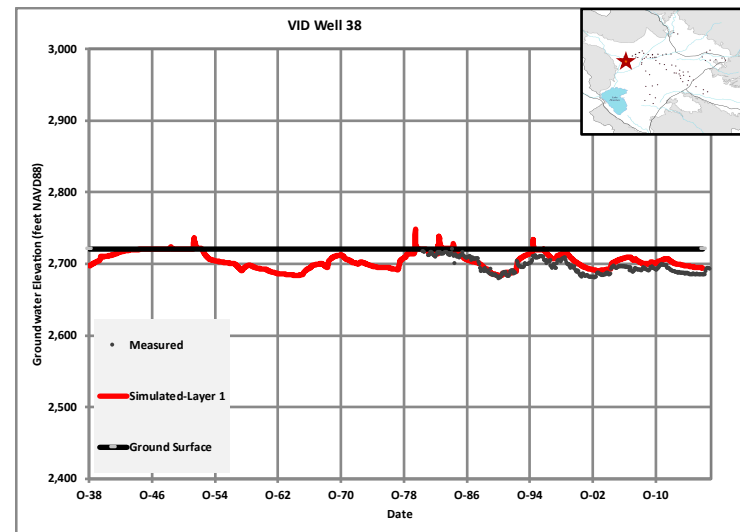
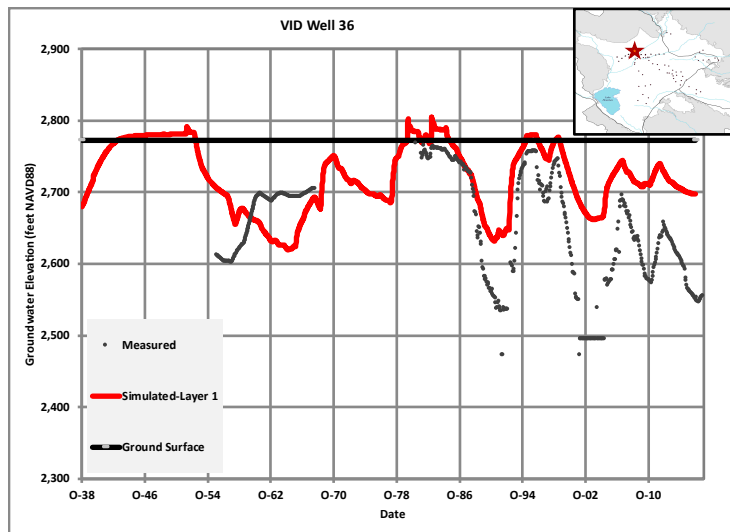
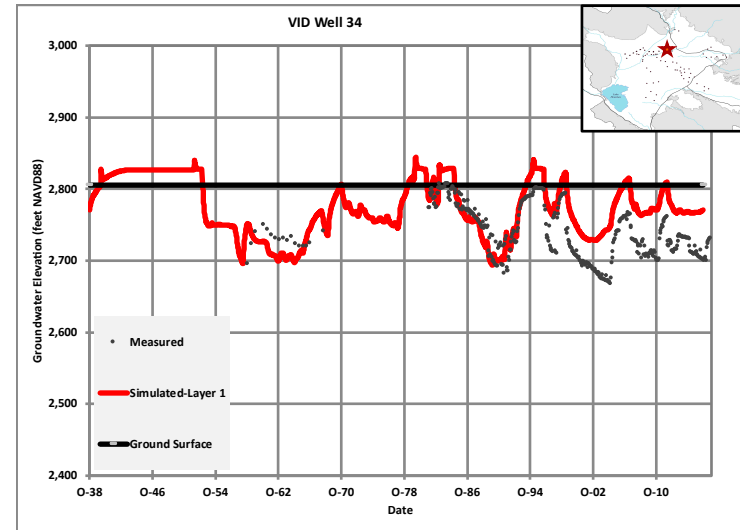
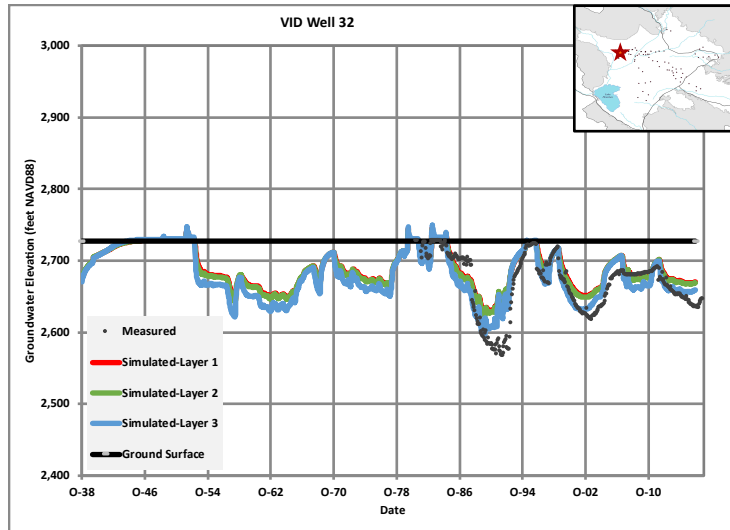
Figure D-1c
Hydrographs



September 2018



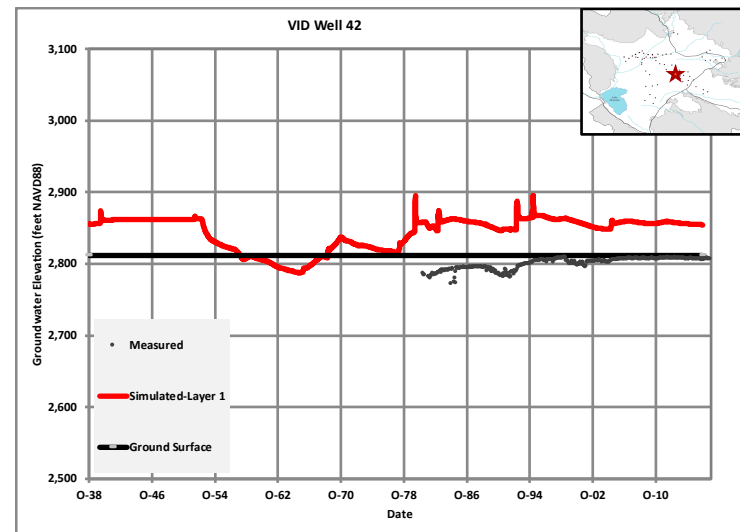
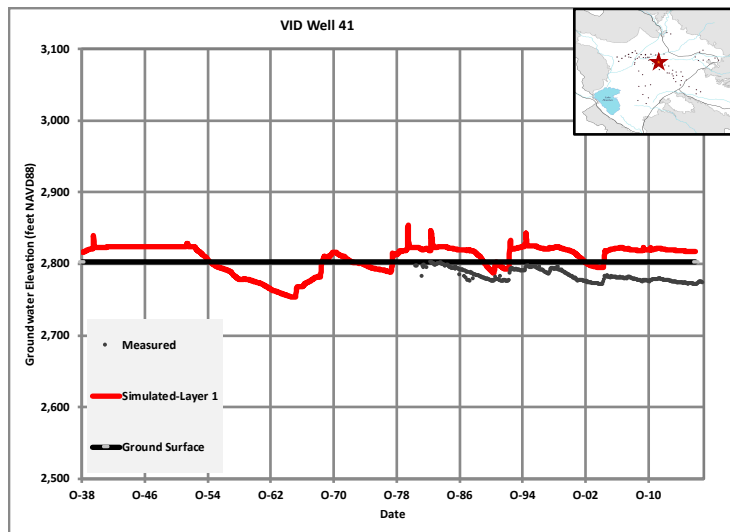
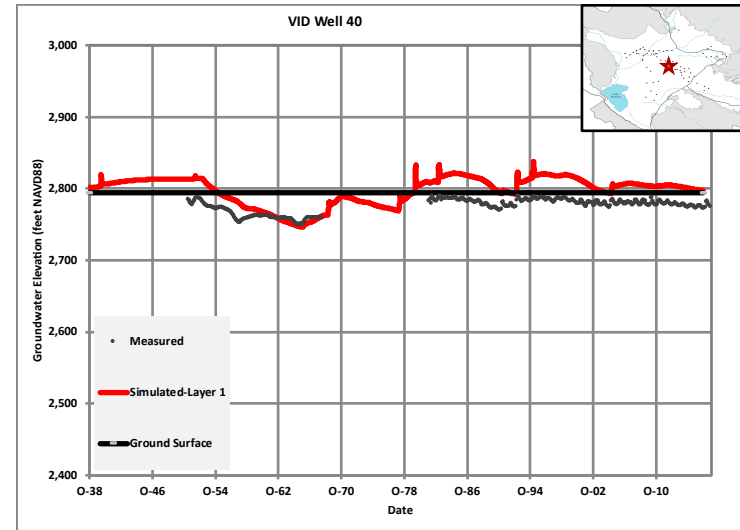
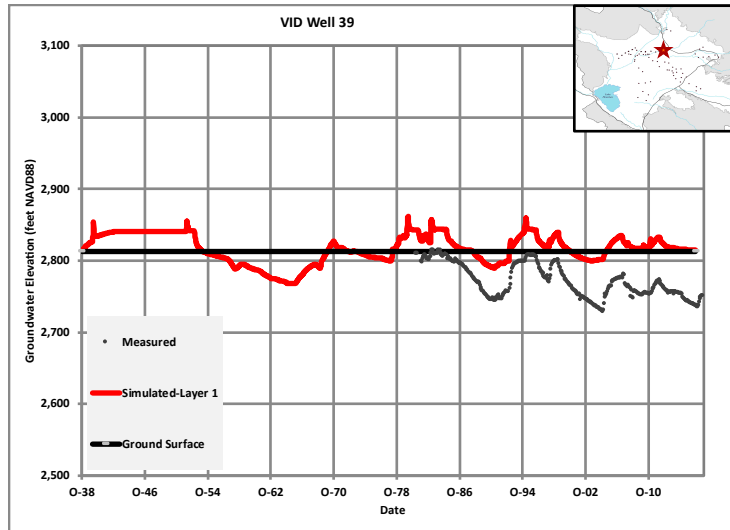
Figure D-1d
Hydrographs



September 2018



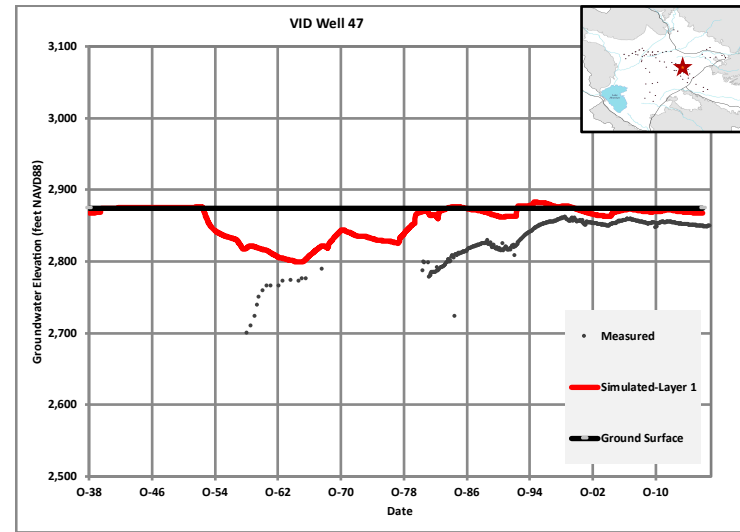
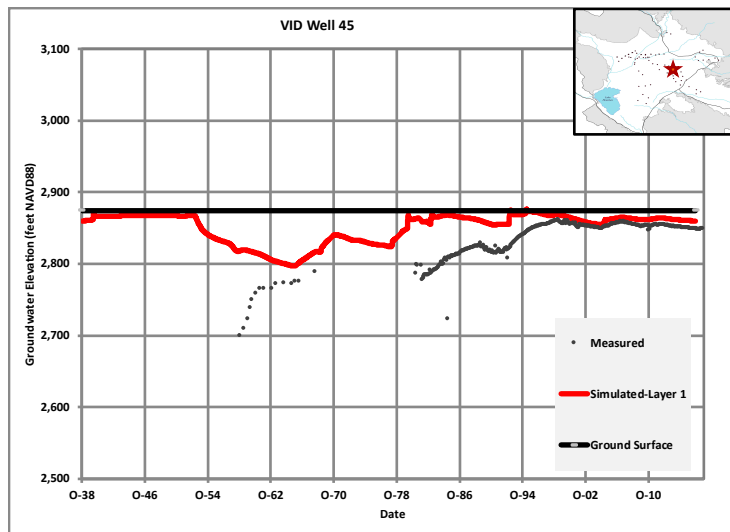
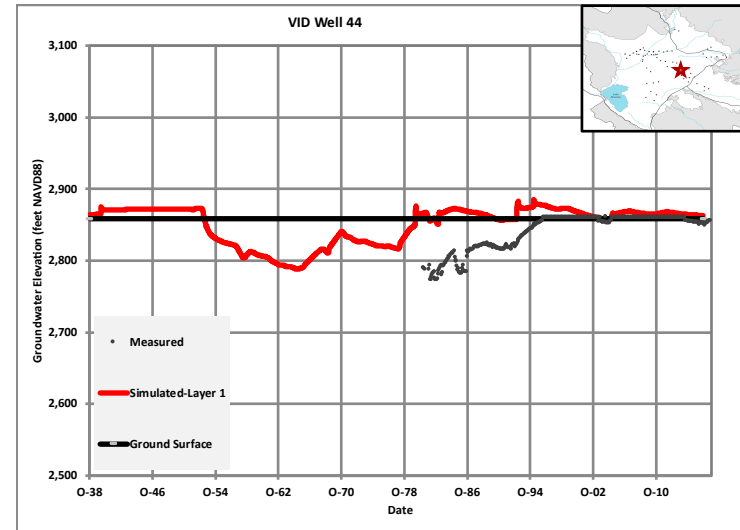
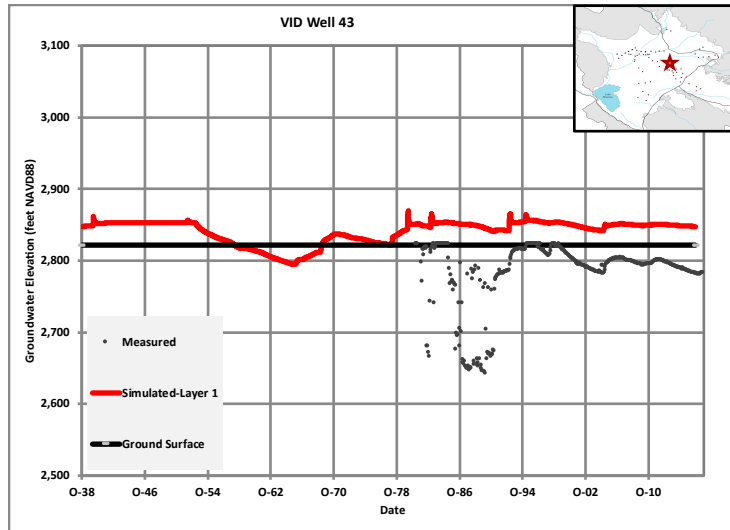
Figure D-1e
Hydrographs



September 2018



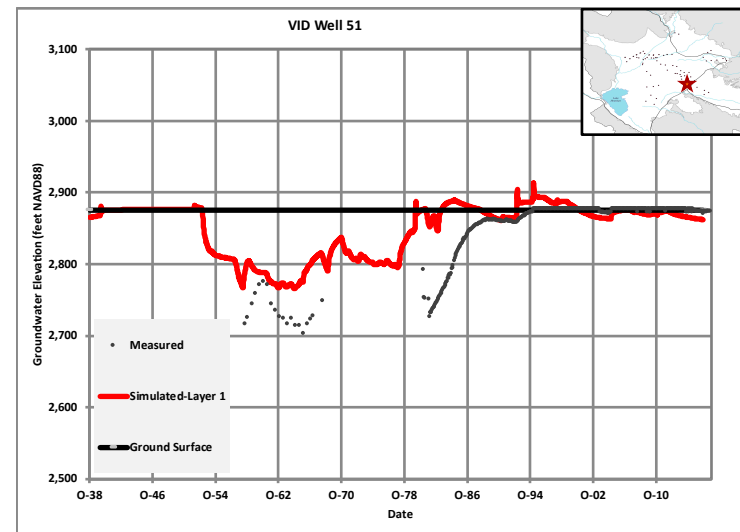
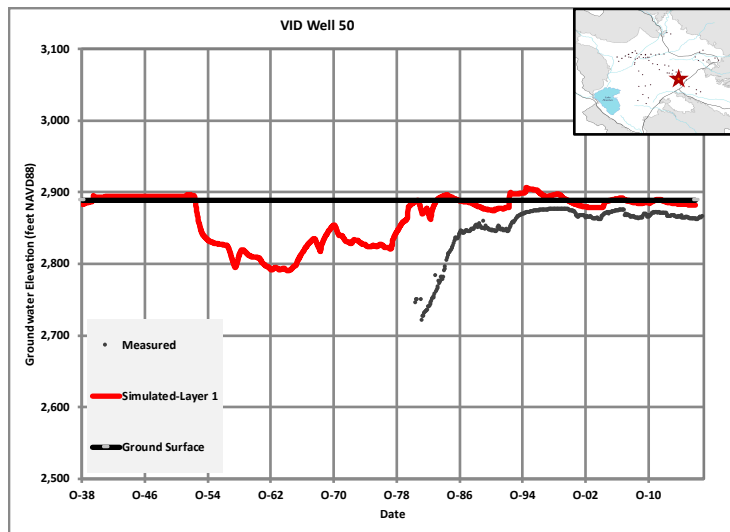
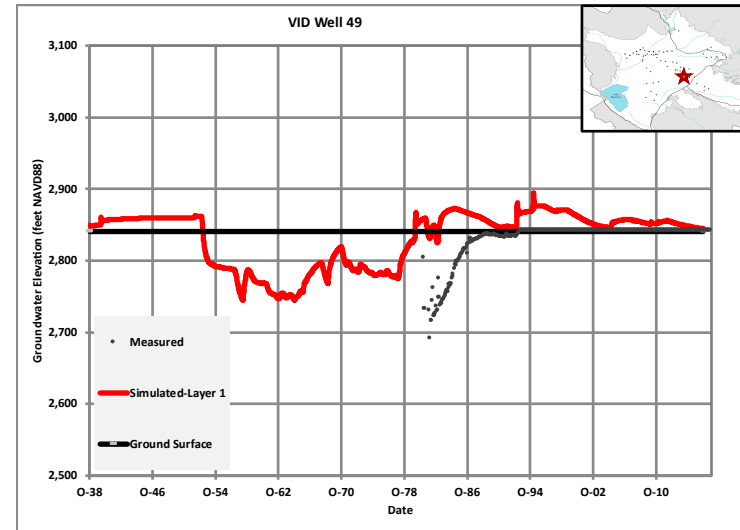
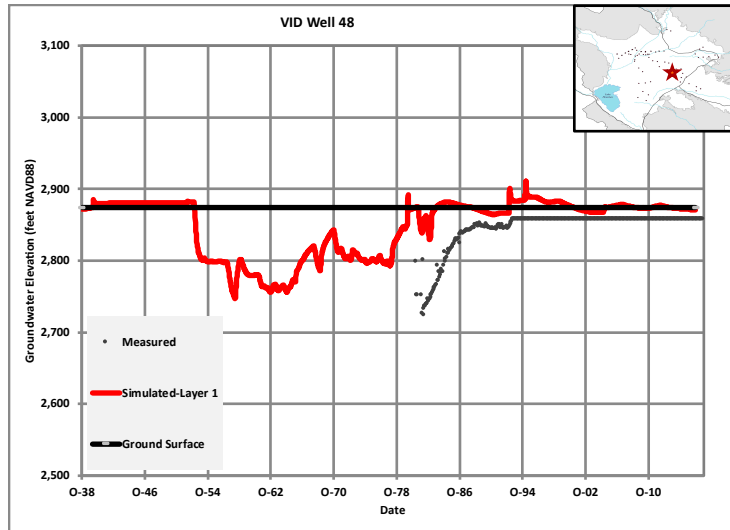
Figure D-1f
Hydrographs



September 2018



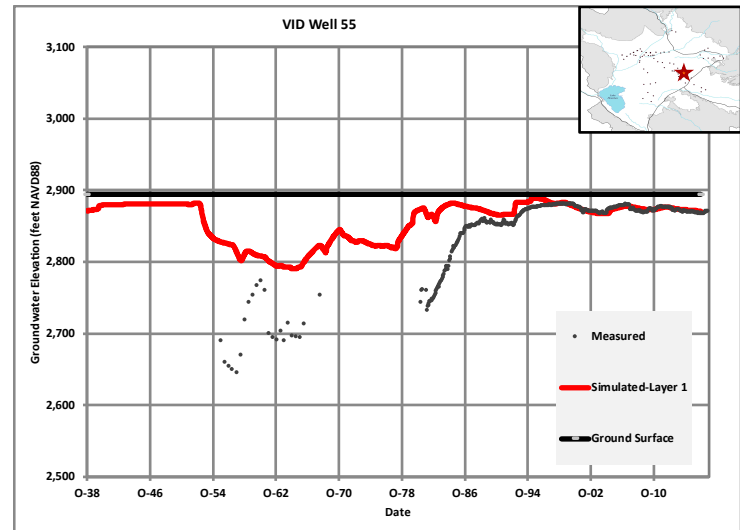
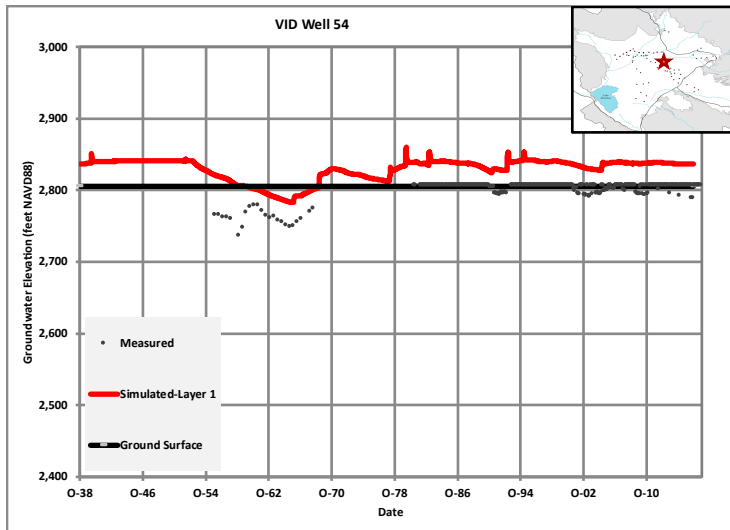
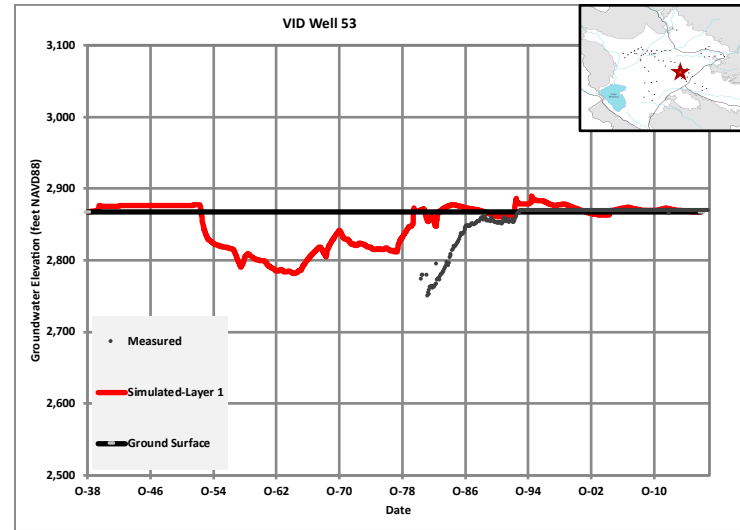
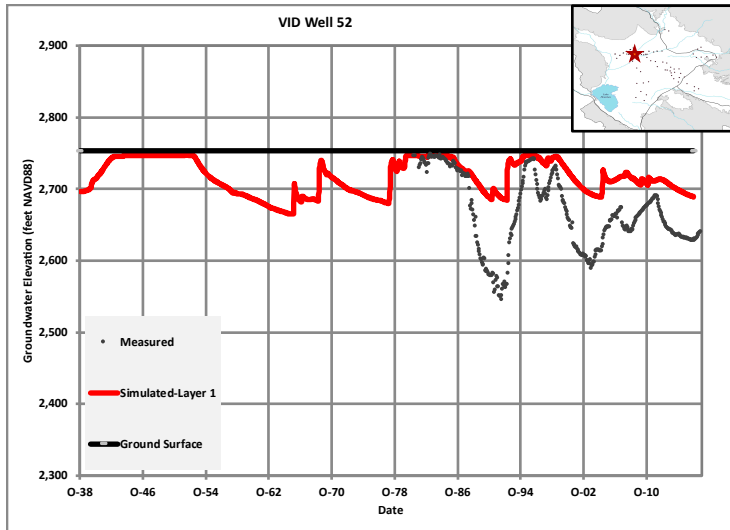
Figure D-1g
Hydrographs



September 2018



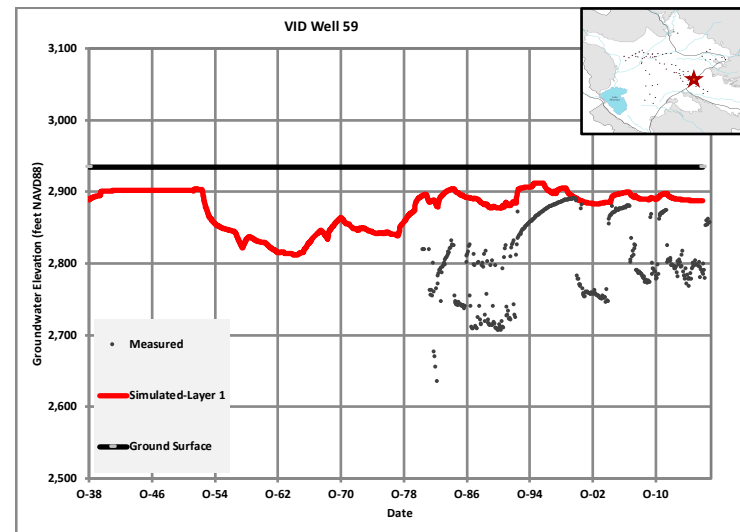
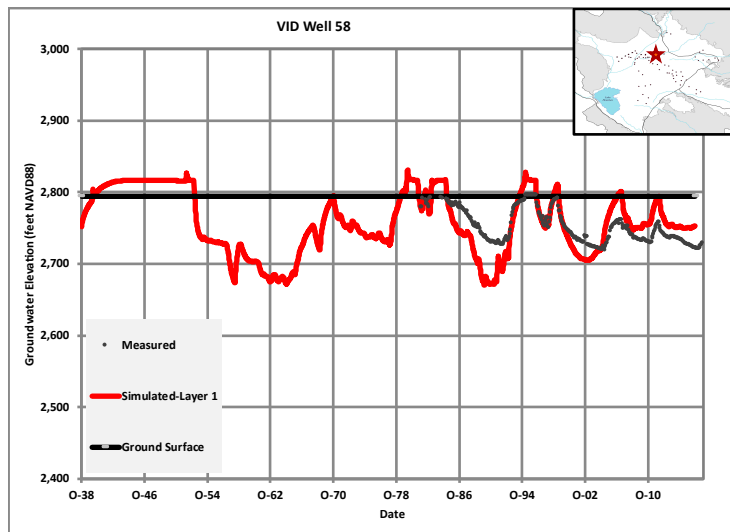
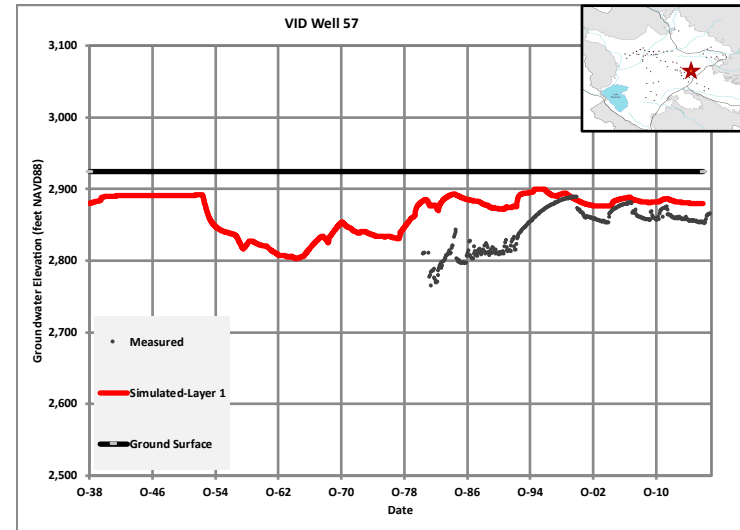
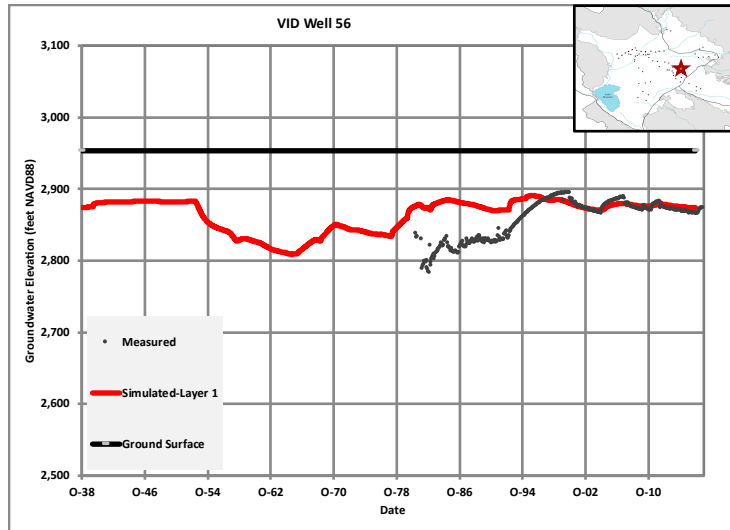
Figure D-1h
Hydrographs



September 2018



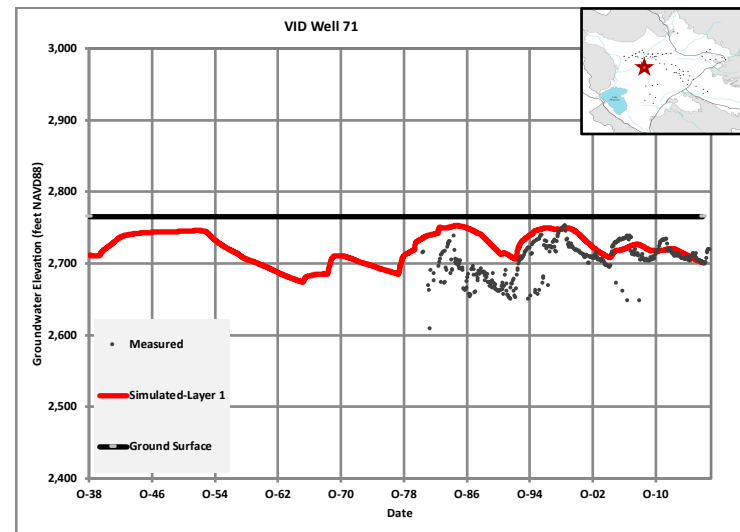
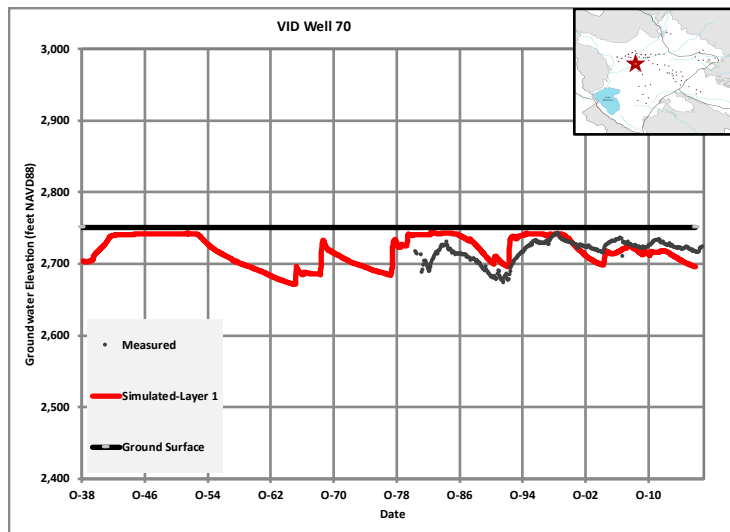
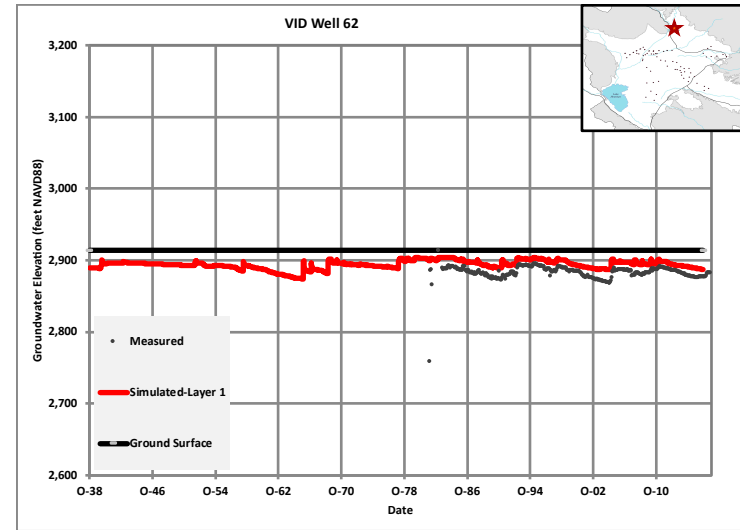
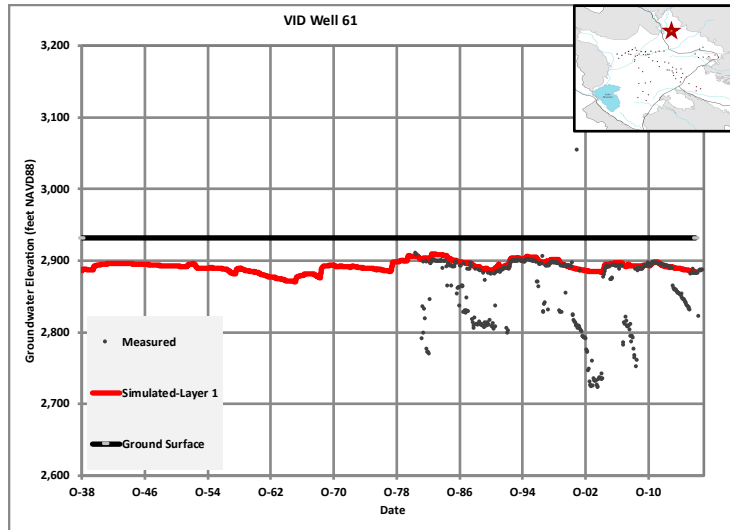
Figure D-1i
Hydrographs



September 2018



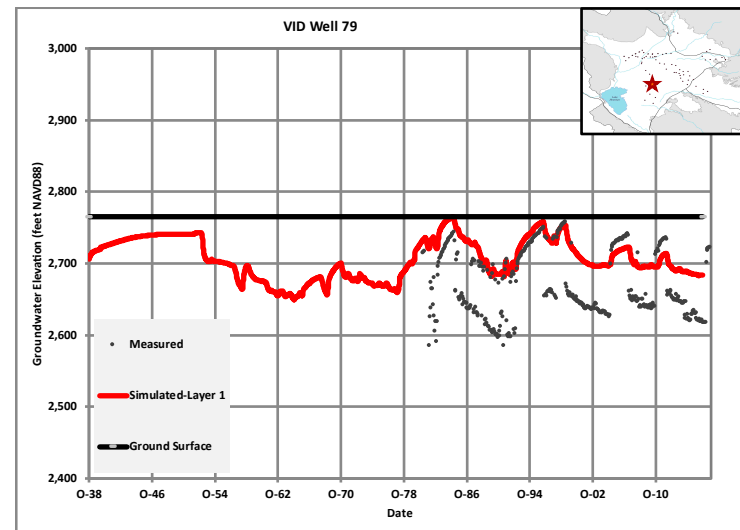
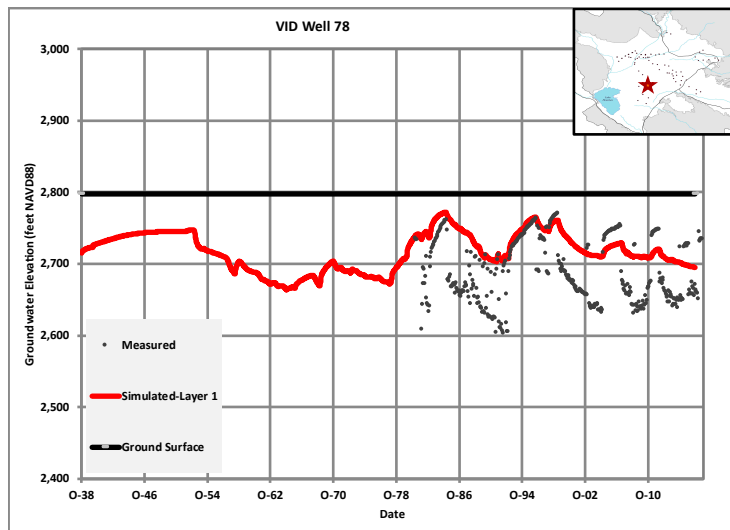
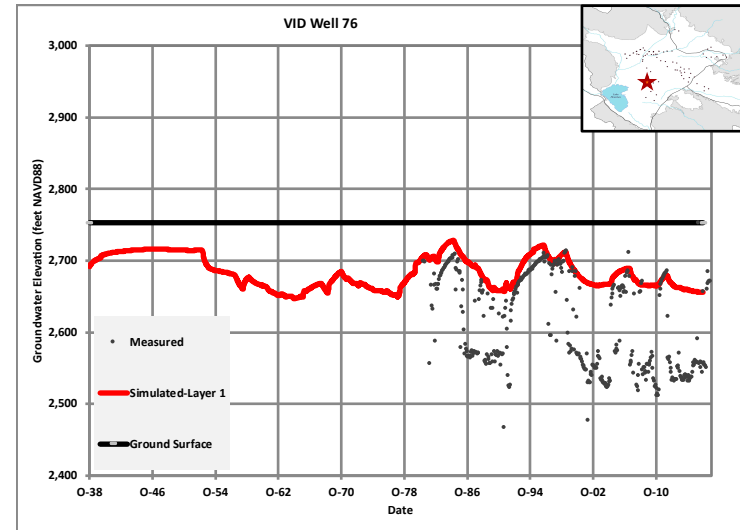
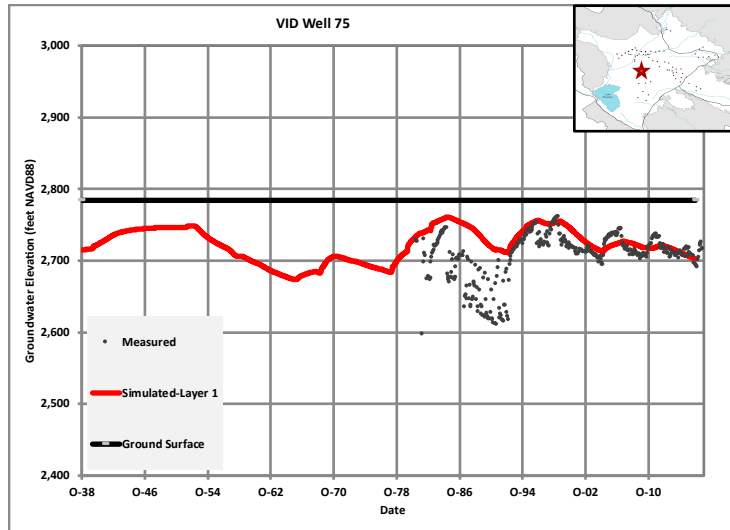
Figure D-1j
Hydrographs



September 2018



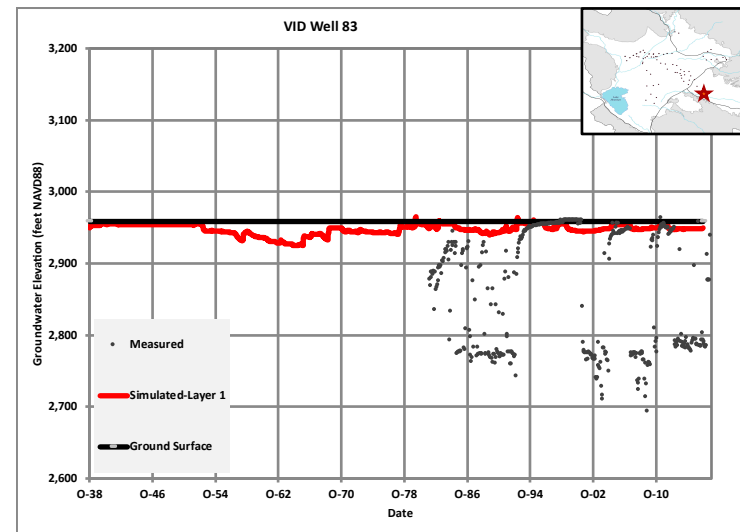
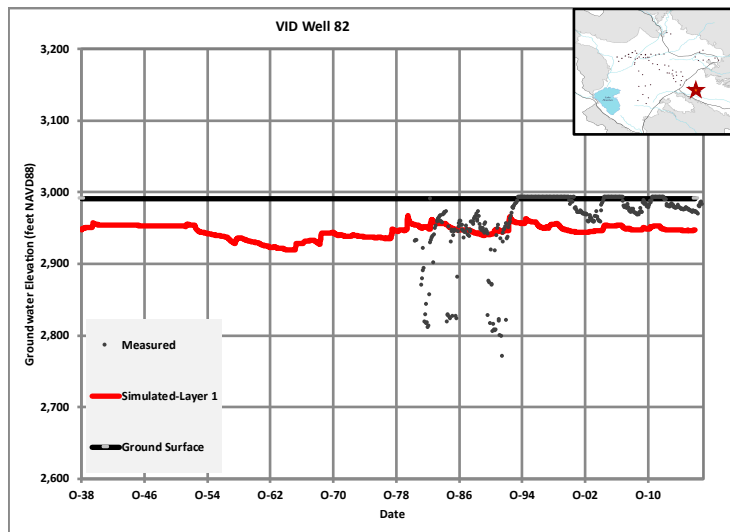
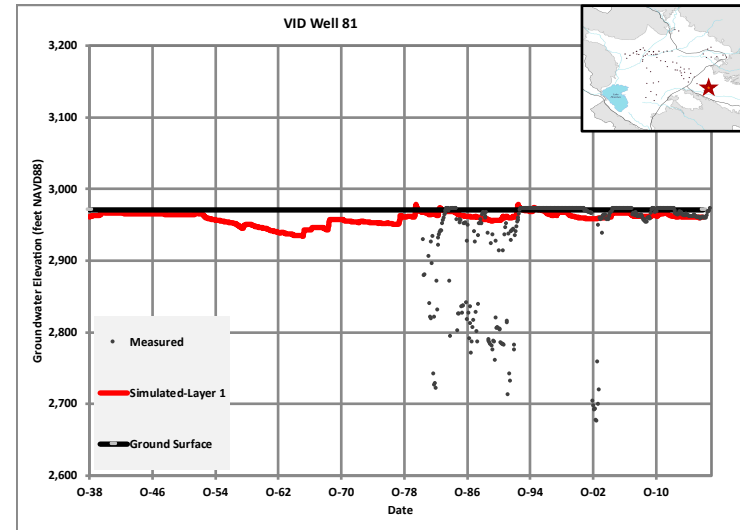
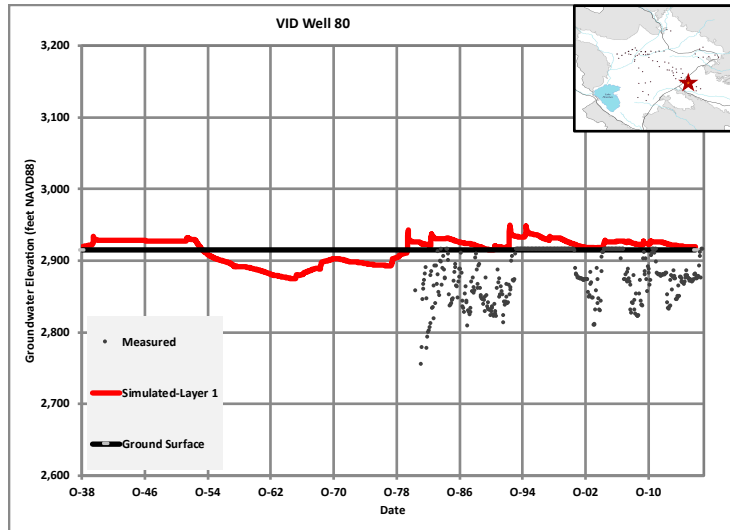
Figure D-1k
Hydrographs



September 2018



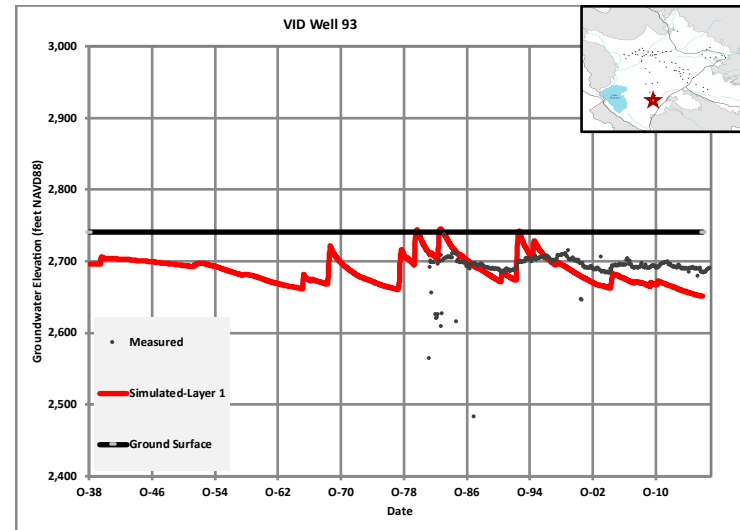
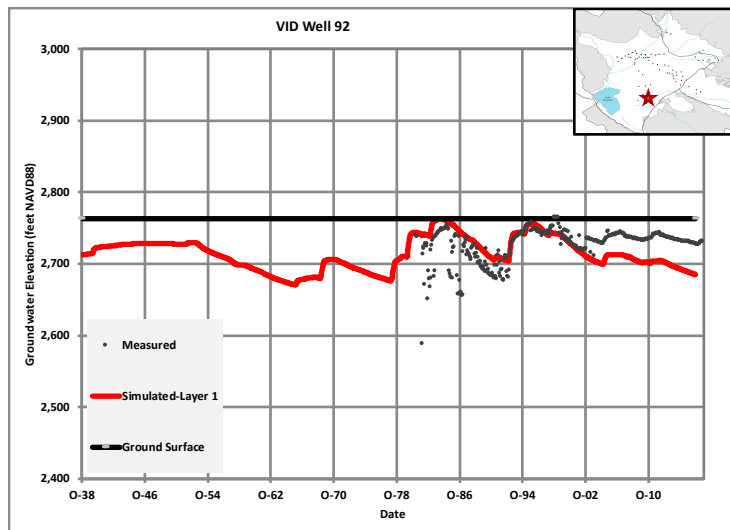
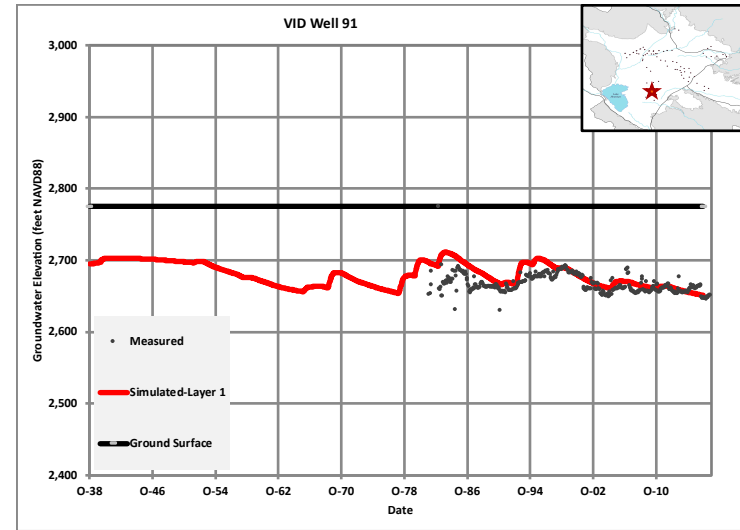
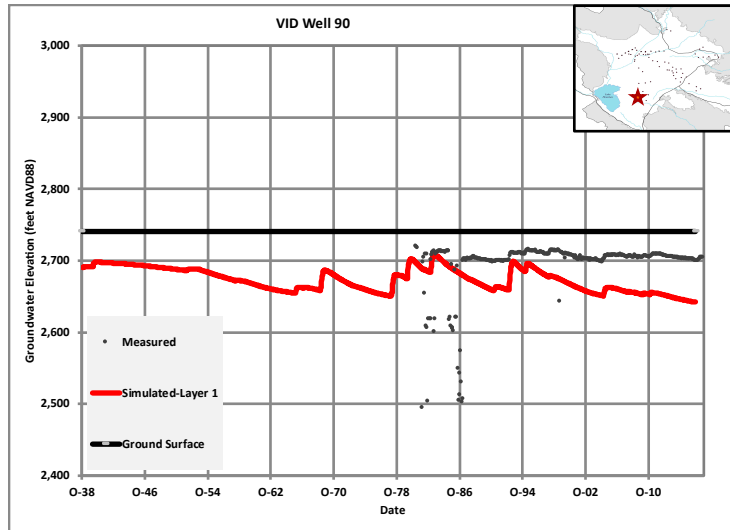
Figure D-11
Hydrographs



September 2018



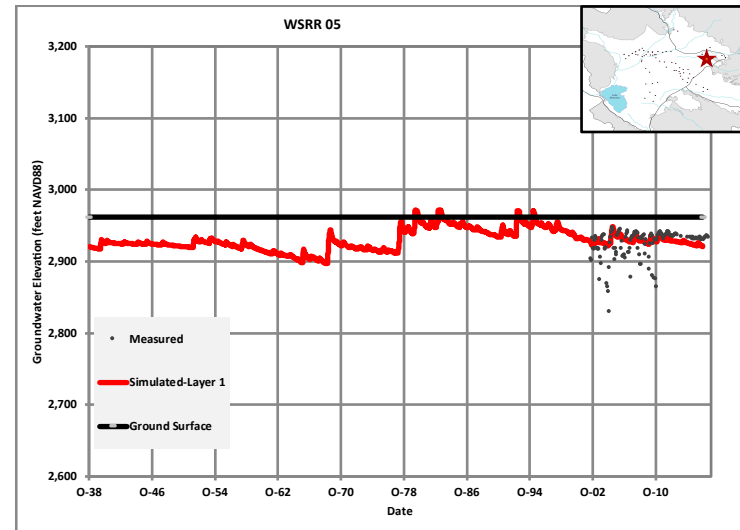
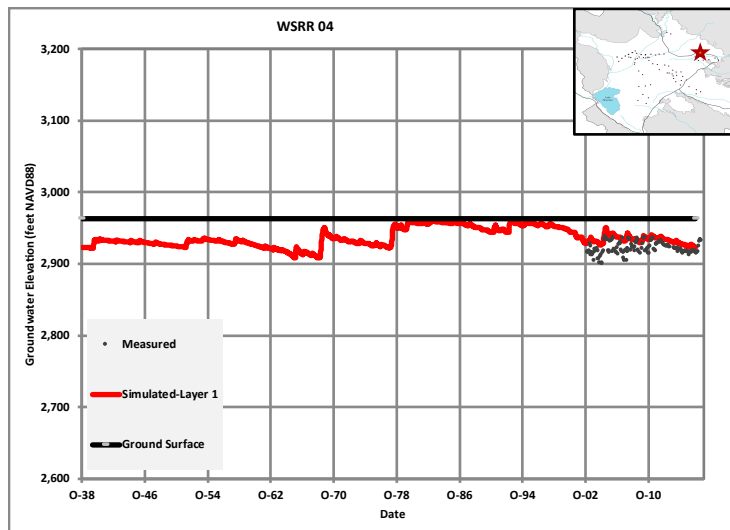
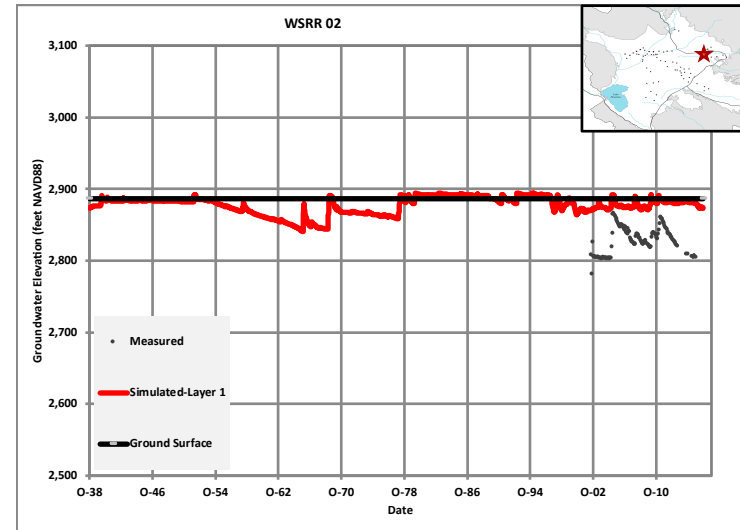
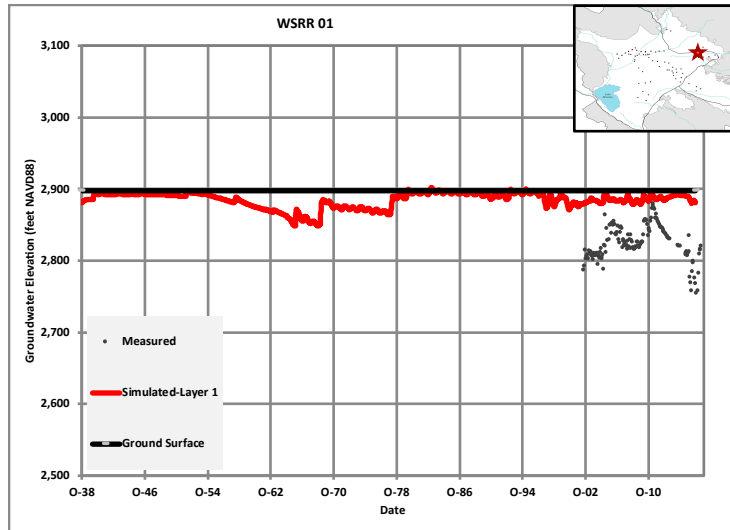
**Figure D-1m
Hydrographs**



September 2018



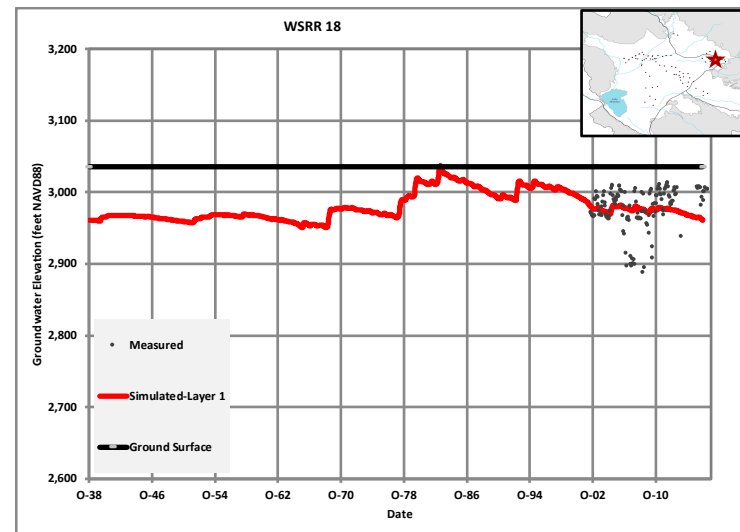
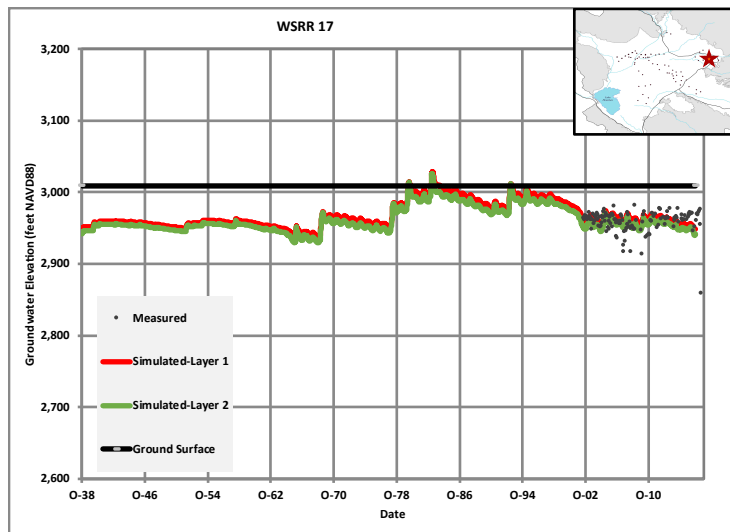
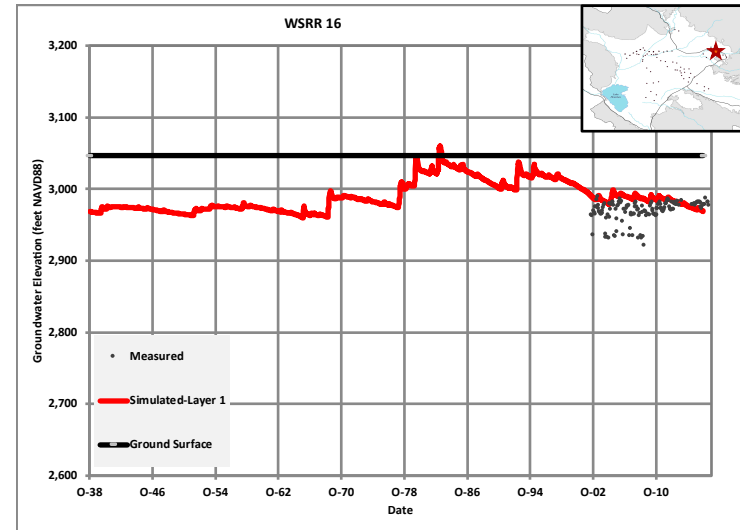
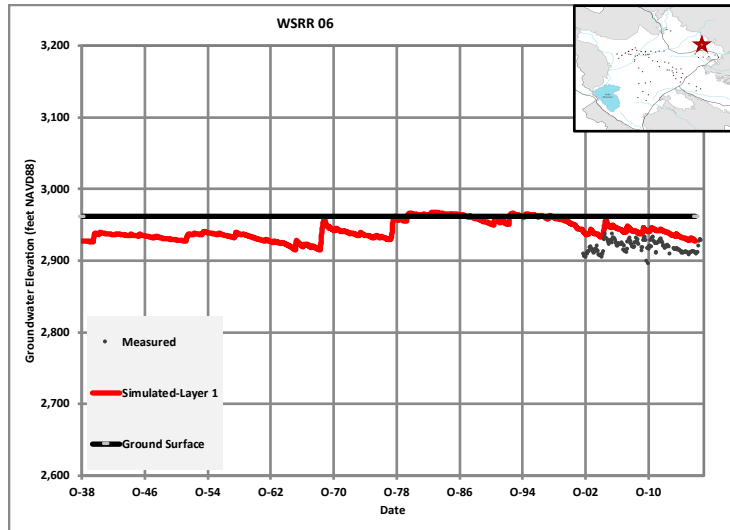
Figure D-1n
Hydrographs



September 2018



Figure D-1o
Hydrographs



September 2018



Figure D-1p
Hydrographs